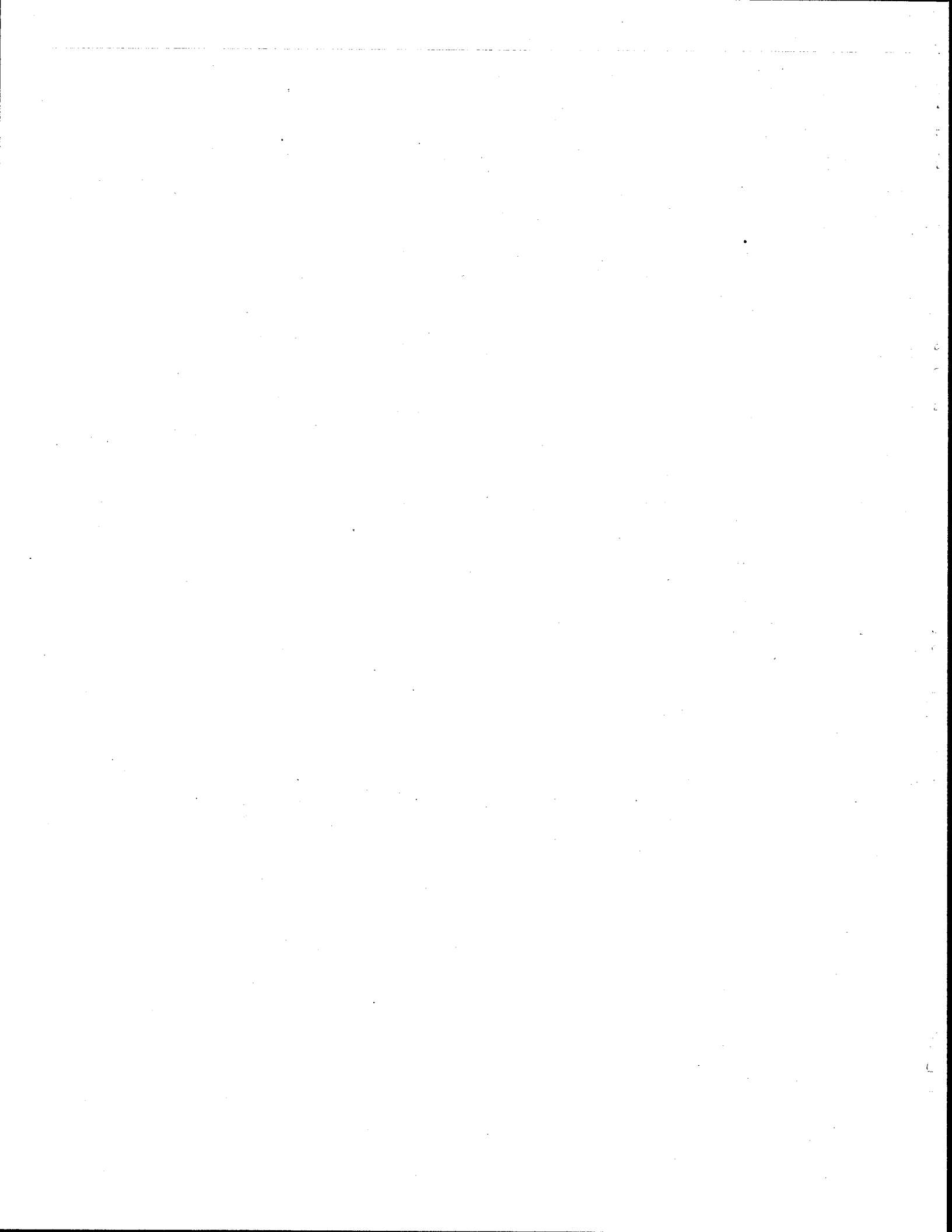


1. Report No. FHWTX77-211-1	2. Government Accession No.	3. Recipient's Catalog No.	
4. Title and Subtitle LATERAL LOAD TEST OF A DRILLED SHAFT IN CLAY		5. Report Date November, 1977	6. Performing Organization Code
		8. Performing Organization Report No. Research Report 211-1	
7. Author(s) Vernon R. Kasch, Harry M. Coyle, Richard E. Bartoskewitz, and William G. Sarver		10. Work Unit No.	
9. Performing Organization Name and Address Texas Transportation Institute Texas A&M University College Station, Texas 77843		11. Contract or Grant No. Research Study 2-5-77-211	
		13. Type of Report and Period Covered September, 1976 Interim - November, 1977	
12. Sponsoring Agency Name and Address Texas State Department of Highways and Public Transportation; Transportation Planning Division P. O. Box 5051 Austin, Texas 78763		14. Sponsoring Agency Code	
		15. Supplementary Notes Research performed in cooperation with DOT, FHWA. Research Study Title: Design of Drilled Shafts to Support Precast Panel Retaining Walls.	
16. Abstract The behavior of a laterally drilled shaft in clay has been investigated by conducting a lateral load test on an instrumented shaft. Lateral deflection, shaft rotation, and soil resistance were measured for each applied load. Dial gages were used to measure lateral deflection, while the shaft rotation was determined by means of an inclinometer. Pneumatic pressure cells were installed in the shaft at various depths to measure the soil resistance. The applied lateral load was measured with a strain gage load cell. Structural failure of the shaft occurred before the soil failed and prevented the attainment of the ultimate lateral soil resistance. However, it was possible to compare the ultimate soil reactions predicted by several analytical procedures with the soil reaction calculated from the maximum recorded soil resistance. Also, an ultimate lateral load for the test shaft was predicted by various analytical methods. A comparison was made between the maximum recorded load and the various predicted ultimates. Finally, a comparison was made between two ultimate test loads obtained from the technical literature and the ultimate loads predicted by the analytical methods. A tentative procedure for the design of the rigid, laterally loaded drilled shafts is presented. However, additional load tests are needed before the design can be finalized.			
17. Key Words Drilled Shaft, Lateral Load Test, Pressure Cells, Soil Reaction, Ultimate Load, Deflection, Rotation, Soil Creep.		18. Distribution Statement No restrictions. This document is available to the public through the National Technical Information Service, Springfield, Virginia 22151	
19. Security Classif. (of this report) Unclassified	20. Security Classif. (of this page) Unclassified	21. No. of Pages 97	22. Price



LATERAL LOAD TEST OF A DRILLED SHAFT IN CLAY

by

Vernon R. Kasch  
Research Assistant

Harry M. Coyle  
Research Engineer

Richard E. Bartoskewitz  
Engineering Research Associate

and

William G. Sarver  
Research Associate

Research Report No. 211-1

Design of Drilled Shafts to Support Precast Panel Retaining Walls  
Research Study Number 2-5-77-211

Sponsored by  
State Department of Highways and Public Transportation  
in Cooperation with the  
U.S. Department of Transportation  
Federal Highway Administration

November 1977

Texas Transportation Institute  
Texas A&M University  
College Station, Texas

## Disclaimer

The contents of this report reflect the views of the authors who are responsible for the facts and accuracy of the data presented herein. The contents do not necessarily reflect the views or policies of the Federal Highway Administration. This report does not constitute a standard, specification or regulation.

There was no invention or discovery conceived or first actually reduced to practice in the course of or under this contract, including any art, method, process, machine, manufacture, design or composition of matter, or any new and useful improvement thereof, or any variety of plant which is or may be patentable under the patent laws of the United States of America or any foreign country.

## ABSTRACT

The behavior of a laterally loaded drilled shaft in clay has been investigated by conducting a lateral load test on an instrumented shaft. Lateral deflection, shaft rotation, and soil resistance were measured for each applied load. Dial gages were used to measure lateral deflection, while the shaft rotation was determined by means of an inclinometer. Pneumatic pressure cells were installed in the shaft at various depths to measure the soil resistance. The applied lateral load was measured with a strain gage load cell.

Structural failure of the shaft occurred before the soil failed and prevented the attainment of the ultimate lateral soil resistance. However, it was possible to compare the ultimate soil reactions predicted by several analytical procedures with the soil reaction calculated from the maximum recorded soil resistance. Also, an ultimate lateral load for the test shaft was predicted by various analytical methods. A comparison was made between the maximum recorded load and the various predicted ultimates. Finally, a comparison was made between two ultimate test loads obtained from the technical literature and the ultimate loads predicted by the analytical methods.

A tentative procedure for the design of rigid, laterally loaded drilled shafts is presented. However, additional load tests are needed before the design can be finalized.

KEY WORDS: Drilled Shaft, Lateral Load Test, Pressure Cells, Soil Reaction, Ultimate Load, Deflection, Rotation, Soil Creep.

## IMPLEMENTATION STATEMENT

The results of the lateral load test and the state of the art survey of the technical literature were combined to produce a tentative procedure for the design of drilled shafts supporting precast panel retaining walls. An important feature in the design of retaining walls is the allowable amount of wall deflection. Consequently, factors of safety were included in the tentative design procedure to control the amount of wall deflection by limiting the shaft rotation.

The tentative design procedure could be implemented but additional testing would undoubtedly result in improvements in the procedure. Future lateral load tests should be conducted to failure in order to obtain ultimate loads and ultimate soil reactions. A maximum value for drilled shaft rotation also needs to be established, and a study of soil behavior under the influence of sustained lateral loads needs to be performed. Finally, load tests on shafts of various depths and diameters in different types of soil should be conducted.

## ACKNOWLEDGEMENTS

The combined efforts of many people were required to successfully complete the objectives of the first year of this research study. Sincere gratitude is expressed to all who participated in the study, especially to the State Department of Highways and Public Transportation (SDHPT) and the Federal Highway Administration (FHWA) whose cooperative sponsorship made the research possible.

The authors are grateful to Mr. H. D. Butler, of the SDHPT Bridge Division, who was the contact representative for the study. His cooperation and suggestions were of much benefit to the research staff. Sincere appreciation is extended to Mr. Bill D. Ray and his support services group of Texas Transportation Institute. The successful completion of the field portion of this study would not have been possible without their dedicated cooperation.

## TABLE OF CONTENTS

INTRODUCTION . . . . .	1
Physical Characteristics of Drilled Shafts . . . . .	1
Historical Development of Drilled Shafts . . . . .	4
Factors Influencing the Use of Drilled Shafts . . . . .	4
Scope of This Study . . . . .	6
DETERMINATION OF DRILLED SHAFT BEHAVIOR . . . . .	10
Methods of Determining Drilled Shaft Behavior . . . . .	10
Discussion of Soil Parameters $E_s$ and $k$ . . . . .	14
Relative Stiffness of Drilled Shafts . . . . .	16
ANALYSIS OF ELASTIC BEHAVIOR OF LATERALLY LOADED CYLINDRICAL FOUNDATIONS . . . . .	22
Solutions Assuming the Winkler Model . . . . .	22
Solution Assuming the Elastic Continuum . . . . .	25
Method by Broms . . . . .	27
Finite Element Method . . . . .	27
ANALYSIS OF RIGID BEHAVIOR OF LATERALLY LOADED CYLINDRICAL FOUNDATIONS . . . . .	29
Soil Pressure Distribution . . . . .	29
Rankine Passive Pressure . . . . .	29
Texas A&M University Research . . . . .	31
University of Florida Research . . . . .	33
Method by Broms . . . . .	36
Method by Hansen . . . . .	36
FIELD LOAD TEST . . . . .	40
Soil Conditions . . . . .	40
Lateral Loading System . . . . .	45

Instrumentation . . . . .	49
Construction of Testing System . . . . .	51
Loading Procedure . . . . .	54
TEST RESULTS . . . . .	57
Pressure Cell Data . . . . .	57
Analysis of Pressure Cell Data . . . . .	67
Load-Deflection Characteristics . . . . .	71
Load-Rotation Characteristics . . . . .	73
Rotation Point of the Test Shaft . . . . .	73
Ultimate Loads on Rigid Shafts . . . . .	76
TENTATIVE DESIGN PROCEDURE . . . . .	79
Force Acting on Retaining Wall . . . . .	79
Application Point of Resultant Force . . . . .	80
Soil Shear Strength . . . . .	80
Allowable Shaft Rotation . . . . .	81
Soil Creep . . . . .	82
Drilled Shaft Design Method . . . . .	83
Proposed Design Procedure . . . . .	83
Example of Design Procedure . . . . .	85
CONCLUSIONS AND RECOMMENDATIONS . . . . .	87
Conclusions . . . . .	87
Recommendations . . . . .	88
APPENDIX I - REFERENCES . . . . .	90
APPENDIX II - NOTATION . . . . .	94

LIST OF TABLES

Table		Page
1	Relative Stiffness of Laterally Loaded Piles or Shafts . . . . .	13
2	Values of $k_s$ , in tons/cu ft for Square Plates, 1 ft x 1 ft, Resting on Pre-Compressed Clay. After Terzaghi (1955) . . . . .	17
3	Initial Pressure Cell Readings . . . . .	57
4	Results of Retaining Wall Loading Simulation of Test Shaft . . . . .	72
5	Comparison of Lateral Load Test Results with Calculated Ultimate Loads . . . . .	77

## LIST OF FIGURES

Figure		Page
1	Principal Classifications of Drilled Shafts (After D'Appolonia et al.) . . . . .	3
2	Precast Panel Retaining Wall . . . . .	7
3	Drilled Shaft Behavior . . . . .	11
4	Soil Modulus, $E_s$ , and Variations with Depth . . . . .	15
5	Relative Stiffness Ratio, D/R, With Constant Soil Modulus, $E_s$ . . . . .	19
6	Relative Stiffness Ratio, D/T, With Constant Soil Modulus Variation, k . . . . .	20
7	Graphical Definition of p and y (After Reese - 1977) . . . . .	24
8	Set of p-y Curves (After Reese - 1977) . . . . .	26
9	Soil Pressure Distribution (After Seiler) . . . . .	30
10	Forces Developed By Overturning Load (After Ivey). . . . .	32
11	Ultimate Lateral Soil Resistance For Cohesive Soils (After Hays et al.) . . . . .	35
12	Ultimate Lateral Soil Resistance For Cohesive Soils According to Broms . . . . .	37
13	Hansen's Ultimate Lateral Soil Resistance . . . . .	39
14	Location of Borings . . . . .	41
15	Boring - S1 . . . . .	42
16	Boring - S2 . . . . .	43
17	Boring - S3 . . . . .	44
18	Texas Cone Penetrometer Test . . . . .	46
19	Lateral Loading System . . . . .	47
20	Terra Tec Pressure Cell . . . . .	50

Figure		Page
21	Location of Pressure Cells . . . . .	53
22	Lateral Load vs. Lateral Pressure, Cell 875 . . . . .	59
23	Lateral Load vs. Lateral Pressure, Cell 877 . . . . .	60
24	Lateral Load vs. Lateral Pressure, Cell 879 . . . . .	61
25	Lateral Load vs. Lateral Pressure, Cells 881 & 883 . . . . .	62
26	Lateral Load vs. Lateral Pressure, Cells 876 & 878 . . . . .	63
27	Lateral Load vs. Lateral Pressure, Cells 880 & 882 . . . . .	64
28	Lateral Load vs. Lateral Pressure, Cell 884 . . . . .	65
29	Lateral Pressure vs. Depth . . . . .	68
30	Ultimate Soil Reaction vs. Depth Below Groundline . . . . .	70
31	Lateral Load vs. Deflection at Groundline . . . . .	74
32	Lateral Load vs. Rotation . . . . .	75
33	Design Chart I (After Lytton) . . . . .	84

## INTRODUCTION

During the last four decades a foundation element referred to variously as a drilled pier, bored pile, drilled shaft, or drilled cassion has come into widespread use. The term "drilled shaft" will be used in this study. A drilled shaft is a concrete foundation element which is cast in a previously drilled cylindrical hole. The shaft is bored with a truck or crane mounted drilling rig equipped with a helical auger or cylindrical drilling bucket. The concrete is reinforced to resist tensile or flexural stresses. Drilled shafts serve the same function as driven piles. The installation procedure is the distinguishing feature between these two foundation elements.

Drilled shafts are used for high rise buildings and heavily loaded industrial facilities where settlement criteria require that the structure be supported on strong soil or bedrock. They are also used as foundations for bridges, retaining structures, and highway sign structures. If suitable equipment is available then battered shafts, shafts skewed from the vertical, may be installed to serve as anchors or tiebacks. The use of drilled shafts has even been extended to offshore structures where they have been used as extensions to large diameter driven pipe piles in order to provide additional foundation penetration.

### Physical Characteristics of Drilled Shafts

Drilled shafts develop their axial bearing capacity from skin friction and end bearing. A drilled shaft may be constructed with an

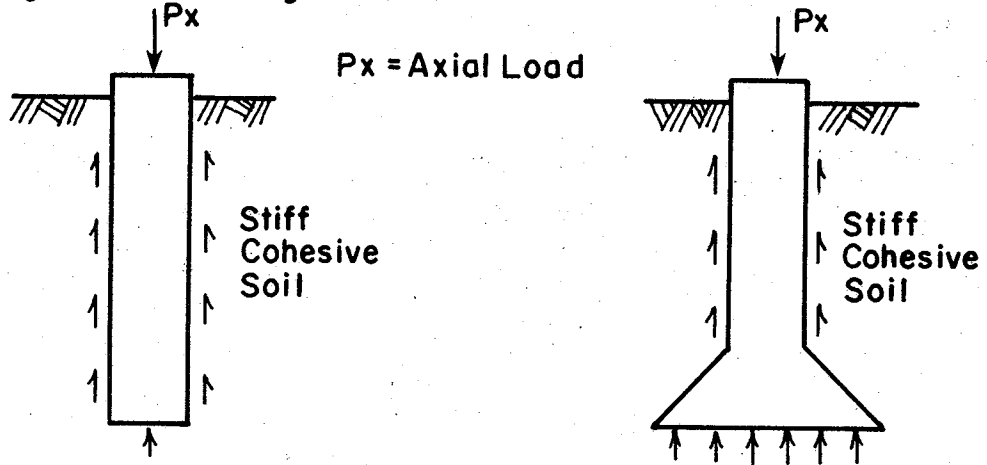
Numbers in parentheses refer to the references listed in Appendix I.

enlarged base in order to provide more axial capacity from end bearing. This type of foundation element is referred to as a belled pier, drilled and underreamed caisson, or underreamed shaft. The underream is hemispherical or conical in shape with the sidewalls making an angle of  $30^{\circ}$  to  $45^{\circ}$  with the vertical. The size of most underreaming tools is limited to three times the diameter of the shaft (41).

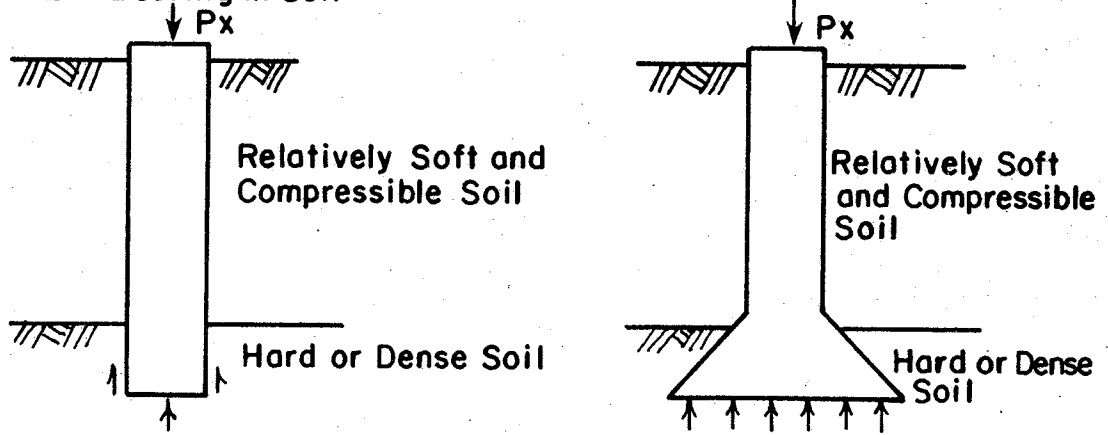
Drilled shafts normally encountered in ordinary construction work have diameters that range from 24 to 48 in. (70 to 121.9 cm) (39). Construction equipment currently available offers the opportunity of drilling shafts that range from 12 in. to 20 ft (30.48 cm to 6.10 m) in diameter. Modern bellling equipment will permit drilled shafts to be constructed with underreams that vary from 2 to 15 ft (0.61 to 4.57 m) in diameter. Shaft depths in excess of 200 ft (61 m) are also attainable with currently available equipment (41).

The manner in which a drilled shaft resists axial load varies according to the subsurface material and physical dimensions of the shaft. Fig. 1 shows three predominant types of drilled shafts (7). A straight shaft in homogeneous soil develops its axial bearing capacity from a combination of skin friction and end bearing. The shafts are sometimes underreamed in order to increase end bearing and resist uplift forces. In areas where a deep stratum of strong bearing soil is overlain by a shallower stratum of weak, compressible soil, the shaft is considered to be primarily an end bearing foundation element. In structures such as this, skin friction is often neglected and the shaft is underreamed to increase the end bearing capacity. In situations where a weak, surface stratum is underlain by a hard, competent material that does not permit underreaming, the shaft may rest directly on the bearing stratum or it may

**A. Floating Shafts in Homogeneous Soil**



**B. Shafts End Bearing in Soil**



**C. Shafts End Bearing in Rock**

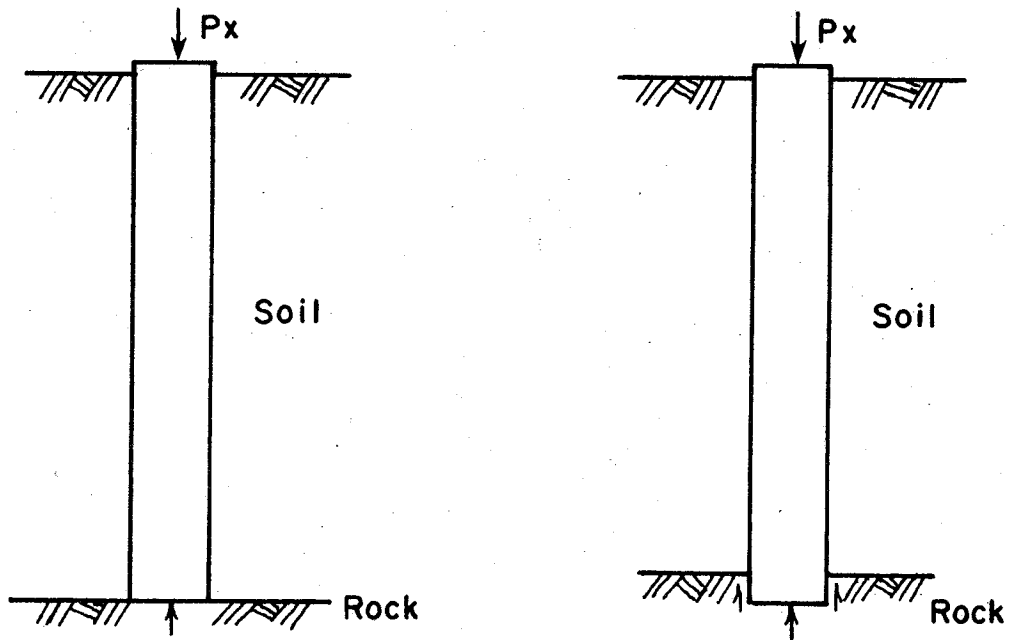


**FIG. 1— Principal Classifications of Drilled Shafts**  
(After D'Appolonia et al.)

be socketed into the stratum to derive both skin friction and end bearing.

### Historical Development of Drilled Shafts

The construction of higher and heavier buildings near the beginning of the twentieth century necessitated the development of high capacity deep foundations. Two methods of deep foundation construction that were used at this time were the Chicago method and the Gow method. Hand-excavated shafts by the Chicago method were carried on inside a wooden shell of vertically placed boards held in place by circular steel compression rings. The boards were left in the shaft as concrete was placed (4). The Gow method employed a series of hand-excavated holes that were made progressively smaller in diameter with depth. They were usually cased with telescoping metal tubes that were withdrawn during concrete placement (24).

Machine excavated shafts began to appear in the 1920's. Many of these machines were horse-powered although steam- and electric-powered machines were developed in the 1920's and 1930's. During World War II the need for rapid construction of lightly loaded structures for the armed services resulted in the widespread use of truck-mounted auger machines for construction of shallow drilled shaft foundations. These machines had originally been used as post hole diggers by utility companies (41). It was not until truck-mounted rotary drilling machines became commercially available after World War II that drilled shafts began to gain widespread acceptance as foundation elements.

### Factors Influencing the Use of Drilled Shafts

When deep foundations are required for a construction project it is necessary to choose piling or drilled shafts. On many jobs economic and

technical factors make the choice of one or the other readily apparent. However, in situations where the superiority of one foundation type over the other is not immediately clear, the advantages and disadvantages of each foundation system should be considered.

The advantages of drilled shaft foundations in comparison to pile foundations are (41, 24):

1. Shafts can be drilled to the anticipated bearing stratum and the quality of the bearing material can be visually inspected.
2. Shafts can be drilled through cobbles, small boulders, weathered rock, and dense sand layers that would deflect piling or cause them to reach refusal.
3. Vibrations and noise that are associated with pile driving are eliminated.
4. A single shaft can replace a pile group, eliminating the need for pile caps and related form work.
5. Ground heave associated with driven displacement piles is eliminated.
6. Uplift resistance can be provided by underreaming the shaft.
7. Increased bearing capacity can be provided by underreaming the shaft.

The disadvantages of drilled shaft foundations in comparison to pile foundations are (41, 24):

1. Complete soil exploration of the construction site is needed. The unexpected occurrence of large boulders, water bearing sand layers, or soft clay may lead to costly construction delays.

2. Wet weather affects drilling and concreting to a greater extent than pile driving.
3. Careful inspection and technical supervision are needed because of problems that can occur during construction.
4. Caving of the shaft and loss of ground is possible in soft clays and loose, dry sands.
5. Termination of a drilled shaft in water bearing granular soil is difficult.

#### Scope of This Study

The Texas State Department of Highways and Public Transportation (SDHPT) has in recent years developed a new concept in retaining wall design and construction. The new type of retaining structure is the precast panel retaining wall. As shown in Fig. 2, this structure makes use of precast panels that are placed between T-shaped pilasters. The pilasters are spaced at even intervals and are supported by drilled shafts. The precast panel derives its restraining ability from the pilasters, which are located at the edges of the panel. The forces acting on the panel are transmitted to the pilasters and must be resisted by the soil in contact with the drilled shafts.

The SDHPT recognizes that improvements in design procedures may result in savings in construction costs. With this thought in mind, a study of lateral earth pressures on retaining walls was recently conducted (42). At the present time it is the opinion in some quarters that improvements in the design of the drilled shafts that support precast panel retaining walls could be economically beneficial. It is in view of this situation that this research study was initiated.

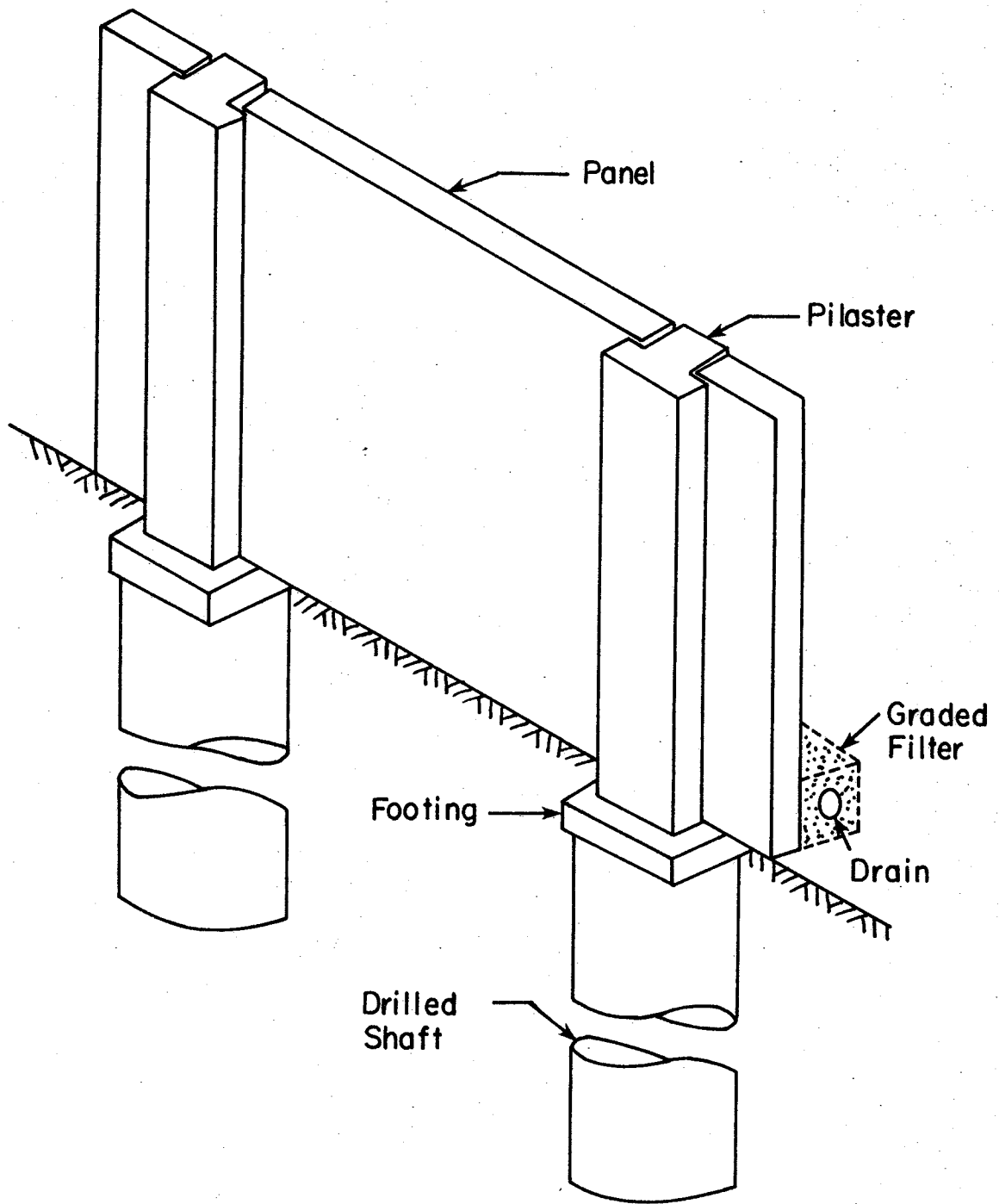


FIG. 2 - Precast Panel Retaining Wall

The drilled shaft must be designed to withstand both axial and lateral loads. However, since the axial load on a shaft supporting a precast panel retaining wall is minimal, it is the lateral load that is of primary interest. Passive and active pressures are developed in the soil as a result of being in contact with the foundation. The magnitude and distribution of these pressures is dependent on many factors, including the size of the lateral load, the type of soil and its physical properties, and the diameter and flexibility of the foundation. Since the forces that resist lateral loads are the resultants of earth pressures, it was felt that field pressure measurements would be beneficial in the development of improved design criteria.

Several investigators have made pressure measurements on cylindrical foundations during the last few decades. Stobie (35), in 1930, used mechanical pressure gages to measure soil pressures on laterally loaded utility poles. The pressures were calculated from the deformation of calibrated lead wire in the gages. Direct measurement of pressures on laterally loaded piles has been reported by Mason and Bishop (21) and Heijnen and Lubking (14). Mason and Bishop report the use of friction-steel ribbon type pressure gages, while Heijnen and Lubking report the use of pressure cells, but do not specify what kind. Adams and Radhakrishna (1) report the use of hydraulic displacement pressure cells on lateral capacity tests of drilled shafts. In addition to these direct measurements of soil pressure, several investigators have reported soil reactions that were determined indirectly from instrumented piles or drilled shafts (20, 22, 30, 31, 39). The soil reactions were determined by double-differentiation of the bending moments that were obtained from

strain gage measurements.

The present research study was initiated with the objective of obtaining field data by the measurement of loads, lateral earth pressures, deflections, and rotations on a laterally loaded drilled shaft. The results of the analysis of the field data will be used to develop rational criteria for the design of drilled shafts that support precast panel retaining walls. The procedure used in conducting the study was:

1. Design and construct a reaction and loading system capable of applying large magnitude lateral loads to large diameter drilled shafts.
2. Construct a large diameter instrumented drilled shaft.
3. Test the shaft by applying lateral loads.
4. Obtain undisturbed soil samples from the drilled shaft construction site and perform laboratory tests to evaluate the engineering properties of the soils.
5. Correlate the engineering properties of the soil and the results of the lateral load test with existing theories and procedures for the design of laterally loaded foundation members.

## DETERMINATION OF DRILLED SHAFT BEHAVIOR

The behavior of a drilled shaft subjected to lateral loads is to a large extent controlled by the flexural stiffness of the shaft relative to the stiffness of the surrounding soil. A deeply embedded shaft will exhibit elastic behavior while one of relatively shallow embedment will behave as a rigid member. As shown in Fig. 3, the load-deflection characteristics of a flexible shaft are quite different from those of a rigid shaft. The designer of the shaft therefore faces the problem of determining the relative flexibility of the proposed shaft before deciding whether to use elastic or rigid design procedures.

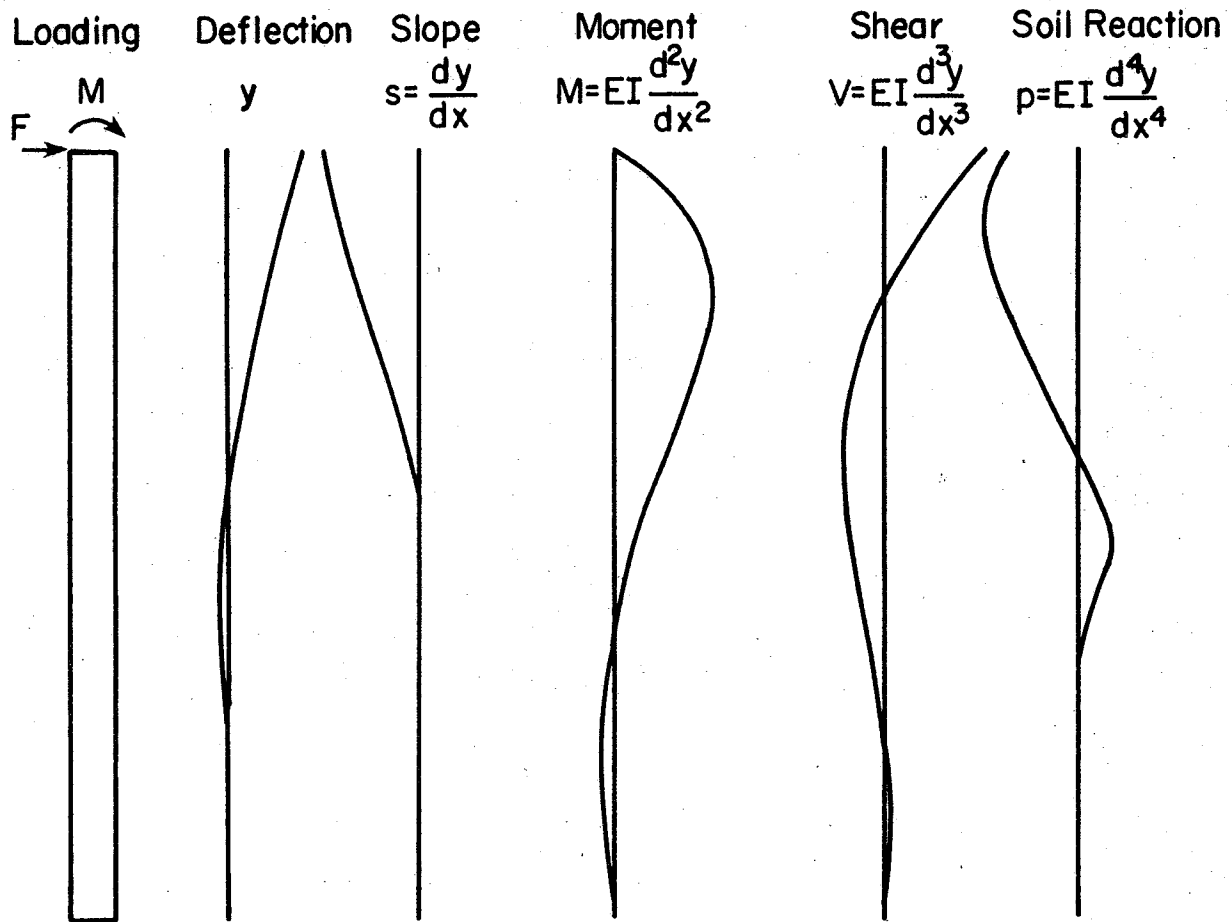
### Methods of Determining Drilled Shaft Behavior

A review of available literature produced two possible means of determining whether a shaft would behave as an elastic or rigid member under the influence of a lateral load. Both methods make use of the flexural stiffness of the shaft and the stiffness of the surrounding soil. Vesic (38) and Broms (5) have used a damping factor,  $\beta$ , while Matlock and Reese (23), Davisson and Gill (8), and Lytton (19) have made use of relative stiffness factors R and T. The expressions for  $\beta$ , R, and T are defined as follows:

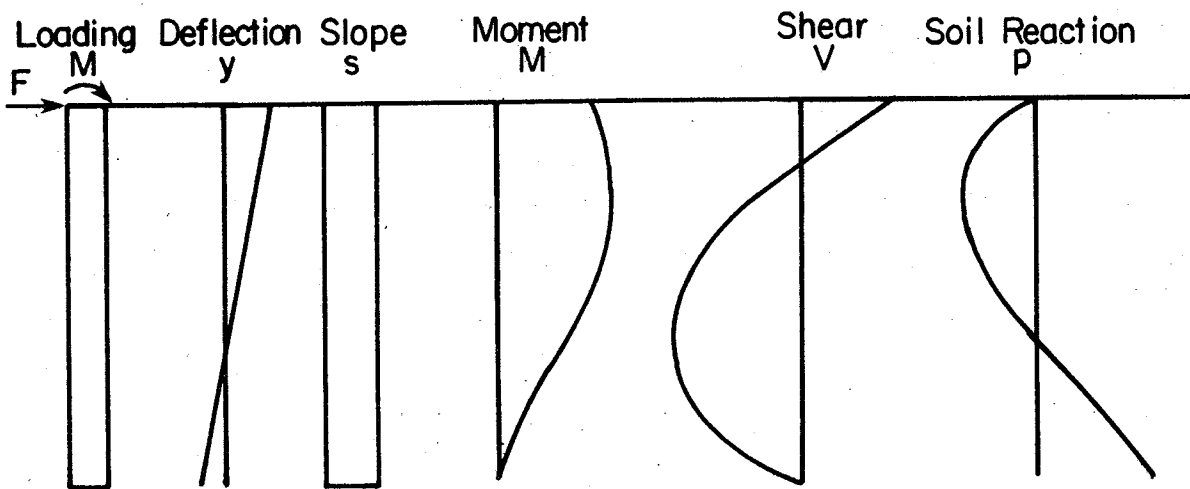
$$\beta = \sqrt[4]{\frac{E_s}{4EI}} \dots \dots \dots (1)$$

$$R = \sqrt[4]{\frac{EI}{E_s}} \dots \dots \dots (2)$$

$$T = \sqrt[5]{\frac{EI}{k}} \dots \dots \dots (3)$$



(a) Elastic Behavior of Flexible Drilled Shaft (After Welch and Reese-1972)  
 $F$ = Applied Lateral Load;  $M$ = Applied Moment;  $EI$ = Flexural Stiffness of Foundation;  $x$ = Depth Below Groundline



(b) Rigid Behavior of Non-Flexible Drilled Shaft ( $F$  and  $M$  same as in (a))

FIG. 3-Drilled Shaft Behavior

where:

$E$  = modulus of elasticity of foundation,

$I$  = moment of inertia of foundation,

$E_s$  = soil modulus, and

$k$  = constant of soil modulus variation.

The damping factor has been used in studies of beams on elastic foundations (38) and on piles subjected to lateral loads (5). The relative stiffness factors have been used on laterally loaded piles (23, 8) and drilled shafts (19). If the damping factor,  $\beta$ , is multiplied by the embedded depth,  $D$ , of the pile or shaft in question, the resulting damping factor product is a dimensionless expression indicating the relative stiffness of the structural member relative to the soil. Likewise, the relative stiffness ratio is obtained if the embedded depth is divided by the relative stiffness factor  $R$  or  $T$ . The results of previous work concerning relative stiffness are summarized in Table 1.

A close examination of the damping factor product,  $\beta D$ , and the relative stiffness ratio,  $D/R$ , indicates that the two expressions give similar results. A comparison of the two expressions for the maximum rigid relative stiffness of  $\beta D = 1.5$  and  $D/R = 2$  indicates a difference of approximately 6%. Likewise, a comparison of the minimum flexible relative stiffness of  $\beta D = 2.5$  and  $D/R = 4$  results in a difference of about 12%. Therefore, it may be concluded that it makes little difference whether the relative stiffness is determined by  $\beta D$  or  $D/R$ . However, for convenience, the expression  $D/R$  will be used for the remainder of the report.

Table 1. - Relative Stiffness of Laterally Loaded Piles or Shafts

$E_s$  = Soil Modulus;  $EI$  = Flexural Stiffness of Foundation;  
 $k$  = Constant of Soil Modulus Variation;  $D$  = Embedded Depth

$\beta = \sqrt[4]{\frac{E_s}{4EI}}$	
Damping Factor Product	Relative Stiffness
$\beta D < 1.5$	Rigid
$\beta D = 1.5 - 2.5$	Intermediate
$\beta D > 2.5$	Flexible
$R = \sqrt[4]{\frac{EI}{E_s}}$	
Relative Stiffness Ratio	Relative Stiffness
$D/R < 2$	Rigid
$D/R = 2 - 4$	Intermediate
$D/R > 4$	Flexible
$T = \sqrt[5]{\frac{EI}{k}}$	
Relative Stiffness Ratio	Relative Stiffness
$D/T < 2$	Rigid
$D/T = 2 - 4$	Intermediate
$D/T > 4$	Flexible

Discussion of Soil Parameters  $E_s$  and  $k$

Before the relative stiffness of a drilled shaft may be determined, either the value of the soil modulus,  $E_s$ , or constant of soil modulus variation,  $k$ , must be determined. The soil modulus is defined as:

$$E_s = - \frac{p}{y} \dots \dots \dots (4)$$

where  $p$  is the soil reaction expressed as force per unit length of shaft and  $y$  is the lateral deflection of the shaft. The negative sign indicates that the direction of the soil reaction is opposite to the direction of shaft deflection. As shown in Fig. 4a, the soil modulus,  $E_s$ , is the slope of a secant drawn from the origin to any point along the  $p$ - $y$  curve. Generally, the relation between soil reaction and shaft deflection is non-linear.

For most clay soils, the value of  $E_s$  increases with depth. According to Matlock and Reese (23) the principal reasons for this are ". . . (1) soils frequently increase in strength characteristics with depth as the result of overburden pressures and of natural deposition and consolidation processes and (2) pile deflections decrease with depth for any given loading, and the corresponding equivalent elastic moduli of soil reaction tend to increase with decreasing deflection." When this statement is considered along with the non-linearity of the  $p$ - $y$  curve, it is concluded that  $E_s$  is a function of both depth,  $x$ , and deflection,  $y$ .

Even though the relationship between lateral load, deflection, and soil modulus is a complicated one, for many practical problems reasonable results may be obtained by a simple assumption of the soil modulus variation with depth. If it is assumed that the soil modulus is a

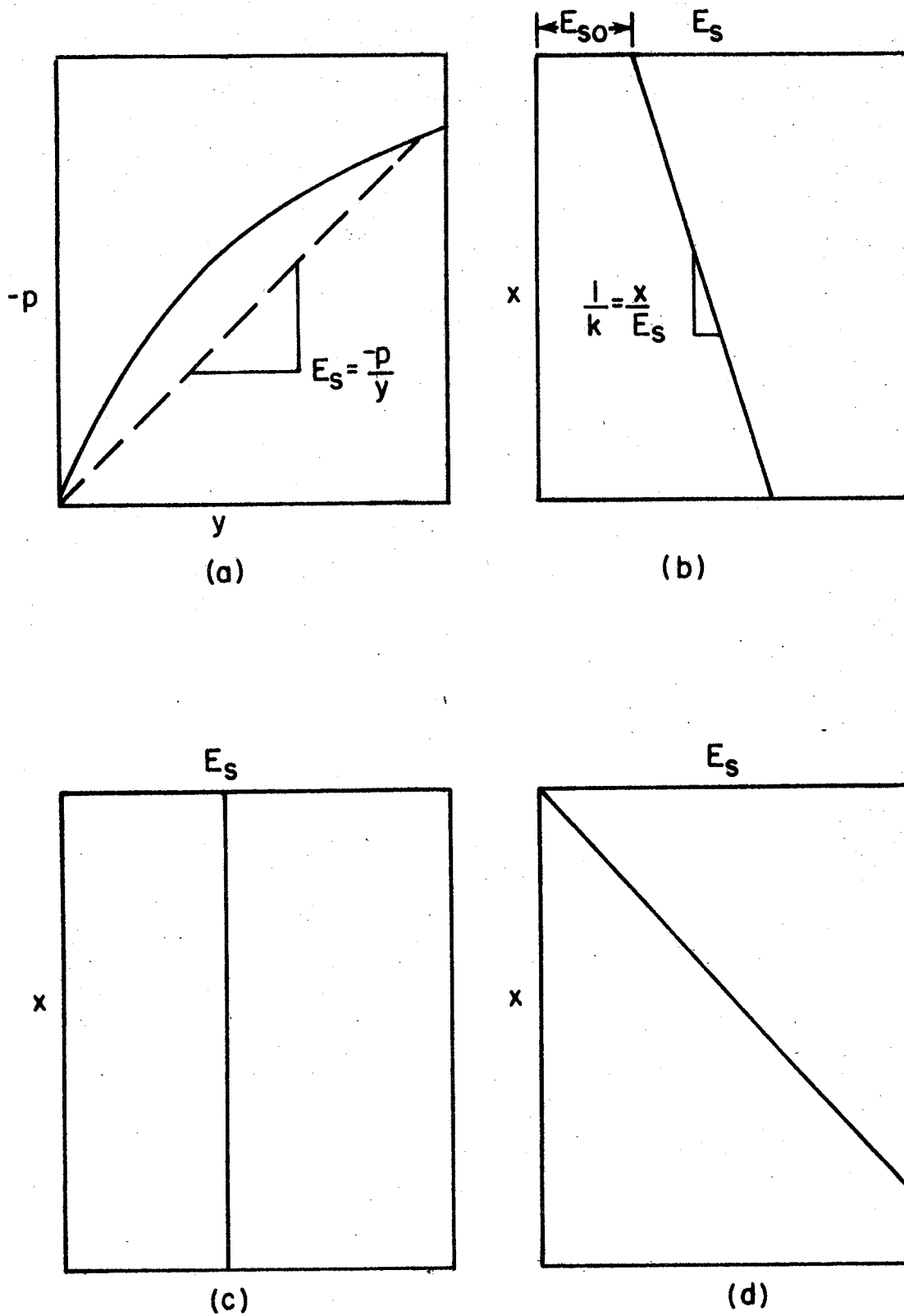


FIG. 4- Soil Modulus,  $E_s$ , and Variations with Depth  
 $p$  = Soil Reaction;  $y$  = Lateral Deflection;  $E_{s0}$  = Initial Modulus;  
 $x$  = Depth;  $k$  = Constant of Soil Modulus Variation

function of depth only, then  $E_s$  may be expressed as:

$$E_s = E_{s0} + kx \dots \dots \dots (5)$$

where  $E_{s0}$  is the initial value of the soil modulus and  $x$  is the depth. The term  $k$  has been defined in Eq. 3 (p. 10). Using this form to describe the variation of the soil modulus with depth,  $E_s$  may be represented in many ways as shown in Figs. 4b, 4c, and 4d.

#### Relative Stiffness of Drilled Shafts

To estimate the relative stiffness of drilled shafts by Eq. 2 and Table 1, it will first be necessary to evaluate  $E_s$ . For shafts embedded to relatively shallow depths in stiff overconsolidated clay,  $E_s$  may be obtained from the values of the coefficient of vertical subgrade reaction,  $k_s$ , given by Terzaghi (36). Terzaghi defined the coefficient of vertical subgrade reaction as:

$$k_s = \frac{q}{w} \dots \dots \dots (6)$$

where  $q$  is the pressure per unit area of contact surface of a loaded beam or slab and the subgrade on which it rests and  $w$  is the settlement produced by load application. The values suggested by Terzaghi are shown in Table 2.

Terzaghi proposed for laterally loaded piles in stiff clay a coefficient of horizontal subgrade reaction,  $k_h$ , be obtained as:

$$k_h = \frac{(1 \text{ ft}) k_s}{1.5B} \dots \dots \dots (7)$$

where  $B$  is the diameter of the pile and the values of  $k_s$  are obtained from Table 2. Values of  $E_s$  may be obtained from  $k_h$  as follows:

$$E_s = Bk_h \dots \dots \dots (8)$$

Table 2. Values of  $k_s$ , in tons/cu ft for Square Plates, 1 ft x 1 ft, Resting on Pre-Compressed Clay. After Terzaghi (1955)  
 $q_u$  = Unconfined Compressive Strength  
 $k_s$  = Coefficient of Vertical Subgrade Reaction

Consistency of Clay	Stiff	Very Stiff	Hard
Values of $q_u$ , tons/sq ft	1 - 2	2 - 4	>4
Range of $k_s$ , square plates	50 - 100	100 - 200	>200
Proposed Values, square plates	75	150	300

Note: 1 ton/sq ft = 95.8 kN/m<sup>2</sup>

therefore

$$E_s = B \cdot \frac{(1 \text{ ft})(k_s)}{1.5B}$$

and

$$E_s = \frac{(1 \text{ ft})(k_s)}{1.5} \dots \dots \dots (9)$$

Eq. 9 may be used to evaluate  $E_s$  when it is assumed that the soil modulus is constant with depth as shown in Fig. 4c. The assumption of a constant soil modulus is probably not bad for shallow drilled shafts in stiff overconsolidated clay.

Using the extreme values of 50 and 200 tcf (15,700 to 62,800 kN/m<sup>3</sup>) given for  $k_s$  in Table 2, values of 33 and 133 tsf (3161 to 12,741 kN/m<sup>2</sup>) were obtained for  $E_s$  by Eq. 9. In order to evaluate shaft flexibility and rigidity for this range of  $E_s$  values, a plot was made of shaft depth

over diameter,  $D/B$ , versus relative stiffness ratio,  $D/R$ . The results are presented in Fig. 5. In the calculation of the relative stiffness factor,  $R$ , the modulus of elasticity,  $E$ , was assumed to be  $3 \times 10^6$  psi ( $2.07 \times 10^7$  kN/m<sup>2</sup>). The embedded depth,  $D$ , was obtained by multiplying a quantity  $D/B$  by a foundation diameter,  $B$ . The moment of inertia term,  $I$ , in the expression for  $R$  contains the quantity  $B^4$  which is consequently brought outside the radical term. The diameter terms,  $B$ , in the numerator and denominator then divide out, making the relationship in Fig. 5 independent of  $B$ . It should also be noted that the  $D/B$  and  $D/R$  relationship is linear.

The variation of soil modulus with depth for normally consolidated clay is probably similar to that shown in Figs. 4b or 4d. Consequently, in order to evaluate the relative stiffness of a drilled shaft in normally consolidated clay, a value of  $k$  for use in Eq. 3 will have to be determined. For the case of a drilled shaft in normally consolidated clay, the extreme values of 0.75 and 20 tcf ( $235.5$  to  $6280$  kN/m<sup>3</sup>) recommended by Bowles (2) for the constant of soil modulus variation,  $k$ , were used to evaluate the relative stiffness factor,  $T$ . As shown in Fig. 6, the shaft depth over diameter ratio,  $D/B$ , is again plotted versus the relative stiffness ratio,  $D/T$ . The modulus of elasticity was assumed to be  $3 \times 10^6$  psi ( $2.07 \times 10^7$  kN/m<sup>2</sup>). The relationship between  $D/B$  and  $D/T$  is linear but in this case it is dependent on the shaft diameter,  $B$ , since the expression for  $T$  contains the fifth root of  $B^4$ .

Table 1 indicates that foundations with relative stiffness ratios,  $D/R$  or  $D/T$ , less than 2 will behave as rigid members. Entering Figs. 5 and 6 at this value with the minimum values of 33 tsf ( $3161$  kN/m<sup>2</sup>) for  $E_s$  and 0.75 tcf ( $235.5$  kN/m<sup>3</sup>) for  $k$ , values of  $D/B$  of about 8.5 to 10

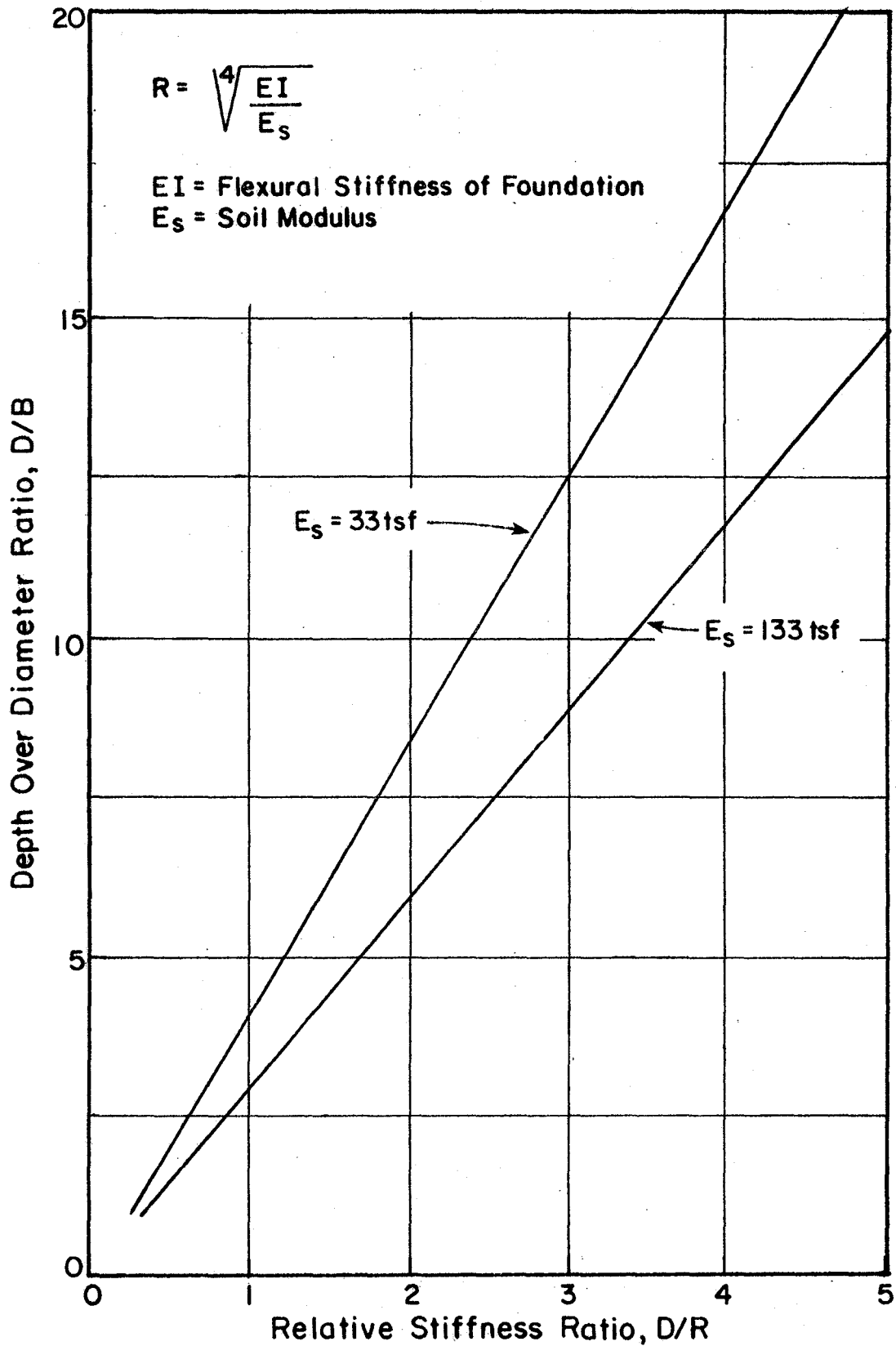


FIG. 5— Relative Stiffness Ratio, D/R, With Constant Soil Modulus, Es; 1 tsf = 95.8 kN/m<sup>2</sup>

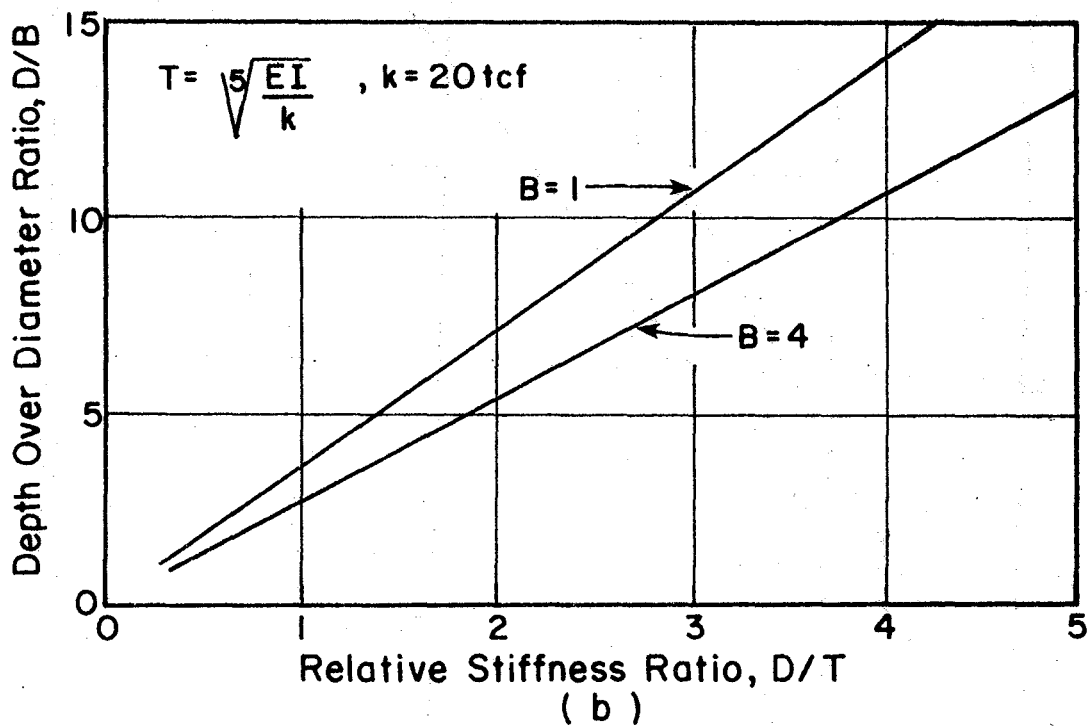
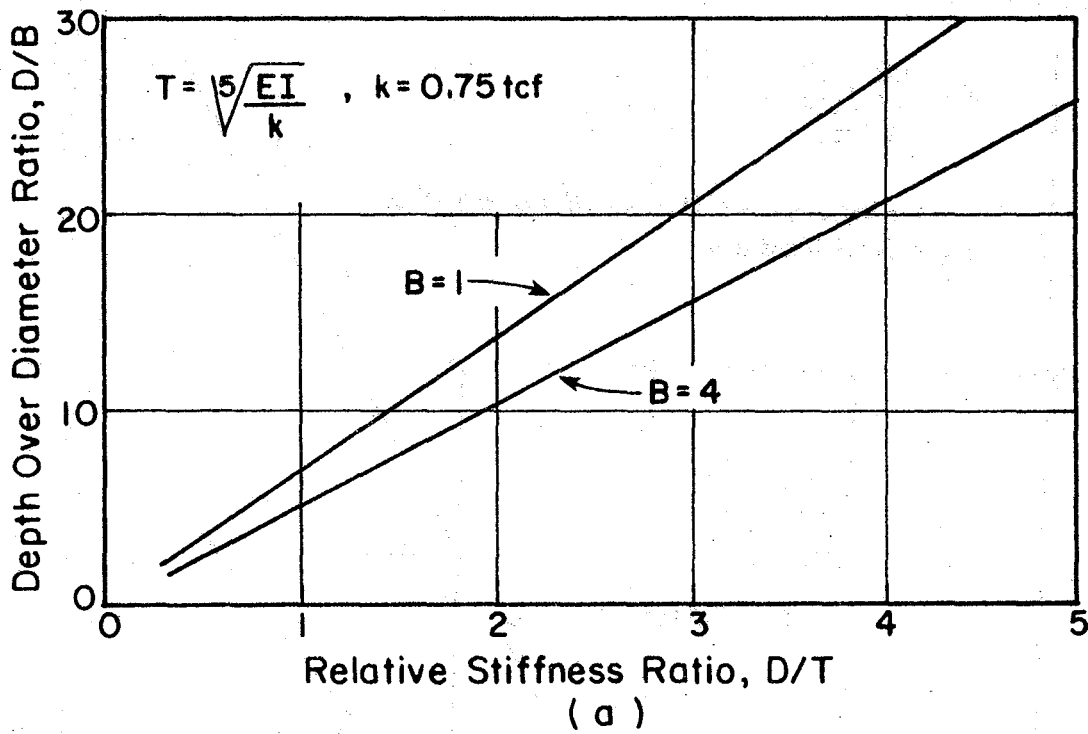


FIG. 6 - Relative Stiffness Ratio,  $D/T$ , With Constant Soil Modulus Variation,  $k$ ;  $EI$  = Flexural Stiffness of Foundation,  $B$  = Foundation Diameter,  $1 \text{ tcf} = 314 \text{ kN/m}^3$

are indicated if rigid behavior is to be insured. Using the maximum values of 133 tsf ( $12,741 \text{ kN/m}^2$ ) for  $E_s$  and 20 tcf ( $6280 \text{ kN/m}^3$ ) for  $k$  with the relative stiffness ratio of 2, values of  $D/B$  of about 6 and 5.5 result. Therefore, under some conditions, a foundation can have a  $D/B$  ratio as high as 10 and still behave as a rigid member. However, in order to insure rigid behavior, the  $D/B$  ratio should be limited to about 6.

Table 1 also indicates that foundations will behave as flexible members if they have relative stiffness ratios greater than 4. Entering Figs. 5 and 6 with a relative stiffness ratio of 4 and using the minimum values of  $E_s$  and  $k$ ,  $D/B$  values of approximately 17 to 27 are indicated for flexible behavior. Using the maximum values of  $E_s$  and  $k$ ,  $D/B$  values of about 10.5 to 14 result. Consequently, flexible foundation behavior will result in some cases with a  $D/B$  ratio as low as about 10.5, but to insure flexible behavior the  $D/B$  ratio should be in excess of 20.

## ANALYSIS OF ELASTIC BEHAVIOR OF LATERALLY LOADED CYLINDRICAL FOUNDATIONS

Several methods of analyzing the elastic behavior of laterally loaded cylindrical foundations are currently in use. A brief review of some of these methods will be presented herein.

### Solutions Assuming the Winkler Model

The behavior of a laterally loaded pile or drilled shaft is closely related to the behavior of a beam on an elastic foundation. However, the laterally loaded foundation element is a more specialized case in the sense that all forces and moments are applied at the top of the pile or shaft, while a beam may be loaded at many points. A complete solution of the beam-on-elastic-foundation problem yields values of deflection, slope, moment, shear, and soil reaction at all points along the beam.

The problem of the laterally loaded pile or drilled shaft may be approached by making the assumption that the soil acts as a series of closely spaced discrete springs. This implies that there is no coupling of adjacent soil elements and the soil deforms only under the loaded area. This approach is attributed to E. Winkler in 1867 (40). The differential equation governing the laterally loaded flexible foundation problem is expressed as:

$$EI \frac{d^4 y}{dx^4} + P_x \frac{d^2 y}{dx^2} - p = 0; \text{ where } p = - E_s y \dots \dots \dots (10)$$

$P_x$  is the axial load on the foundation and  $x$  is the depth below the groundline. The terms  $E$ ,  $I$ , and  $E_s$  have been defined in Eqs. 1 - 3 (p. 10) while  $p$  and  $y$  have been defined in Eq. 4 (p. 14).

Eq. 10 may be readily solved if an expression for the soil modulus,

$E_s$ , can be found. The soil modulus may be estimated as a function of depth or a series of p-y curves may be predicted to describe the  $E_s$  variation. Solving Eq. 10 will yield the lateral deflection for any load capable of being sustained by the foundation. Successive differentiation of the lateral deflection will yield slope, bending moment, shear, and soil reaction (29).

Matlock and Reese (23) have presented a method by which non-dimensional solutions for Eq. 10 may be computed for any desired variation of soil modulus with respect to depth. The soil modulus variation may be expressed as a power form ( $E_s = kx^n$ ) or as a polynomial form ( $E_s = k_0 + k_1x + k_2x^2$ ). In this method a soil modulus variation is selected and the problem solutions are determined through the use of non-dimensional coefficients. The soil modulus variation is then adjusted in a series of repetitive trials until satisfactory compatibility is obtained between the soil modulus function and the problem solutions.

The best representation of the soil modulus variation is a numerical description of the soil modulus presented as a set of curves showing the soil reaction, p, as a function of deflection, y. The soil modulus,  $E_s$ , has been defined through the use of p and y in Eq. 4. Reese (29) offers a further explanation of the p-y concept:

Fig. 7(a) shows a section through a deep foundation at some depth  $x_j$  below the ground surface. Fig 7(b) shows a possible stress distribution in the soil around the foundation, after it has been installed and before it has been loaded laterally. The deflection of the foundation through a distance,  $y_j$ , as shown in Fig. 7(c) generates unbalanced soil stresses, possibly as indicated in the figure. Integration of the soil stresses yields an unbalanced force,  $p_j$ , per unit of length of pile.



If the decision is made to describe the soil modulus variation through the use of p-y curves, it will then be necessary to predict a set of p-y curves, such as those shown in Fig. 8, in order for Eq. 10 to be solved. Eq. 10 is normally expressed in finite difference form and solved by digital computer. Computer programs for its solution are readily available (29).

Methods of predicting p-y curves are also readily available. The use of p-y curves for the laterally loaded pile problem was first proposed by McClelland and Focht in 1956 (20). Since that time studies conducted on laterally loaded piles have resulted in methods for prediction of p-y curves in soft clay (22), in stiff clay (31), and in sand (30). A p-y curve prediction method has also resulted from the lateral load testing of a drilled shaft (39).

#### Solution Assuming Elastic Continuum

Some writers have expressed the opinion that the Winkler assumption of soil behavior is unsatisfactory because the continuity of the soil mass is not taken into account (34, 27). These investigations feel that a more satisfactory analysis would be achieved if the soil were assumed to be an elastic continuum.

Poulos (27) has presented a method in which the soil is assumed to be an ideal, elastic, homogeneous, isotropic mass, having constant elastic parameters of soil modulus,  $E_s$ , and Poisson's ratio,  $\nu_s$ . The pile is assumed to be a thin rectangular vertical strip of width,  $d$ , length  $L$ , and constant flexibility,  $EI$ . Deflections, rotations, and moments may be determined through the use of dimensionless influence factors. A comparison is made between solutions obtained using the elastic continuum

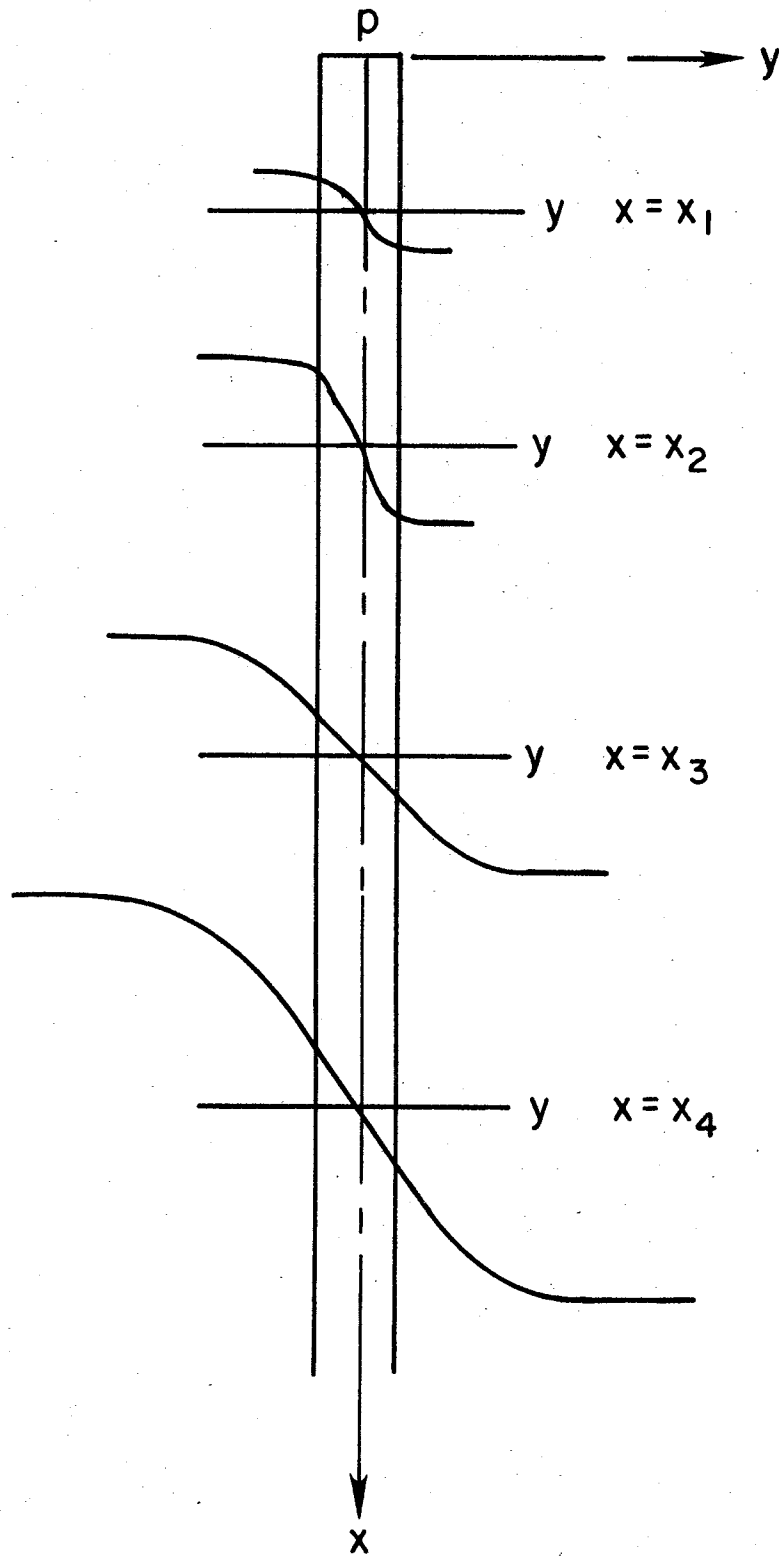


FIG. 8— Set of  $p$ - $y$  Curves (After Reese—1977)  
 $p$ = Soil Reaction,  $x$ = Depth Below Groundline,  
 $y$ = Lateral Deflection

model and the Winkler model. Solutions obtained from the Winkler model are shown to be the more conservative of the two.

Poulos states that the quantity of primary importance in the solution of the problem is the soil modulus,  $E_s$ . According to Poulos if an accurate value of  $E_s$  is desired, a field load test should be conducted so that  $E_s$  may be backfigured from the results. If this is not possible estimated values of  $E_s$  will have to be used.

#### Method by Broms

Broms (5) has presented methods for the calculation of deflections, ultimate lateral resistances, and maximum bending moments for laterally loaded piles. Non-dimensional charts are included for quick determination of these items. The lateral deflection calculations utilize the concept of a coefficient of subgrade reaction. Methods for the evaluation of the coefficient are presented. The ultimate lateral resistance of laterally loaded piles is based on the assumption that the piles fail through the formation of plastic hinges. The failure occurs when a plastic hinge forms at the location of the maximum bending moment. Calculated deflections and maximum bending moments were compared to available test data. Fairly good agreement was found between the measured and calculated values.

#### Finite-Element Method

Bowles (3) has proposed a finite-element solution of the laterally loaded foundation problem. Bowles has a favorable opinion of the finite-difference method using the Winkler model for the solution of the beam-on-elastic-foundation problem and has presented this method in the past

(2). However, Bowles feels that the finite-difference solution has several disadvantages:

1. It is troublesome to account for general boundary conditions because of the formulation of the coefficient matrix.
2. It is difficult to correct for negative deflections, i.e., eliminating the Winkler springs when the footing tends to separate from the soil foundation.
3. It is fairly difficult to write a computer program to generate a general coefficient matrix.
4. It is extremely difficult to account for different load conditions.
5. It is difficult to account for non-linear soil deformation.

According to Bowles, the finite-element method proposed is somewhat similar to the finite-difference solution but eliminates the five major difficulties just cited. Agreement between computed and measured data is reasonable for the cases cited.

## ANALYSIS OF RIGID BEHAVIOR OF LATERALLY LOADED CYLINDRICAL FOUNDATIONS

Several methods for the analysis of rigid laterally loaded cylindrical foundations have been presented during the last several years. This section presents a brief review of some of these methods.

### Soil Pressure Distribution

In 1932 Seiler (32) presented the soil pressure distribution shown in Fig. 9. Seiler's pressure distribution was confirmed by Rutledge (26) and by Shilts, Graves, and Driscoll(33). Later tests by Osterberg (25) also gave further confirmation of the assumed pressure distribution. Seiler used the distribution to develop design charts for the embedment depth of standard timber poles and Rutledge developed an embedment chart for the Outdoor Advertising Association of America, Inc.

### Rankine Passive Pressure

Ivey and Hawkins (17) proposed a method to calculate the embedment depth of drilled shafts of specified diameter for the support of sign structures. They used Rankine's passive earth pressure formula (37) along with the soil pressure distribution presented by Seiler. The Rankine formula is based on the assumption of the horizontal movement of an infinitely long frictionless wall into the soil. In reality, the tilting of a cylindrical foundation element is resisted by friction along the two planes which pass tangent to the sides of the foundation and parallel to the plane of tilting. Normal and tangential forces are also developed at the bottom of the footing. Use of the Rankine formula also implies that the soil is in a state of plastic equilibrium, that is, on the verge of failure. The presence of friction and the non-fulfillment

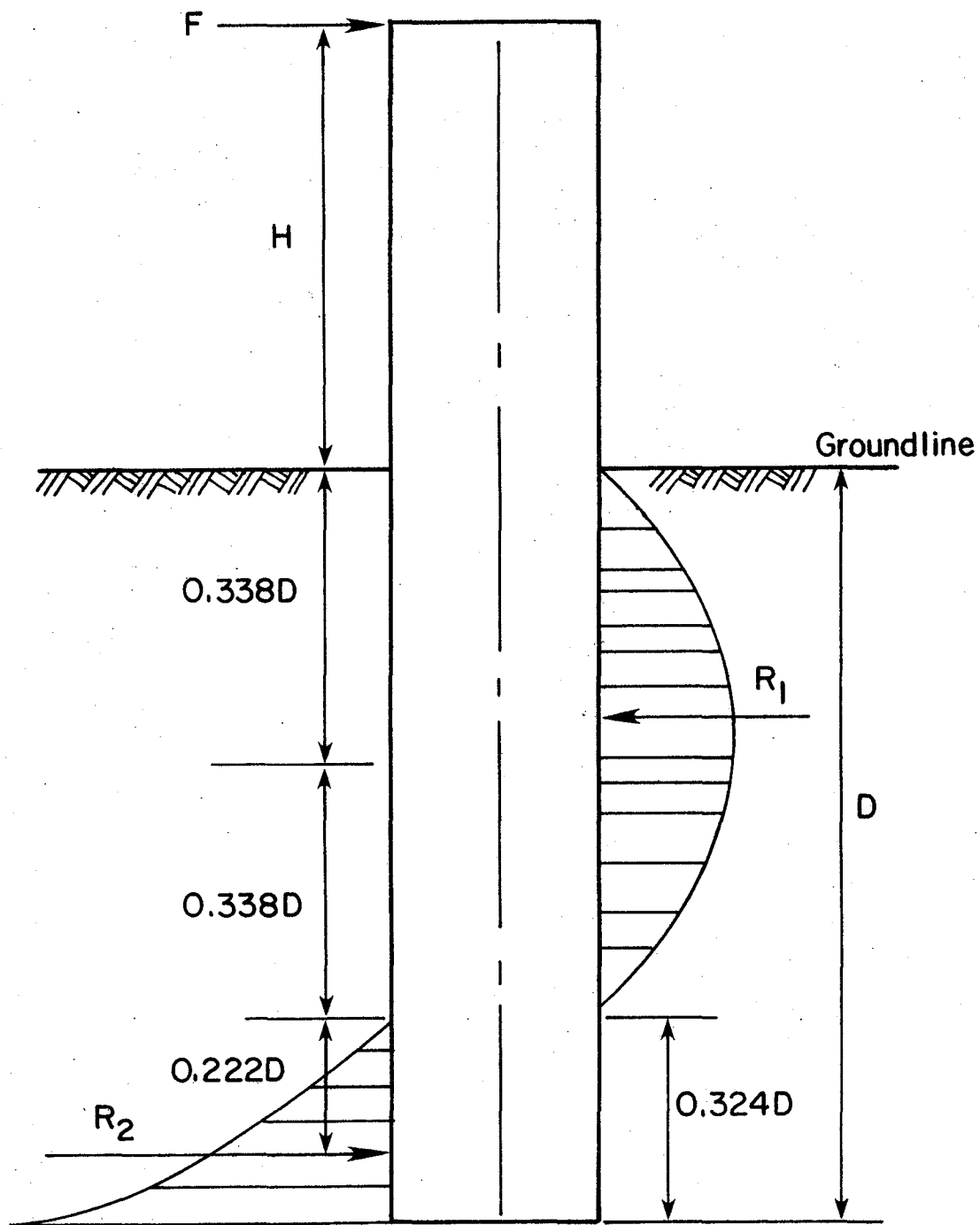


FIG. 9 — Soil Pressure Distribution (After Seiler)  
 F = Lateral Load; H = Height of Load Application;  
 D = Embedded Depth of Foundation;  $R_1$  = Top Resultant Force;  
 $R_2$  = Bottom Resultant Force

of the plastic equilibrium state results in a very conservative solution. The need for research to refine the design procedure to a more rational one was recognized by Ivey and Hawkins.

#### Texas A&M University Research

Ivey et al. (15, 16, 18) working at Texas A&M University developed a procedure for determining the ultimate resistance of drilled shaft foundations subjected to lateral loads. As shown in Fig. 10, the analysis takes into account all shear forces acting on the shaft. This includes the shear forces in the horizontal direction along the sides of the shaft, the shear forces in the vertical direction along the sides of the shaft, and the shear forces in the horizontal direction developed beneath the shaft. Consequently, the solution is a three dimensional analysis of the laterally loaded drilled shaft problem.

A part of the theoretical analysis presented in the first research report (15) included the use of Rankine earth pressure coefficients with the realization that the Rankine assumptions are not satisfied for the problem at hand. In the second part of the research study (18), model tests on laboratory rigid shafts were conducted with the results being correlated with the theoretical analysis. As a result of the model tests, a modifying factor for the Rankine coefficients of passive and active earth pressure was introduced. The ultimate load of each model test was then calculated and compared with the results of the tests. The new semi-empirical method proved to be slightly unconservative by overpredicting ultimate loads. The ultimate loads were overpredicted by about 2% for the cohesive soils and by approximately 13% for the cohesionless soils. If the conventional theory as presented by Ivey and Hawkins in 1966 (17)

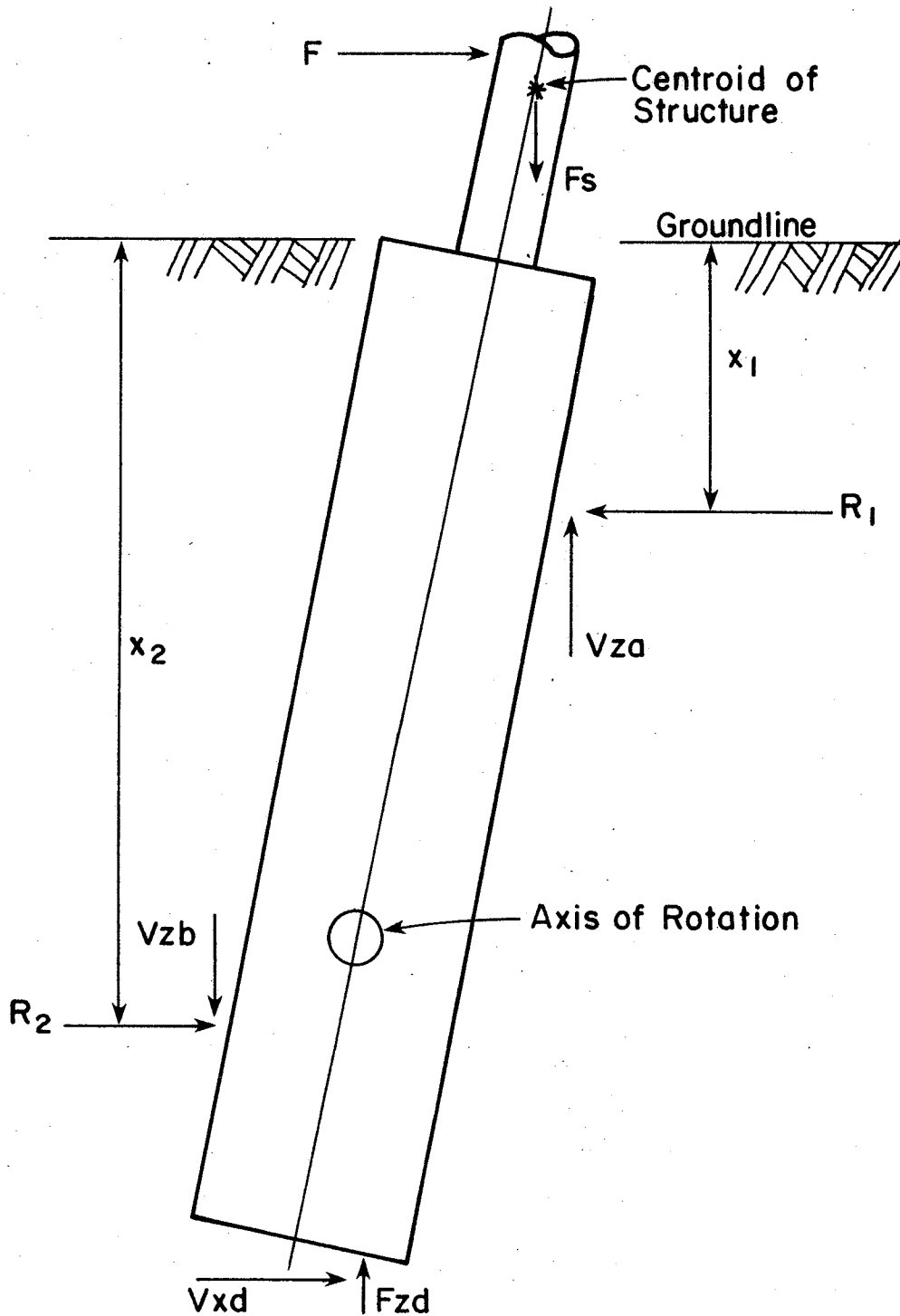


FIG. 10— Forces Developed By Overturning Load (After Ivey)  
 $F$  = Lateral Load;  $F_s$  = Weight of Structure and Footing;  $x_1$  = Depth to  $R_1$ ;  
 $x_2$  = Depth to  $R_2$ ;  $R_1$  = Top Resultant Force;  $R_2$  = Bottom Resultant Force;  
 $V_{za}$  = Top Verticle Shear Force;  $V_{zb}$  = Bottom Verticle Shear Force;  $V_{xd}$  =  
Horizontal Shear Force Beneath Foundation;  $F_{zd}$  = Verticle Force  
Beneath Foundation.

is used, the ultimate loads for the cohesionless and cohesive soils were underpredicted by an average of approximately 450% and 78% respectively, thus confirming the highly conservative nature of that particular method. The ultimate load for most of the models corresponded to a foundation rotation of  $5^{\circ}$ .

The third report of the research project presented the results of lateral load tests on three full-scale drilled shafts (16). The ultimate loads were calculated using the new semi-empirical method and compared to the results obtained from the load tests. The drilled shafts were 2 ft (0.610 m) in diameter and 6 ft (1.829 m) deep. The first test was performed in sand (Navasota) and resulted in an observed load 7% below the analytical prediction. The second test was conducted at a site (Galveston) consisting of soft to firm clay with a thin upper crust of very stiff clay. The observed load was 91% higher than the predicted load. The site (Bryan) for the third test consisted of very stiff clay. For this test the actual load was 18% below the calculated value. The authors noted that even though the observed ultimate load was lower than the predicted load at the failure rotation of  $5^{\circ}$  in two of the three cases, the predicted load was conservative up to a rotation of  $3^{\circ}$  in all three cases.

#### University of Florida Research

Hays et al. (13) studied two methods of solution for the rigid pile or drilled shaft problem. The first was a discrete element solution utilizing the Winkler assumption and p-y curves. A solution of the problem using the discrete element method results in values of deflection, shear, bending moment, soil reaction, and rotation. It was noted from

solutions obtained with this method that the rotation point of rigid foundations varies along the shaft length at the ultimate load for different soils. It was also noted that as the ultimate load was approached the soil resistance along most of the foundation length increased to essentially its ultimate value similar to that shown in Fig. 11. However, this observation assumed that premature material failure did not occur and that the p-y curves experienced continued deflection at the maximum value of soil reaction. The second solution method, termed the maximum load solution, resulted from these observations.

The assumed soil resistance distribution at failure for cohesive soils is shown in Fig. 11. It is assumed that the soil resistance is at its maximum value along the whole length of the pile, even though the maximum resistance will never be reached around the rotation point. The soil is assumed to be homogeneous and the ultimate soil resistance varies linearly with depth. Using this assumed distribution the applied lateral load and moment were solved for in terms of the soil parameters and unknown distance to the rotation point. Design charts are presented to expedite the solution. The solution is an iterative process involving the selection of trial embedment depths.

In order to determine how the maximum load solution compared with actual data, the method was used to calculate the ultimate loads for the model tests conducted at Texas A&M. The ultimate load was under-predicted by an average of 76% for the cohesionless soil and by an average of 42% for the cohesive soil. The maximum load solution was also used to calculate the ultimate loads for the full-scale tests conducted at Texas A&M. Using this method, the ultimate load for the Navasota test in sand was underpredicted by 165%. The calculated ultimate load for the

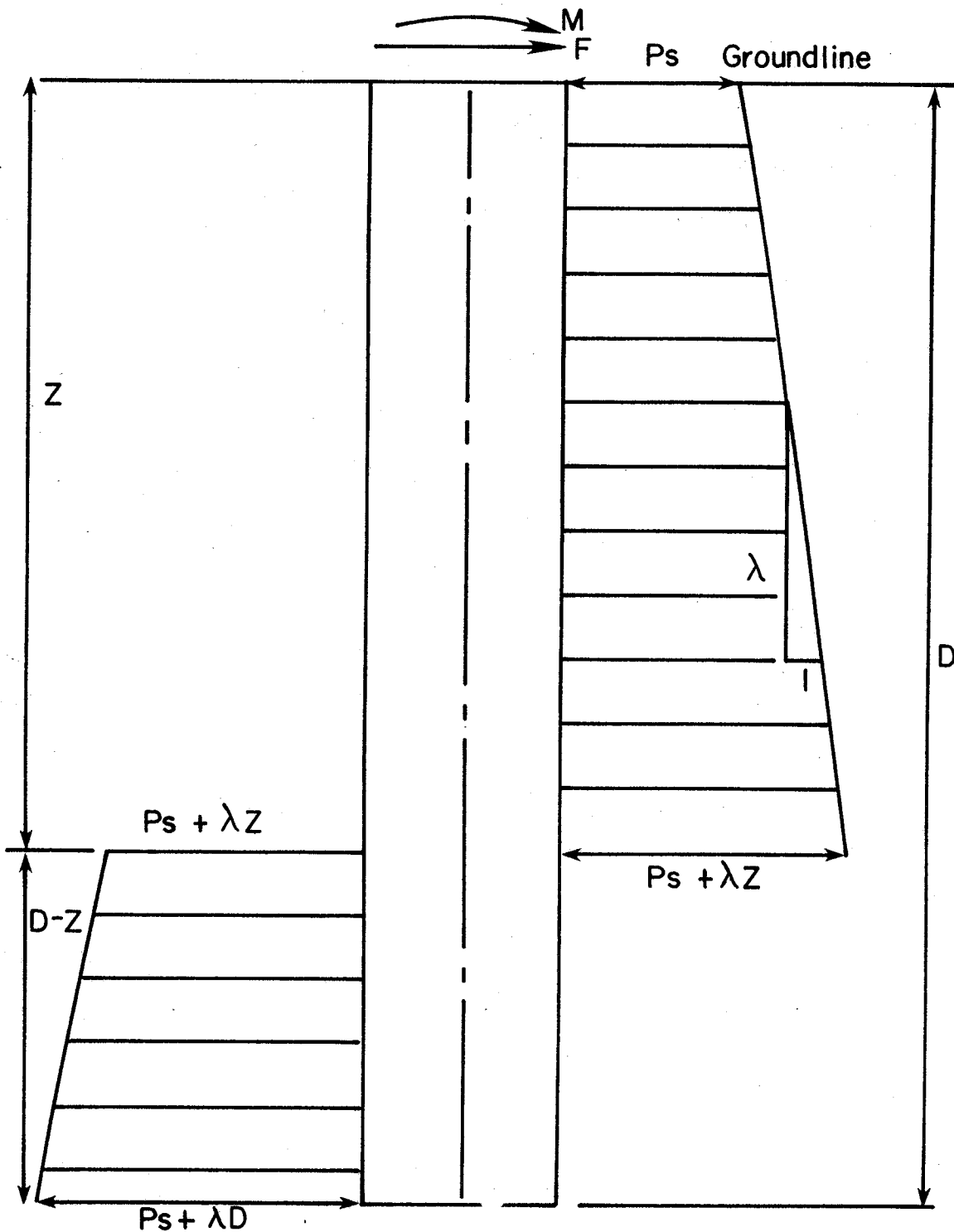


FIG. 11— Ultimate Lateral Soil Resistance For Cohesive Soils (After Hays et al.);  $F$  = Lateral Load;  $Z$  = Distance to Rotation Point;  $M$  = Moment;  $D$  = Embedded Depth;  $P_s$  = Ultimate Soil Resistance at Groundline;  $\lambda$  = Slope of Soil Resistance Diagram

Galveston test in soft clay was 211% under the actual observed load. A comparison of the calculated and observed ultimate loads for the Bryan test in very stiff clay resulted in an underprediction of 41%. Therefore, the maximum load solution appears to give consistently conservative results.

#### Method by Broms

In addition to his work on laterally loaded flexible foundations, Broms (5) has also studied the case of short, rigid piles. The design procedure he presents for cohesive soils is based on the soil resistance distribution shown in Fig. 12. The ultimate lateral soil reaction,  $p_u$ , is calculated as follows:

$$p_u = 9C_u B \dots\dots\dots (11)$$

where  $C_u$  is the undrained cohesive shear strength of the soil and  $B$  is the pile diameter. The resistance for 1.5 times the pile diameter below the ground surface is neglected. The soil is also assumed to be homogeneous and isotropic. Deflections, embedment depths, and maximum bending moments may be solved for through the use of dimensionless design charts.

#### Method by Hansen

Hansen's (12) method for the design of rigid foundations is based on a calculated earth pressure coefficient,  $K_c$ . The term  $K_c$  has been derived from the bearing capacity factor,  $N_c$ , and is presented graphically.  $K_c$ , plotted as a function of  $D/B$ , varies from 2.55 to 8.14. The ultimate lateral soil reaction,  $p_u$ , is calculated as:

$$p_u = K_c C_u B \dots\dots\dots (12)$$

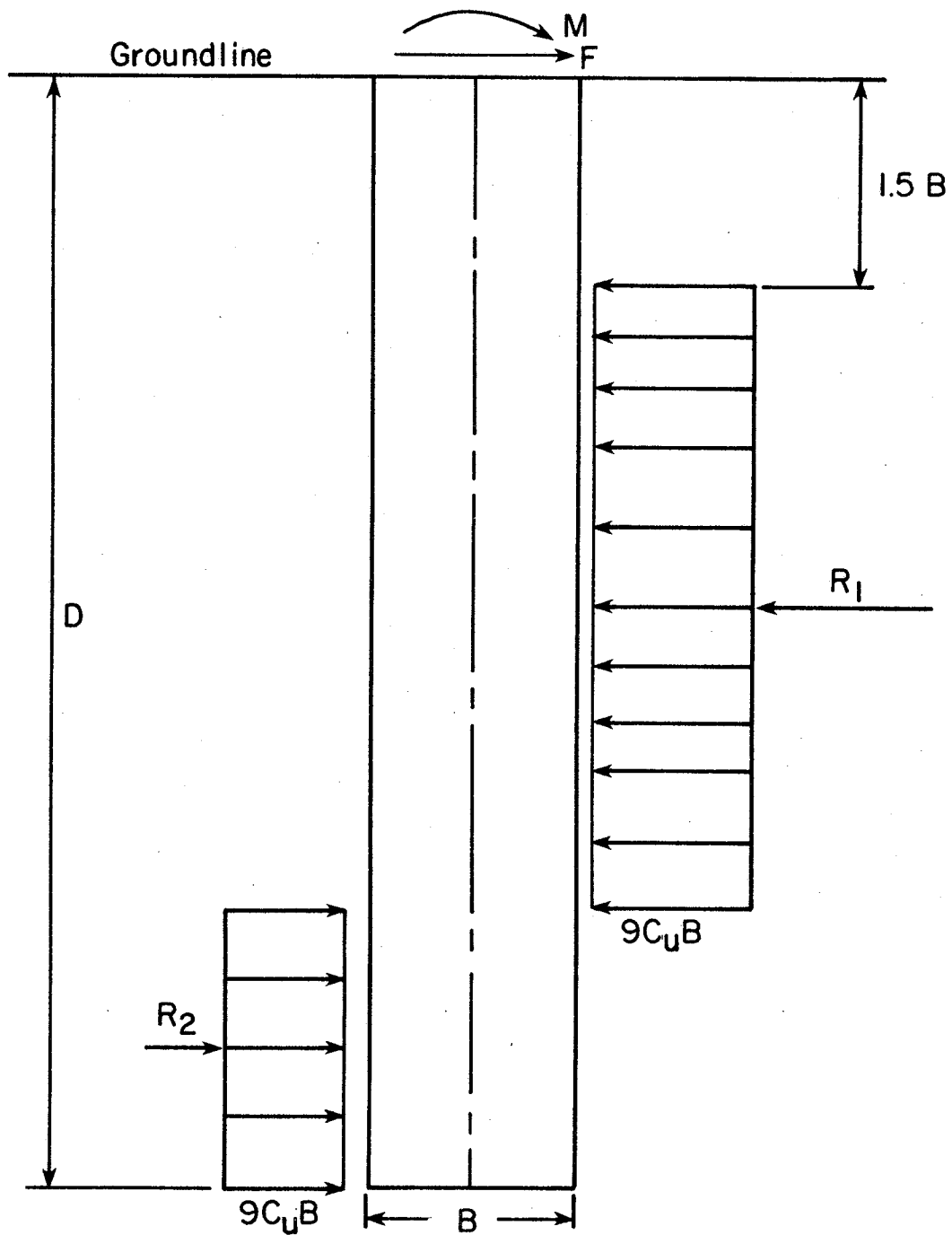


FIG. 12 - Ultimate Lateral Soil Resistance for Cohesive Soils According to Broms;  $F$ = Lateral Load;  $M$ = Moment;  $B$ =Diameter;  $D$ = Embedded Depth;  $C_u$ = Undrained Cohesive Shear Strength;  $R_1$ = Top Resultant Force;  $R_2$  = Bottom Resultant Force

where  $C_u$  and  $B$  are the same as defined in Eq. 11. The ultimate lateral resistance distribution is shown in Fig. 13. The solution is an iterative process involving the summation of moments about an assumed rotation point.

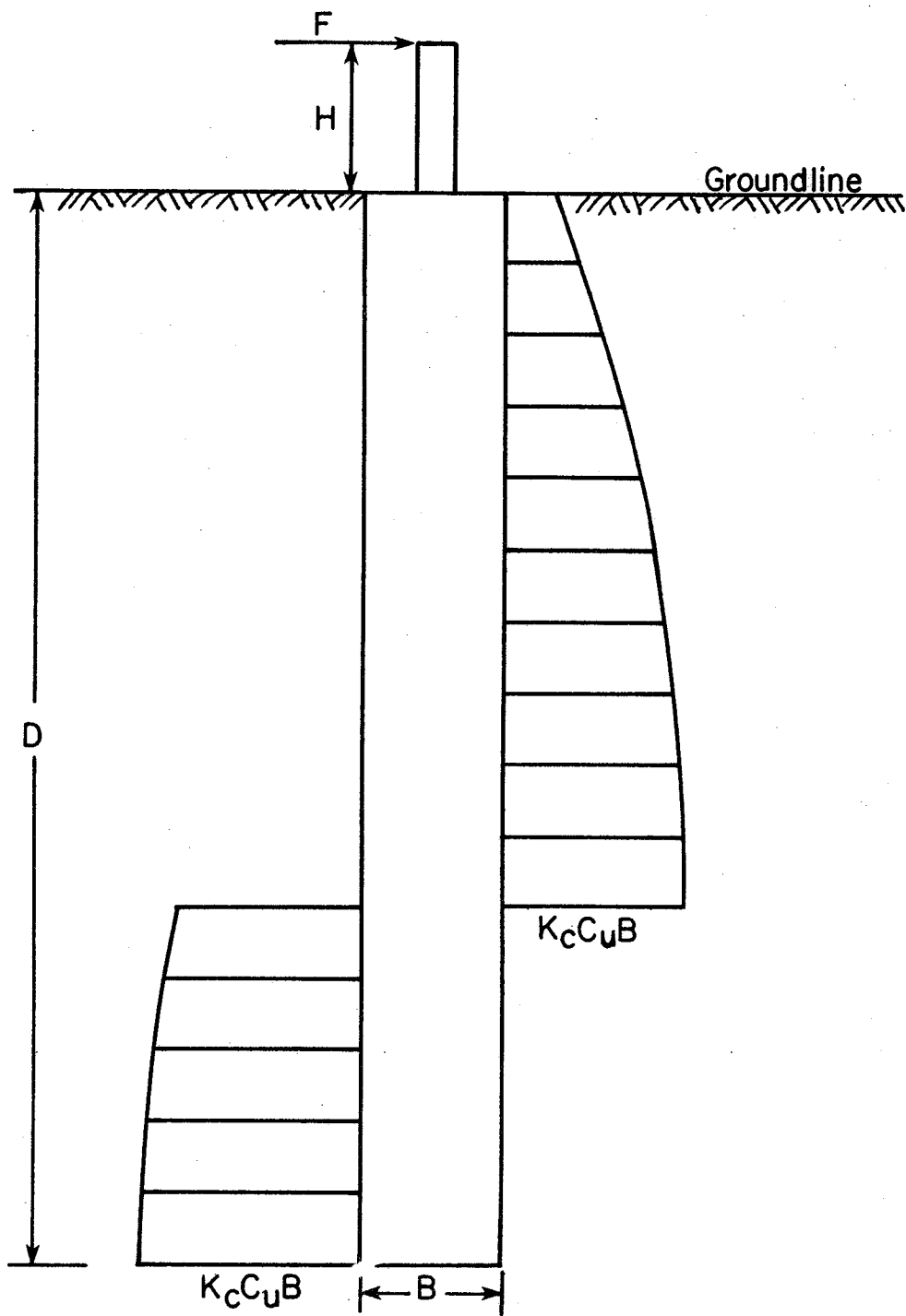


FIG. 13- Hansen's Ultimate Lateral Soil Resistance  
 $F$ = Lateral Load;  $H$ = Height of Lateral Load Application;  
 $D$ = Embedment Depth;  $K_c$ = Earth Pressure Coefficient;  
 $C_u$ = Undrained Cohesive Shear Strength;  $B$ = Diameter

## FIELD LOAD TEST

As stated earlier, the objective of this research study is to conduct lateral load tests on instrumented drilled shafts in order to collect field data for use in the development of rational design criteria. For this first year of study it was decided that a shaft embedded entirely in clay would be tested. A suitable test site was found at the southwest end of the northeast-southwest runway on the Texas A&M University Research and Extension Center.

### Soil Conditions

Soil conditions at the test site were investigated with three soil borings and one Texas Cone Penetrometer (TCP) Test. The soil borings were drilled on January 7, 1977, March 15, 1977, and July 26, 1977. The boring locations, designated B-S1, B-S2, and B-S3, are shown in Fig. 14. Undisturbed soil samples were taken with a 1.5 in. (3.81 cm) thin-wall tube sampler. The TCP Test was conducted with a drilling rig furnished by the SDHPT on March 9, 1977. The location of the TCP Test, designated TCP-1, is also shown in Fig. 14.

Laboratory tests on the undisturbed samples included Atterberg limits, moisture contents, and unit weights. The undrained cohesive shear strength,  $C_u$ , of the samples was determined by unconfined compression tests and miniature vane tests. The results of the tests are plotted on the boring logs presented in Figs. 15, 16, and 17. The test results indicated that the soil conditions in the immediate area of the borings were fairly uniform. The site consisted of stiff to very stiff clay with an average undrained cohesive shear strength of about 1.3 tsf ( $124.5 \text{ kN/m}^2$ ). The clay to a depth of approximately 5 ft (1.52 m) was

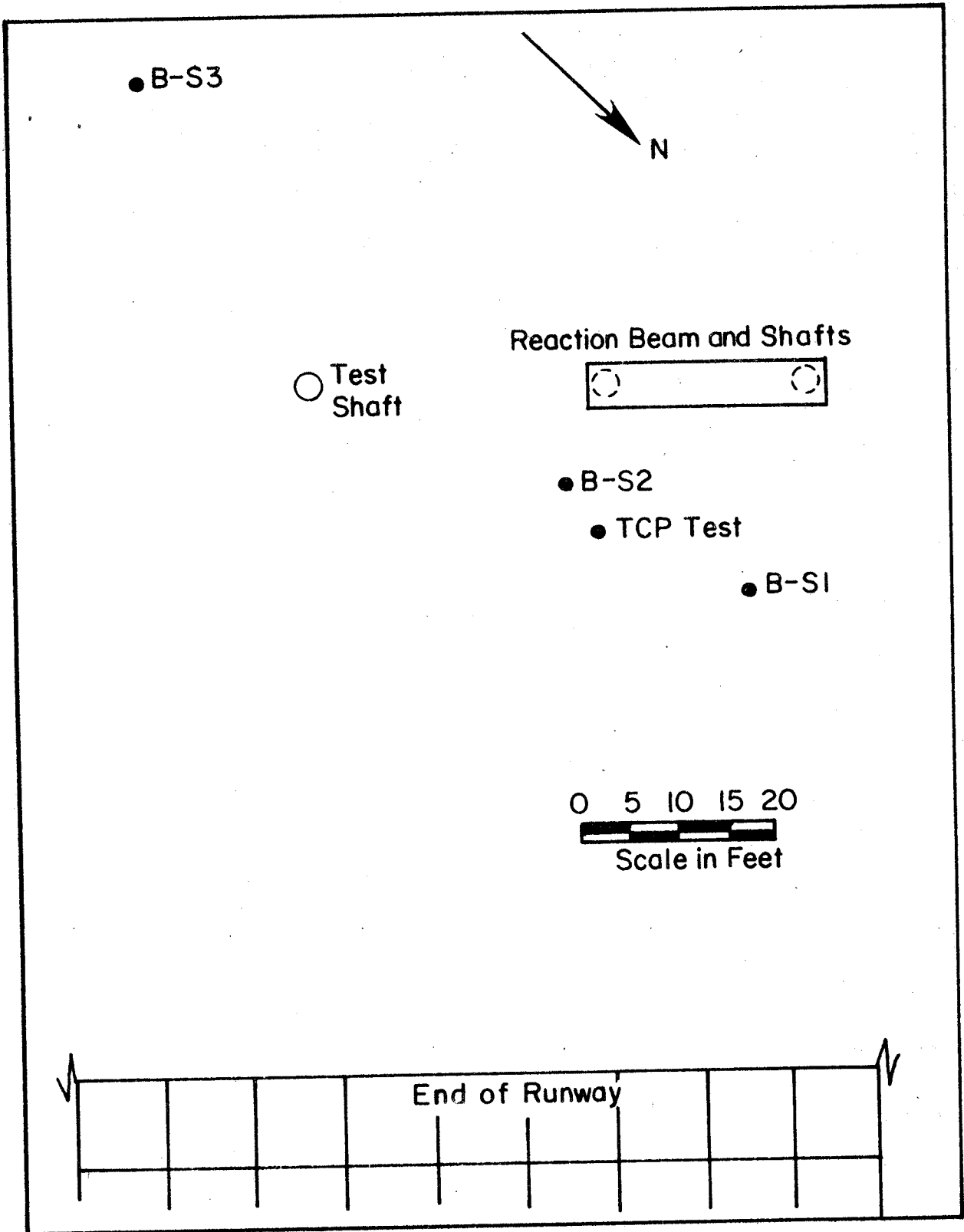


FIG. 14 - Location of Borings  
 1 ft = 0.3048 m

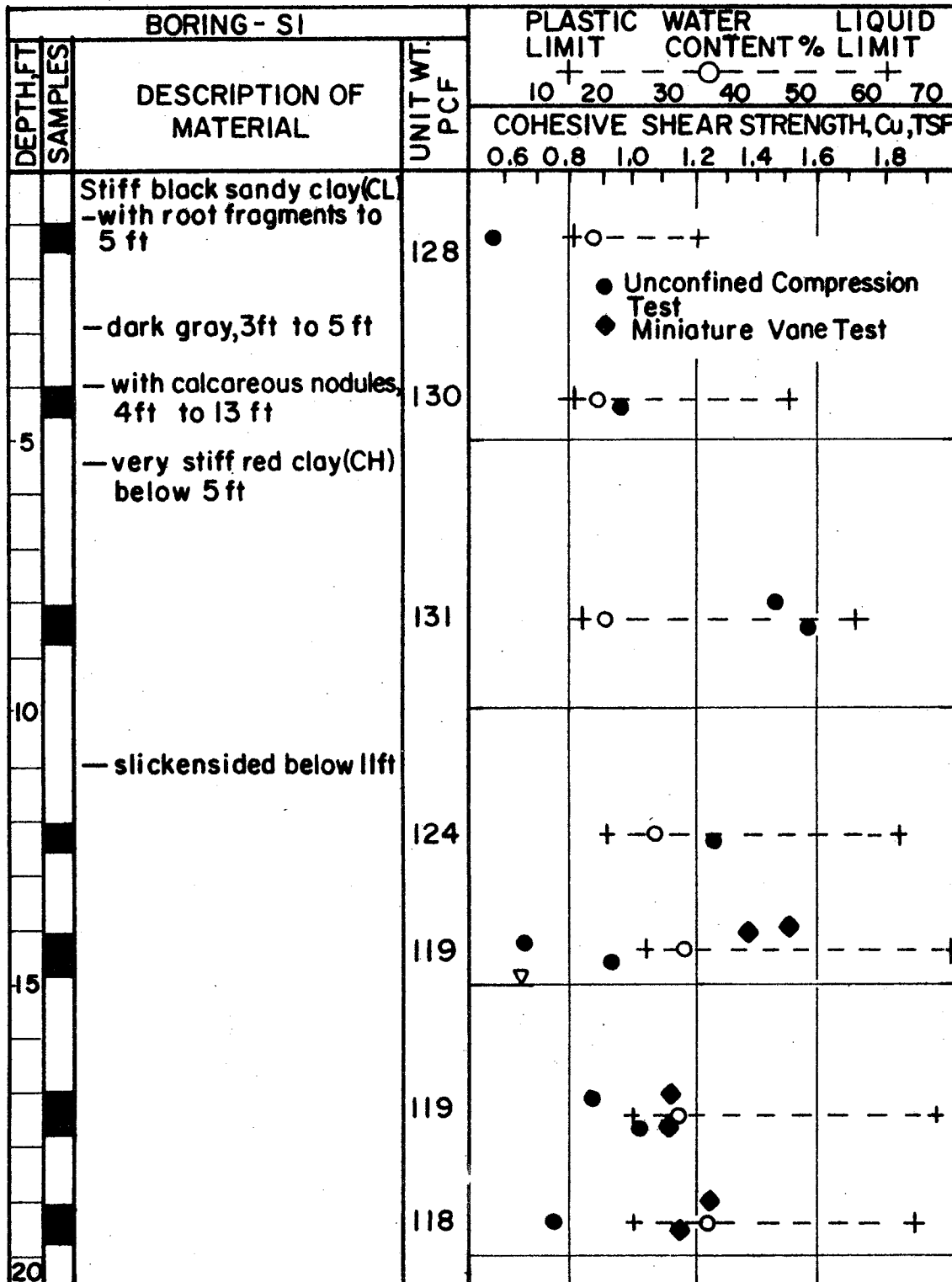


FIG. 15- Boring - S1  
 1 ft = 0.3048m, 1 tsf = 95.8 kN/m<sup>2</sup>, 1pcf = 0.157 kN/m<sup>3</sup>

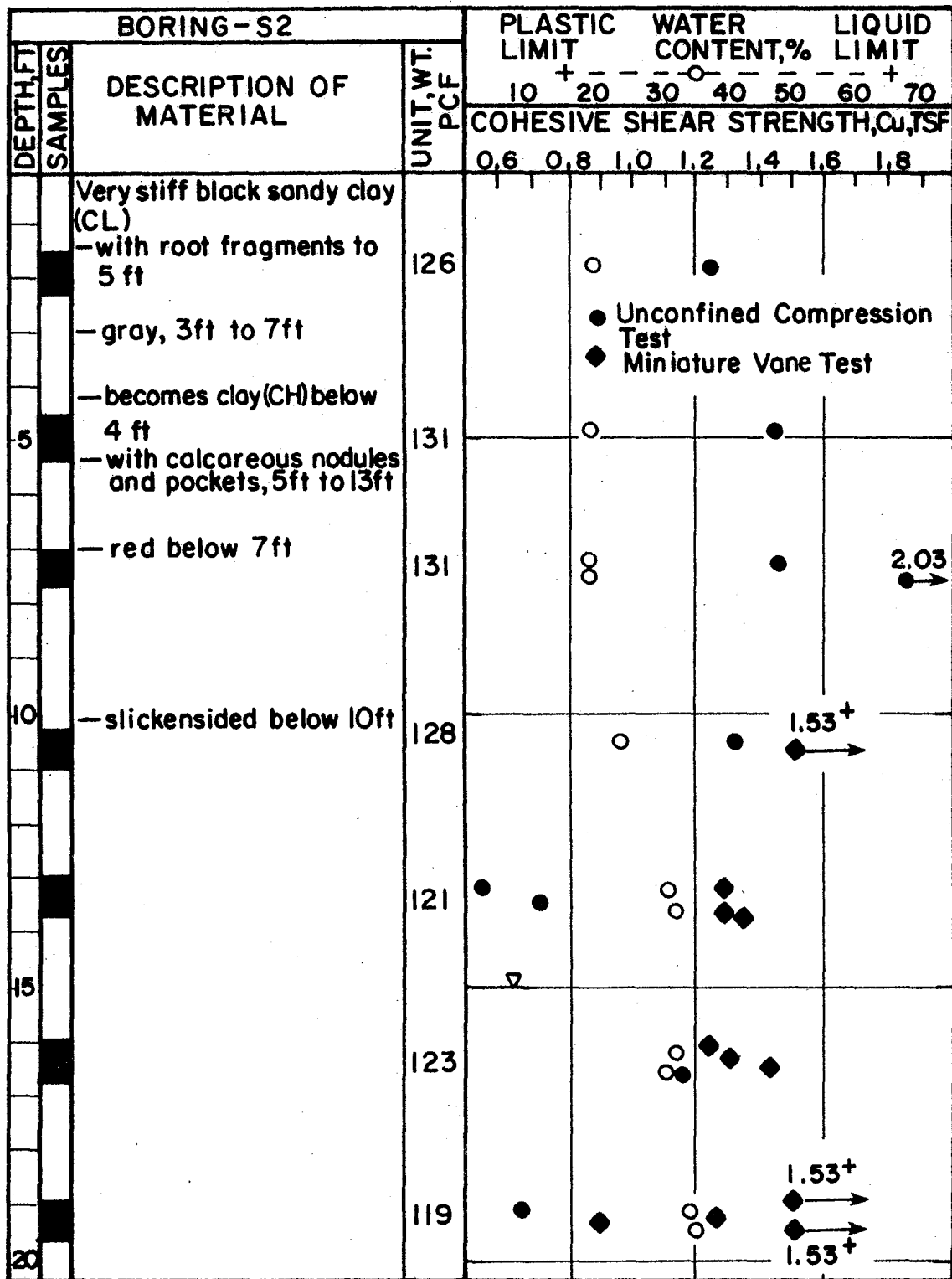


FIG. 16 - Boring - S2  
 1ft = 0.3048m, 1tsf = 95.8 kN/m<sup>2</sup>, 1pcf = 0.157 kN/m<sup>3</sup>

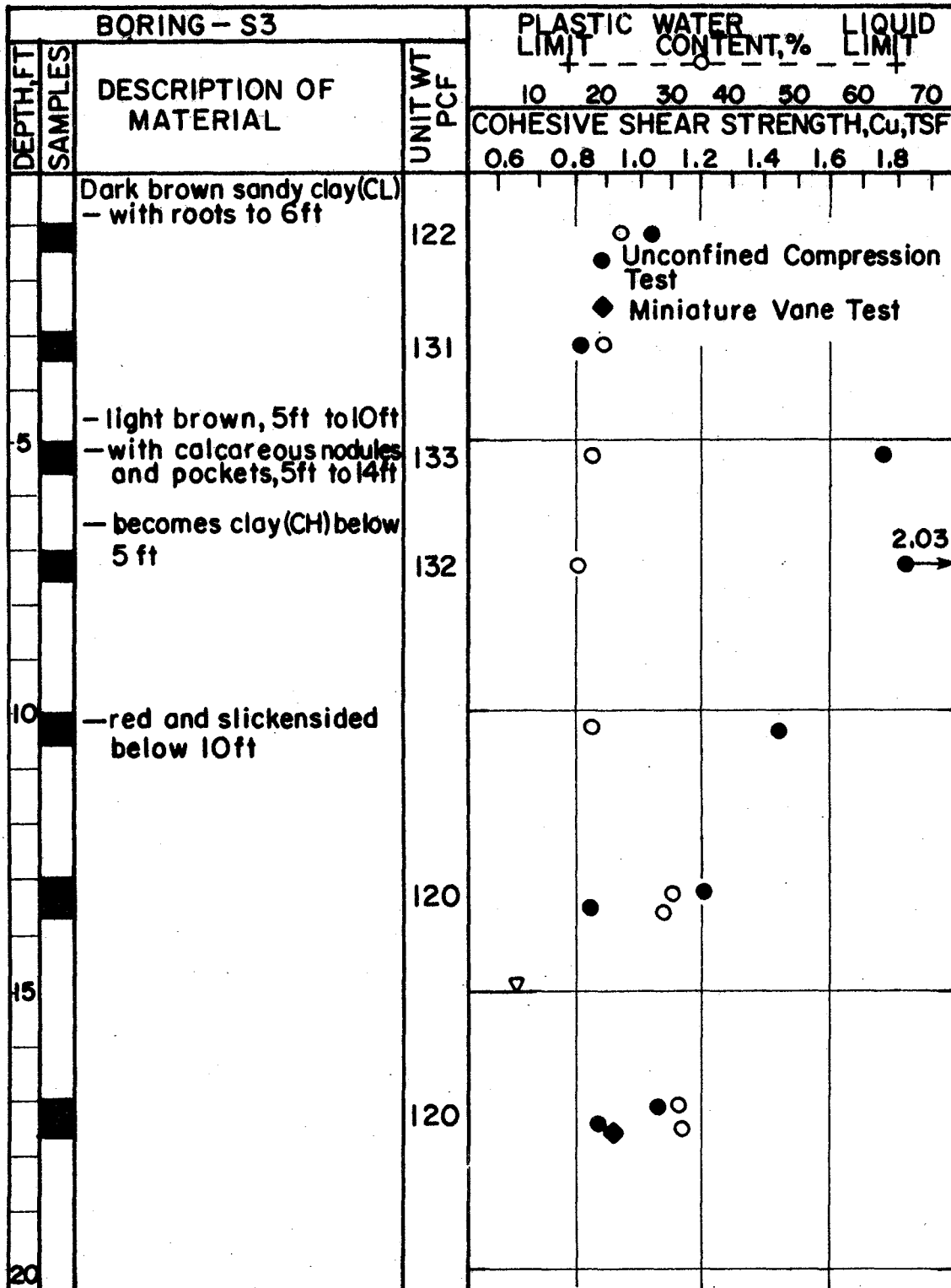


FIG. 17 — Boring - S3  
 1ft = 0.3048m, 1tsf = 95.8 kN/m<sup>2</sup>, 1pcf = 0.157 kN/m<sup>3</sup>

a CL according to the Unified Soil Classification system. The clay below approximately 5 ft (1.52 m) was classified as CH. A slickensided structure was noted in the clay below about 10 ft (3.05 m) depth. The soil shear strength in the upper 4 to 7 ft (1.22 to 2.13 m) of the site was somewhat higher in March and July than in January. The strength increase was apparently the result of a decrease in water content near the surface.

The N-values (blow counts) obtained from the TCP Test were also used to develop a shear strength profile. The correlation developed by Duderstadt et al. (10) was used to determine the undrained cohesive shear strength from the N-values. An average undrained cohesive shear strength of about 1.15 tsf ( $110.2 \text{ kN/m}^2$ ) was obtained using this method. This value compares quite well with the shear strength of 1.3 tsf ( $124.5 \text{ kN/m}^2$ ) obtained from the unconfined compression and miniature vane tests. The results of the TCP Test are shown in Fig. 18.

Upon completion of Boring S3 an open standpipe was installed for ground water observations. A perforated PVC pipe, covered with screen wire, was placed in the bore hole and surrounded with clean gravel. Water level readings in August, 1977 indicated the water level was steady at a depth of 15 ft (4.57 m).

#### Lateral Loading System

The loading and reaction system used in testing the instrumented drilled shaft is shown in Fig. 19. The reaction system consisted of two reinforced concrete drilled shafts connected by a reinforced concrete tie beam. Each shaft was drilled to a depth of 20 ft (6.10 m) and was 3 ft (0.91 m) in diameter. The shaft spacing was 20 ft (6.10 m), center-to-center. The steel reinforcing cages for each shaft consisted of twelve

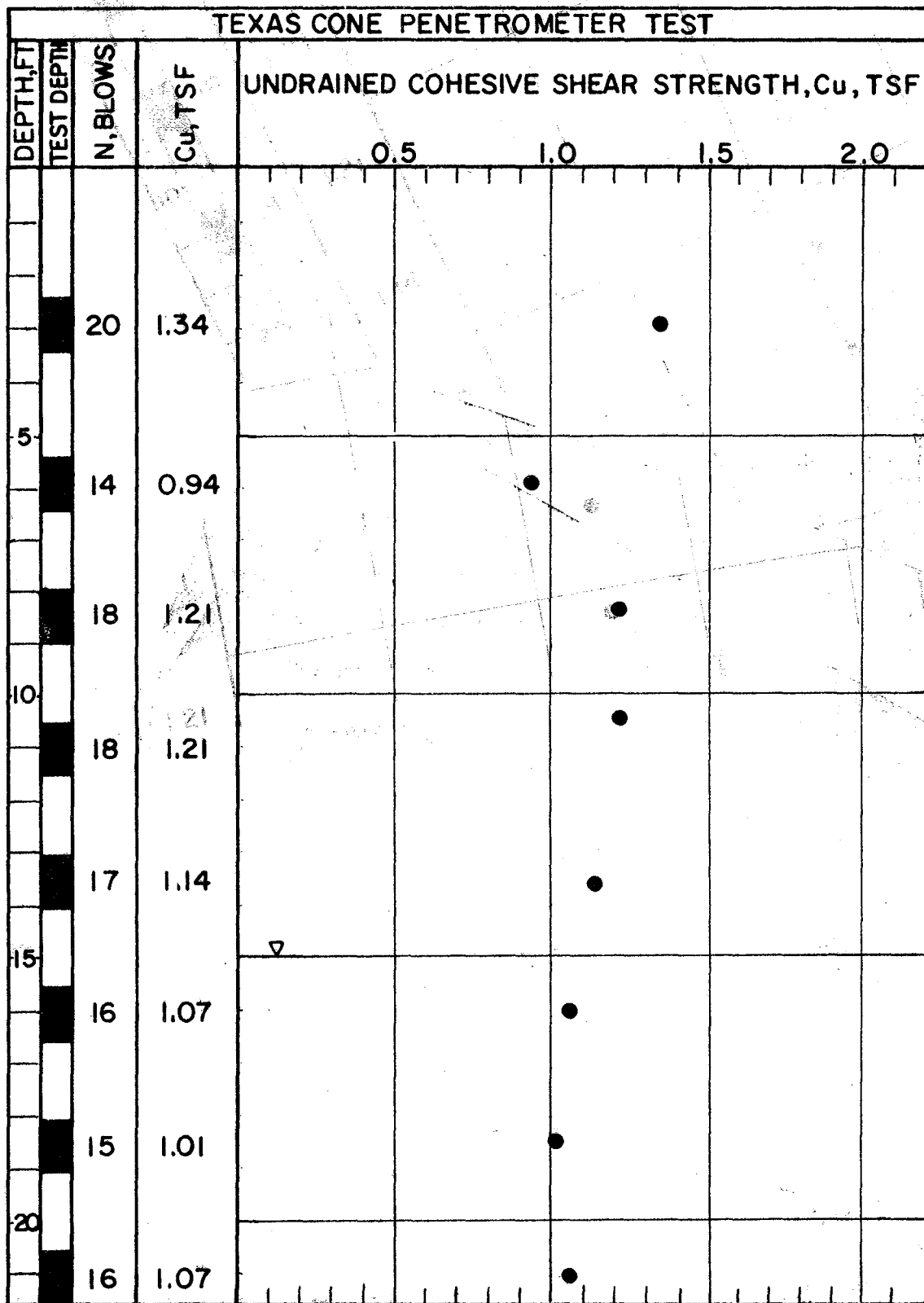


FIG. 18— Texas Cone Penetrometer Test  
 1ft = 0.3048m, 1tsf = 95.8 kN/m<sup>2</sup>

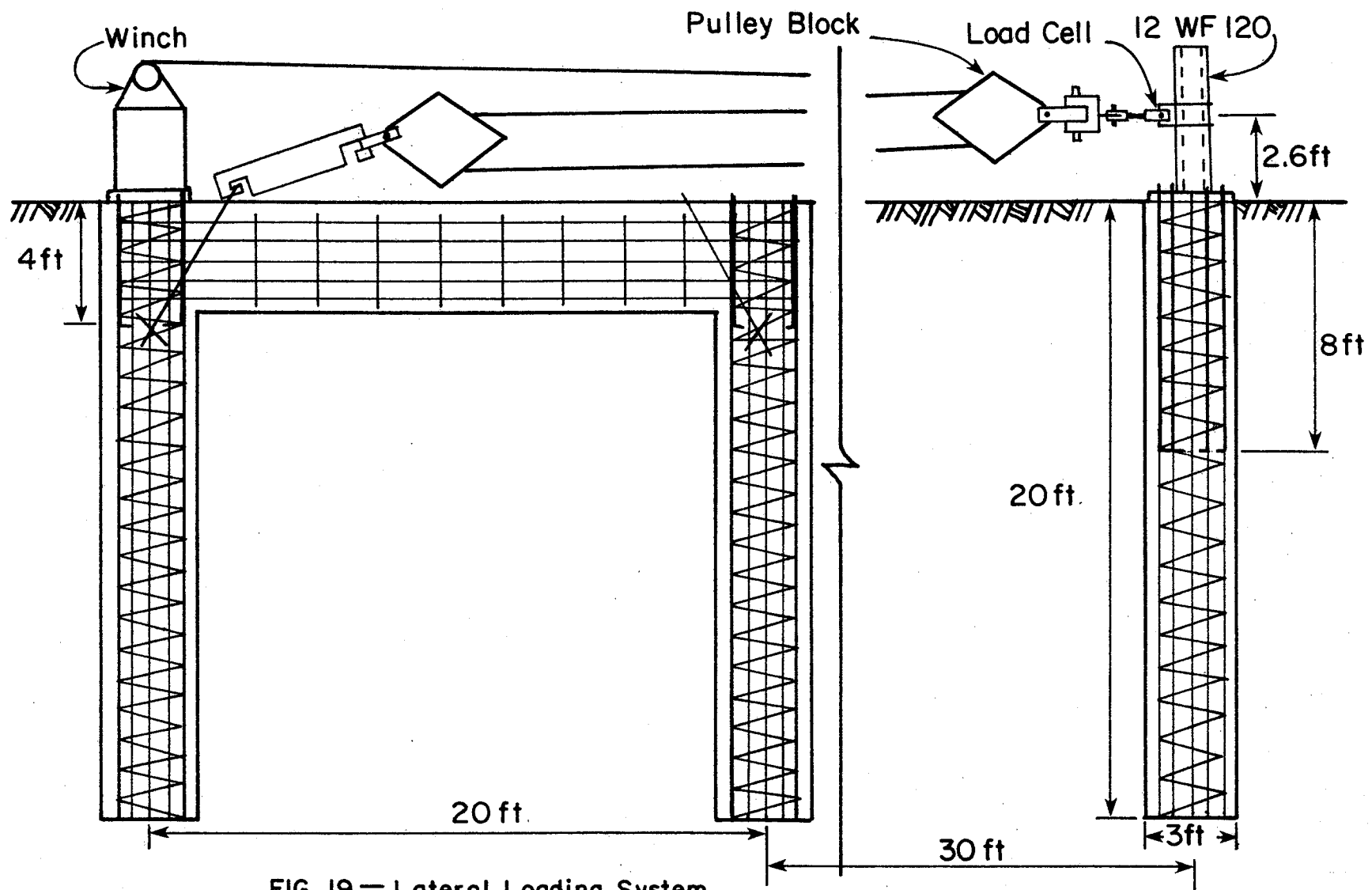


FIG. 19 — Lateral Loading System  
 1ft = 0.3048 m

No. 11 bars (Grade 60) with No. 3 spiral at 6 in. (15.2 cm) pitch. The beam connecting the shafts was approximately 4 ft (1.22 m) wide and 3.5 ft (1.07 m) deep. It was reinforced with fourteen No. 6 steel bars with No. 3 stirrups at 24 in. (0.61 m) spacing. A 2 in. (5.1 cm) diameter steel reaction bar was embedded about 4 ft (1.22 m) deep on both reaction shafts. An 18 x 18 x 1 in. (45.7 x 45.7 x 2.54 cm) steel plate was welded to each reaction bar to increase the bearing area. The winch was anchored to the rear reaction shaft by six 1.25 in. (3.2 cm) anchor bolts embedded to a depth of approximately 4 ft (1.22 m).

The test shaft was located on line with the centers of the reaction shafts at a center-to-center distance of approximately 30 ft (9.10 m) from the front reaction shaft. The shaft was nominally 3 ft (0.91 m) in diameter by 20 ft (6.10 m) deep. Wobble in the auger produced a diameter of about 39 in. (0.99 m) at the ground surface decreasing to 36 in. (0.91 m) at about 16 ft (4.88 m) depth. The shaft depth was approximately 20.2 ft (6.16 m). The reinforcing cage for the test shaft was the same as for the reaction shafts. As shown in Fig. 19, the lateral load was applied to a steel column which was bolted to the test shaft. The column was a 12 WF 120 which was welded to a 1 in. (2.54 cm) steel base plate. Twelve 1.25 in. (3.2 cm) anchor bolts were used to connect the column to the shaft. The bolts were embedded to a depth of 8 ft (2.44 m).

The lateral load was applied to the test shaft by a winch and pulley system. The winch was a single drum, 20 ton (178 kN) capacity Garwood cable winch driven through a four to one gear reduction unit by a gasoline powered hydraulic unit. A twelve to one mechanical advantage was provided by two, six sheave, 100 ton (890 kN) capacity pulley blocks. The cable was a 3/4 in. (1.91 cm) 6 x 19 standard hoisting wire rope. As

shown in Fig. 19, one block was connected to the anchor bar while the other was connected to the test shaft. The load cell was placed between the block and the test shaft at a height of 2.6 ft (0.79 m) above the groundline.

### Instrumentation

Pressure Cells. - The test shaft was instrumented with Terra Tec pressure cells. The Terra Tec cells were used with good results by Wright et al. (42) in a study of active pressures on precast panel retaining walls. A sketch of the pressure cell is shown in Fig. 20. The following is a description of the cell according to Corbett et al. (6).

The cell is constructed of two 9 in. (22.9 cm) diameter steel plates welded together at the circumference. The void between the plates is filled with an incompressible, non-corrosive fluid which transmits the applied pressure to the sensing unit; the sensing unit consists of a double-bellows assembly. Air pressure from the control unit is applied through a closed loop system inside the bellows to balance the external total pressure. This pressure is read directly on the gauge in the control unit.

Before the cells were installed in the test shaft, they were individually checked in a pressure chamber. The zero reading of each cell was determined and no malfunctions were observed in any of the cells.

Load Cell. - The load applied to the test shaft was measured by a 200 kip (890 kN) capacity strain gage load cell. The load is indicated on a Budd P350 indicator in units of microstrain and is converted from microstrain to kips by a predetermined calibration constant. The accuracy of the load cell and Budd indicator unit is approximately  $\pm 0.04$  kips (0.178 kN).

Inclinometer. - The rotation of the shaft was determined by a

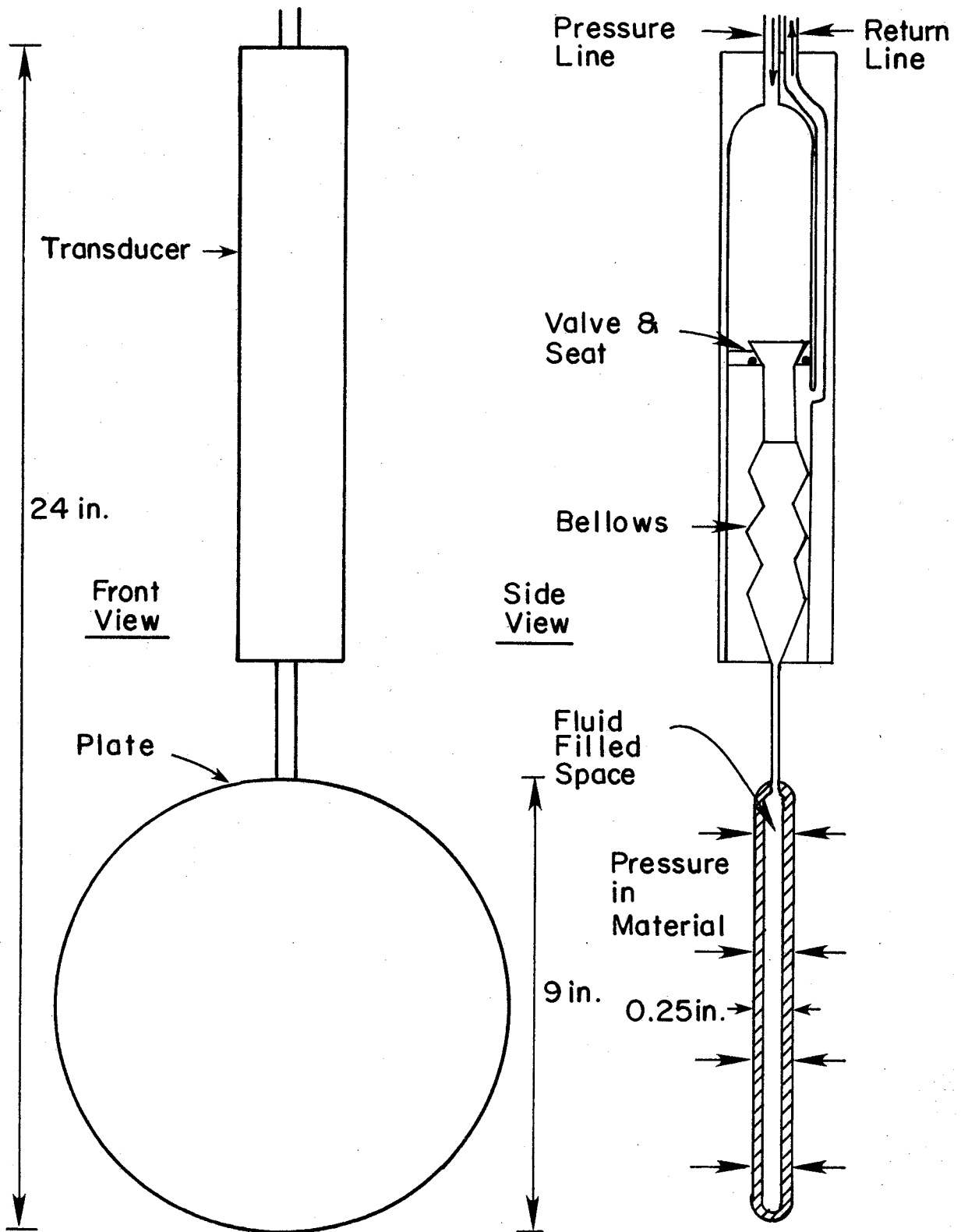


FIG. 20— Terra Tec Pressure Cell  
1 in. = 2.54 cm

Hilger & Watts TB108-1 inclinometer. The rotation could be read in degrees to an accuracy of approximately plus or minus one minute. Rotational readings were taken by placing the inclinometer at five predetermined locations on the steel column. A back-up system was also devised for the determination of the shaft rotation. Horizontal measurements from a vertical reference line to five points on the steel column allowed the determination of the relative movements of the points. The reference line was established by a plumb-bob suspended from a frame welded to the top of the column. Initial measurements were made before the lateral load was applied. The initial measurements were subtracted from subsequent measurements to obtain the movement relative to the initial position of the plumb line.

Dial Gages. - The deflection of the shaft at the groundline was measured by two 0.001 in. (0.0254 mm) dial gages. The gages were mounted on a steel beam behind the shaft which was bolted to footings that were placed approximately 10 ft (3.05 m) on each side of the shaft. A bench mark was also set about 50 ft (15.24 m) behind the shaft as a safety measure in case the dial gages were disturbed.

#### Construction of Testing System

The shafts for the loading and reaction system were constructed on March 15, 1977. At that time the excavation for the tie beam had not been completed, so the concrete placement was stopped about 5 ft (1.52 m) below ground level. Concreting was completed on April 8, 1977, after the beam excavation was finished and reinforcing steel had been installed.

Before the test shaft was installed, it was realized that some method of shoring the shaft excavation would be needed. The shoring was

necessary due to the length of time required for the installation of the pressure cells and because of the caving potential of the slickensided clay below 10 ft (3.05 m) depth. The excavation was shored by tying 20 ft (6.10 m) long 1 x 4 in. (2.54 x 10.16 cm) boards to the outside of the reinforcing cage. In order to leave room for the installation of the pressure cells, openings were left at two locations along the length of the shaft. To protect the exposed area from caving, metal flashing was tied to the outside of the cage. Holes were cut in the flashing at selected locations to permit the installation of the pressure cells. The reinforcing cage was set in the shaft excavation after the drilling was completed. The tie wires were then cut and the boards and flashing were forced against the side of the excavation by wooden wedges driven between the cage and shoring.

The spacing and location of the pressure cells on the test shaft is shown in Fig. 21. The cells were installed directly in line with the direction of the applied load. Five cells were located on the front of the shaft facing the reaction system and five cells were located directly opposite on the backside. The cells were placed in the soil along the side of the excavation and held in place by steel pins.

Because of the time involved in the installation of the pressure cells, two days were needed to complete the test shaft. The shaft was drilled and reinforcing cage set on Monday morning, May 23, 1977. Pressure cell installation was begun Monday afternoon and completed Tuesday afternoon. After the cells were in place, all wedges between the shoring and reinforcement were removed. Concrete placement then began with the use of a rubber tremie. Sections of the tremie were removed as the level of concrete rose. A vibrator was used to

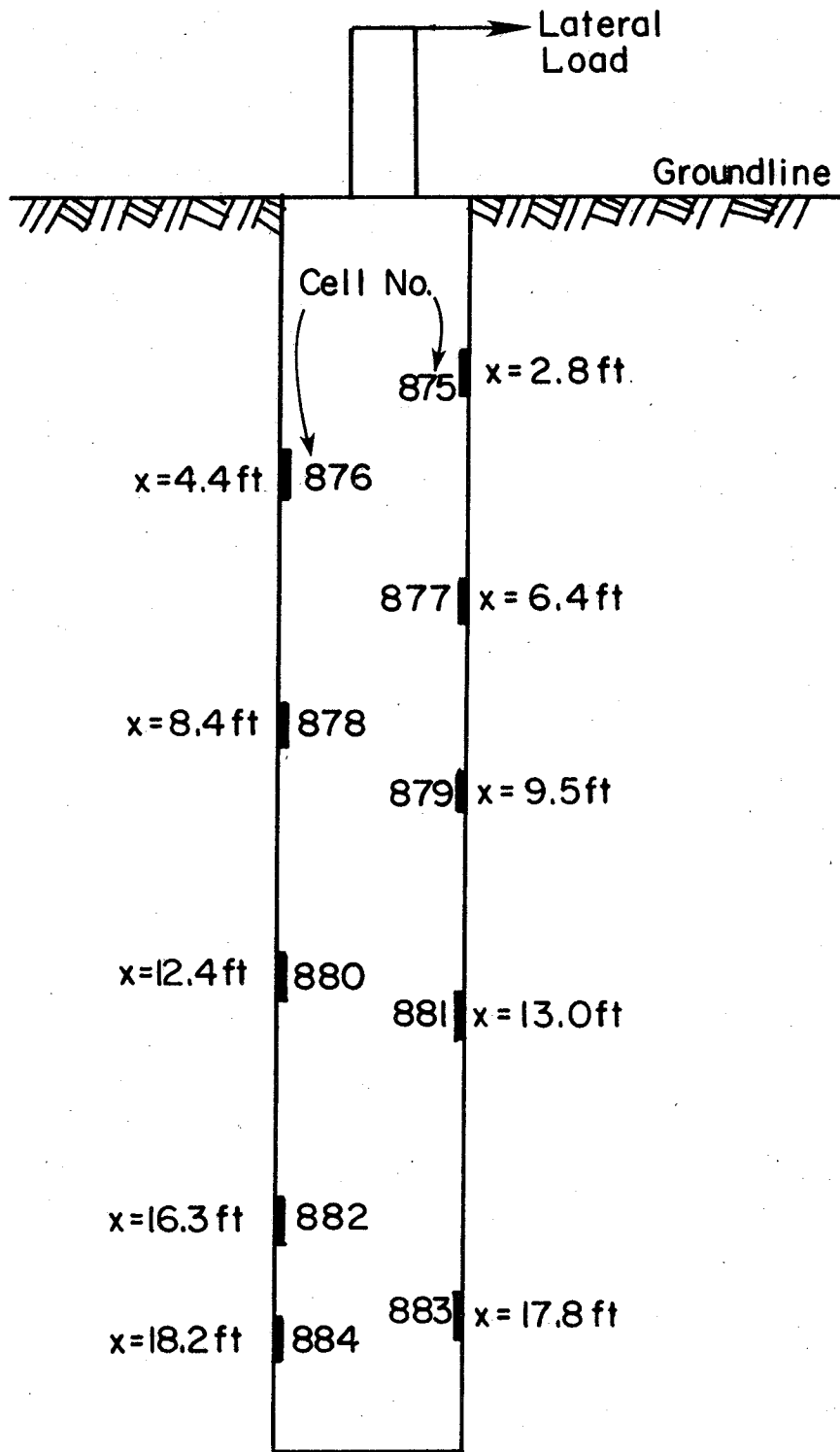


FIG. 21— Location of Pressure Cells  
 $x$  = Depth Below Groundline; 1 ft = 0.3048 m

consolidate the concrete at various intervals. After several feet of concrete had been placed in the shaft the boards were slowly removed from the excavation, the level of concrete always staying ahead of the bottom of the boards. When the concrete level was approximately 6 ft (1.83 m) below ground level the anchor bolts were set in the shaft. Concrete placement then continued until the shaft was completed at ground level.

Class C concrete as specified by the SDHPT was used in the shaft. Concrete cylinders taken during the placement of the test shaft had an average 28 day strength of 3000 psi (20,700 kN/m<sup>2</sup>). The test shaft was cured for 30 days before the first load was applied on June 23, 1977.

#### Loading Procedure

The decision to load test a drilled shaft with dimensions of 20 ft (6.10 m) depth and 3 ft (0.91 m) diameter was based on the study reported by Wright et al. (42). The precast panel retaining wall instrumented in that study was founded on drilled shafts with these dimensions. Since the lateral load acting on a drilled shaft supporting a precast panel retaining wall is the resultant of the backfill acting on the panel, it was decided that the initial loads applied to the test shaft should simulate those loads resulting from the backfilling of this retaining wall.

Wright et al. presented a method for calculating the maximum resultant force of the backfill acting on a retaining wall. For the retaining wall reported in their study the maximum resultant force was calculated to be 34.9 kips (155 kN) per shaft. The backfill producing the resultant force in that study was deposited over an eight day period. In order to simulate the backfilling of that particular retaining wall

as closely as possible, the initial loads on the test shaft in this study were applied over a six day period. The applied force on the test shaft at the end of the six day period was 34.5 kips (153.5 kN). Minor inaccuracies in the loading system prevented the exact simulation of the retaining wall backfill.

It was also decided to simulate the overburden pressure imposed by the retaining wall backfill. The simulation was accomplished by stacking concrete blocks of various sizes behind the test shaft. The blocks were stacked directly behind the shaft for a length of 17 ft (5.18 m) along a width of 3.5 ft (1.07 m). Each day a number of blocks were added to the stack, such that the weight being added was roughly equal to the overburden pressure on the retaining wall reported by Wright et al. After the final blocks were added on the sixth day, the overburden was approximately 1050 psf (7245 kN/m<sup>2</sup>). The base of the retaining wall in the study reported by Wright et al. also had a 3 ft (0.91 m) overburden of soil in front of it. This overburden was simulated by steel stock that was stacked in front of the test shaft. The surcharge was equivalent to approximately 300 psf (2070 kN).

After the load of 34.5 kips (153.5 kN) was applied, no additional loads were added for a period of 13 days in order to try to determine whether any creep was occurring in the soil in front of the shaft. However, it was soon realized that it was not possible to hold a constant load of 34.5 kips (153.5 kN) on the shaft. Daily temperature changes caused the cables in the loading system to expand and contract, thus creating a cyclic effect in the applied load. Daily load cycles of as much as 7 kips (31 kN) were recorded.

At the conclusion of the 13 day "constant load" period, the load

was increased daily in increments of roughly 9 kips (40 kN). This continued until the lateral load reached 144 kips (641 kN). At that point two steel pins connecting the load cell to the loading assembly and the shaft fractured. Consequently, the load had to be taken off the shaft and a two week delay occurred while the connections were redesigned and rebuilt. When repairs were completed the shaft was reloaded and the load test continued until a structural failure of the shaft occurred at 169 kips (752 kN). Excavation of the shaft indicated the reinforcing bars on the back of the shaft had fractured along with the concrete at a depth of 8 ft (2.44 m). The fracture occurred directly below the level of the anchor bolts.

## TEST RESULTS

The results of the lateral load test are given in this section. Pressure cell data are presented and analyzed along with test shaft deflection and rotation characteristics, shaft rotation point, and ultimate loads.

### Pressure Cell Data

Initial Pressures. - Four sets of pressure cell readings are shown in Table 3. The readings presented are: (1) the zero readings from the laboratory calibration; (2) the initial readings taken after the cells

Table 3. - Initial Pressure Cell Readings

Cell	Zero Reading from Lab, psi April, 1977	In Shaft Before Concrete, psi May 24, 1977	In Shaft After Concrete, psi May 24, 1977	In Shaft Before Lateral Load, psi June 23, 1977
875	9.2	7.4	8.8	7.4
876	16.6	16.5	18.6	16.4
877	7.7	7.2	9.8	8.6
878	7.0	6.5	8.3	6.5
879	10.0	9.0	11.4	10.4
880	10.0	7.6	9.0	8.0
881	10.5	10.0	12.4	11.5
882	15.2	14.1	16.9	17.3
883	7.7	6.6	10.8	10.5
884	11.5	10.8	15.0	15.4

Note: 1 psi = 6.9 kN/m<sup>2</sup>

were installed in the shaft, but before the concrete was placed; (3) the readings taken after the concrete was placed; (4) and the readings taken 30 days after concrete placement before the application of the first lateral load. As shown in the table, the initial zero readings taken in the shaft differed from the zero readings obtained from the laboratory calibration. In most cases the readings taken in the shaft were 0.5 to 1.5 psi (3.45 to 10.35 kN/m<sup>2</sup>) lower than the laboratory calibration. The reason for the lower pressure readings is not known. As expected, the readings taken after the placement of the concrete were higher than the initial readings and the largest pressure increases were recorded by the cells on the bottom of the shaft. Thirty days later, before the first lateral load was applied, cell readings indicate that most of the pressures had dropped by 1 psi (6.9 kN/m<sup>2</sup>) or more. Concrete shrinkage during the 30 day curing time could account for this pressure decrease.

Pressures During Lateral Loading. - The lateral soil pressures resulting from the lateral loads on the shaft were obtained by subtracting the initial cell readings from the cell readings obtained for a particular lateral load. The initial cell readings used were those obtained on June 23, just prior to the application of the first lateral load. The resulting lateral soil pressures are plotted on Figs. 22 through 28. The solid curve represents the pressures that were obtained from lateral loads up to 144 kips (640.5 kN) before the load cell connections had to be redesigned. The dashed curve represents pressures that were obtained when the shaft was reloaded. It should be noted that on most of the solid curves the last two points do not appear to be in line with the previous ones. A problem with the pressure readout unit caused this discrepancy. It can also be seen that for most cells the initial portion

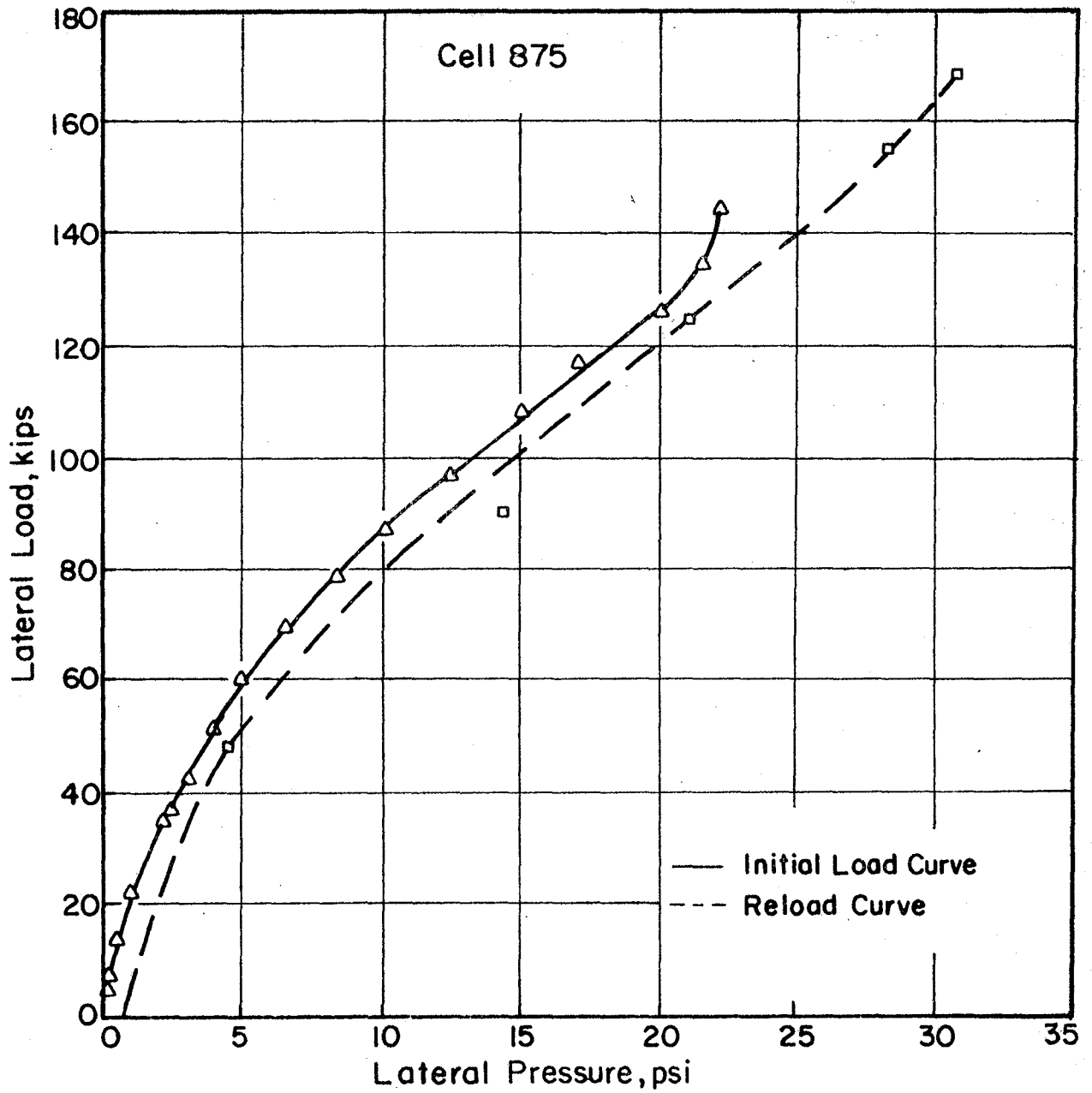


FIG. 22— Lateral Load vs. Lateral Pressure, Cell 875  
 1 kip = 4.45 kN; 1 psi = 6.9 kN/m<sup>2</sup>

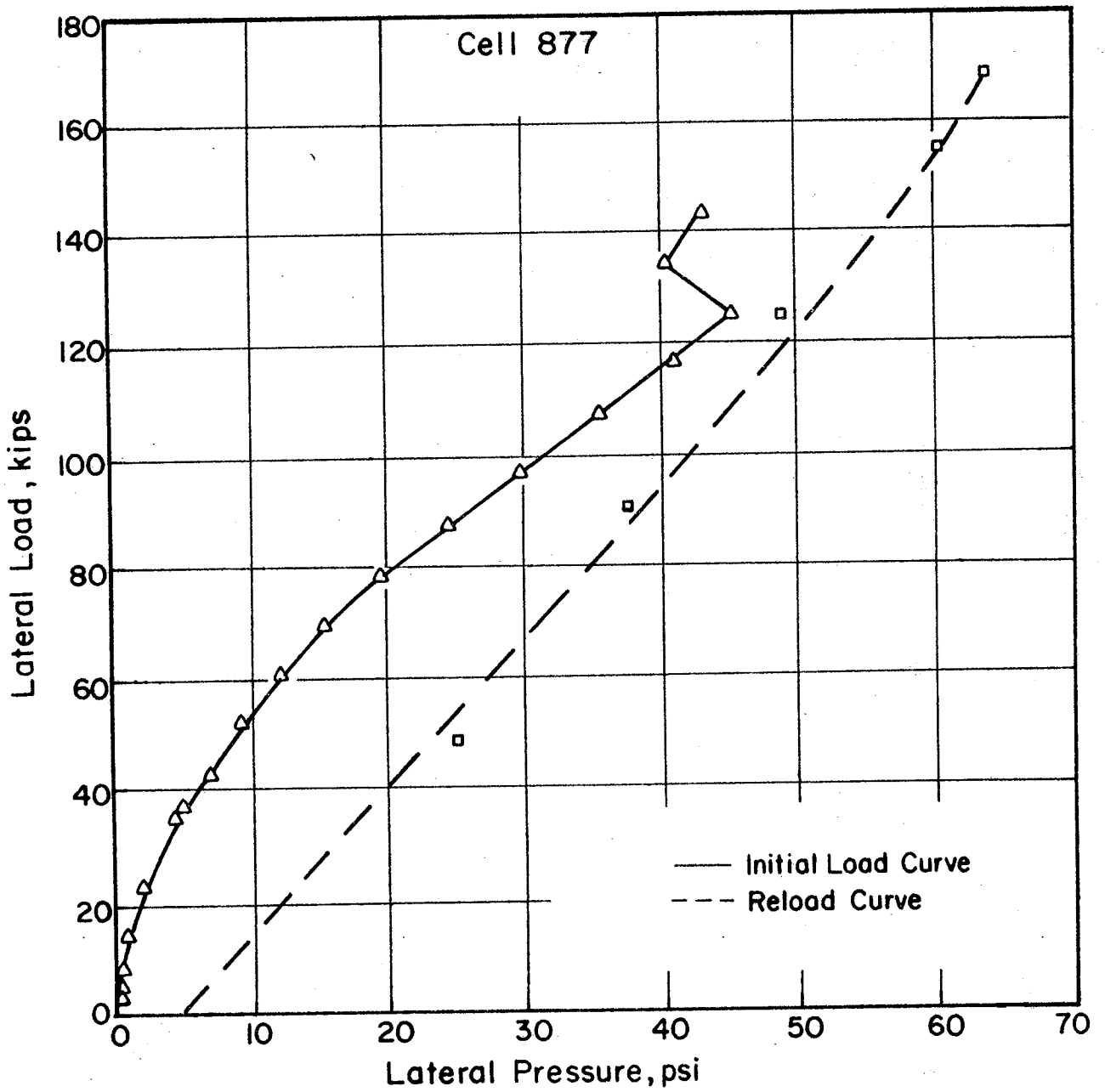


FIG. 23— Lateral Load vs. Lateral Pressure, Cell 877  
 1 kip = 4.45 kN; 1 psi = 6.9 kN/m<sup>2</sup>

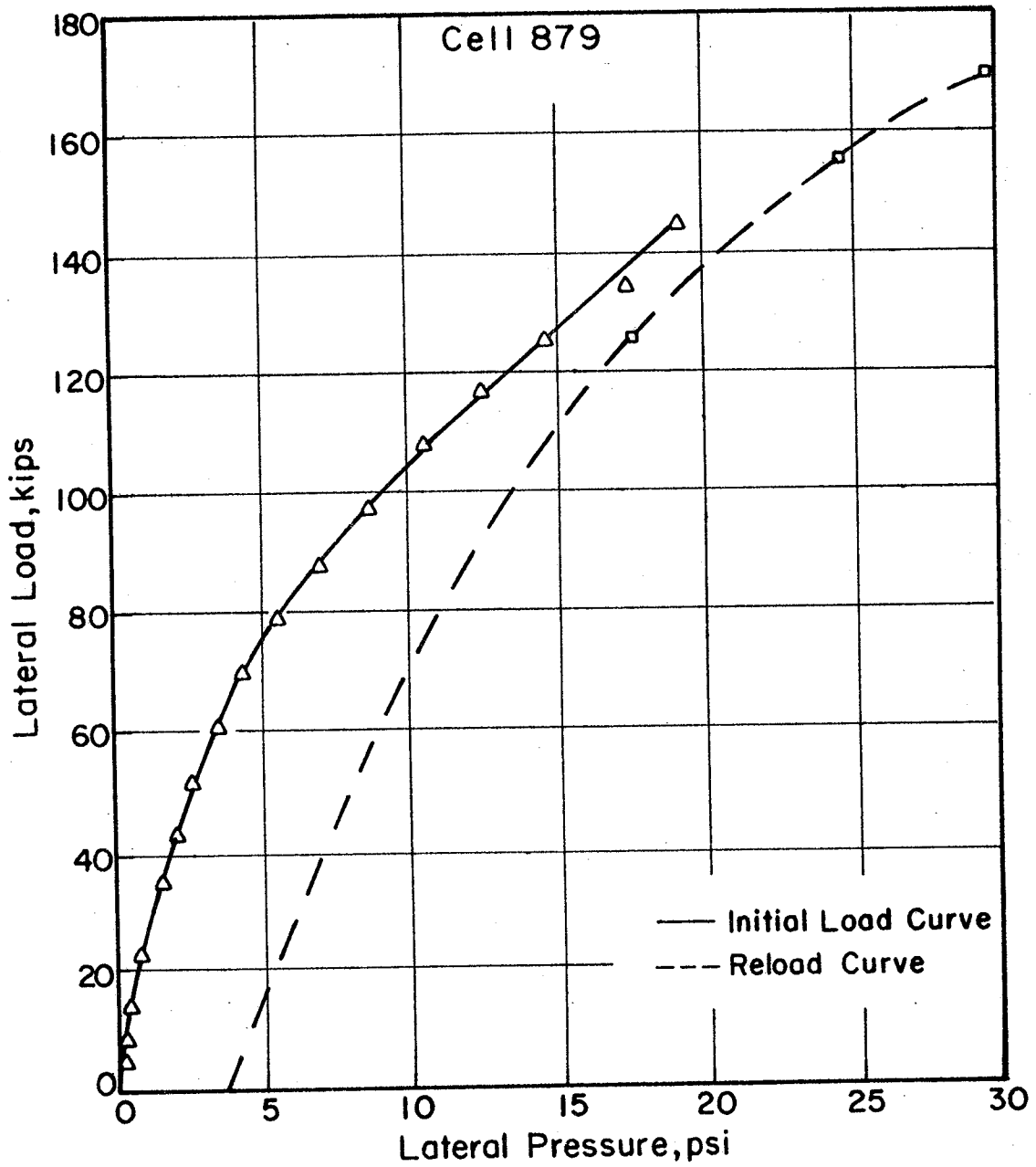


FIG. 24 — Lateral Load vs. Lateral Pressure, Cell 879  
 1 kip = 4.45 kN; 1 psi = 6.9 kN/m<sup>2</sup>

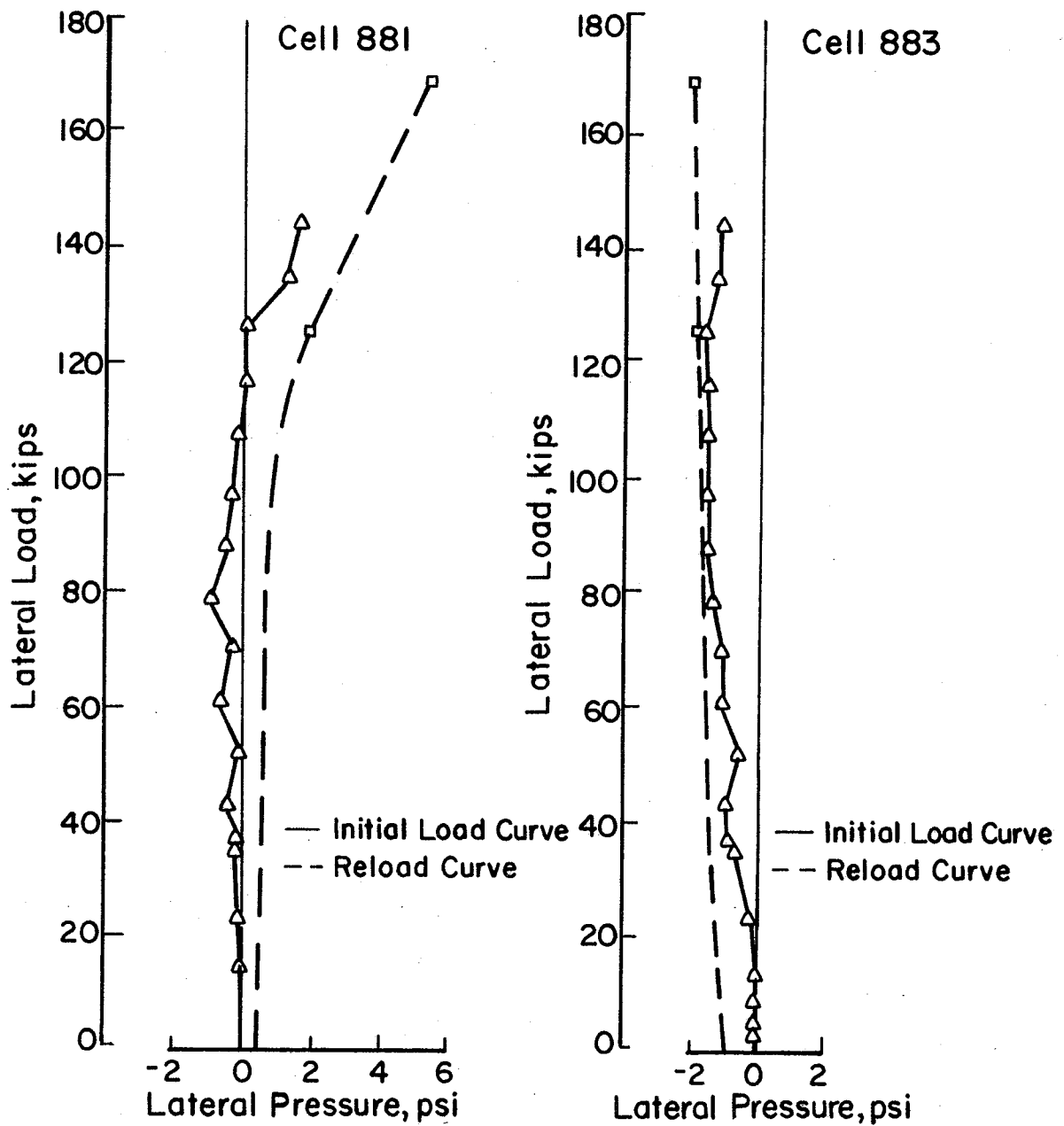


FIG. 25— Lateral Load vs. Lateral Pressure, Cells 881 & 883  
 1 kip = 4.45 kN; 1 psi = 6.9 kN/m<sup>2</sup>

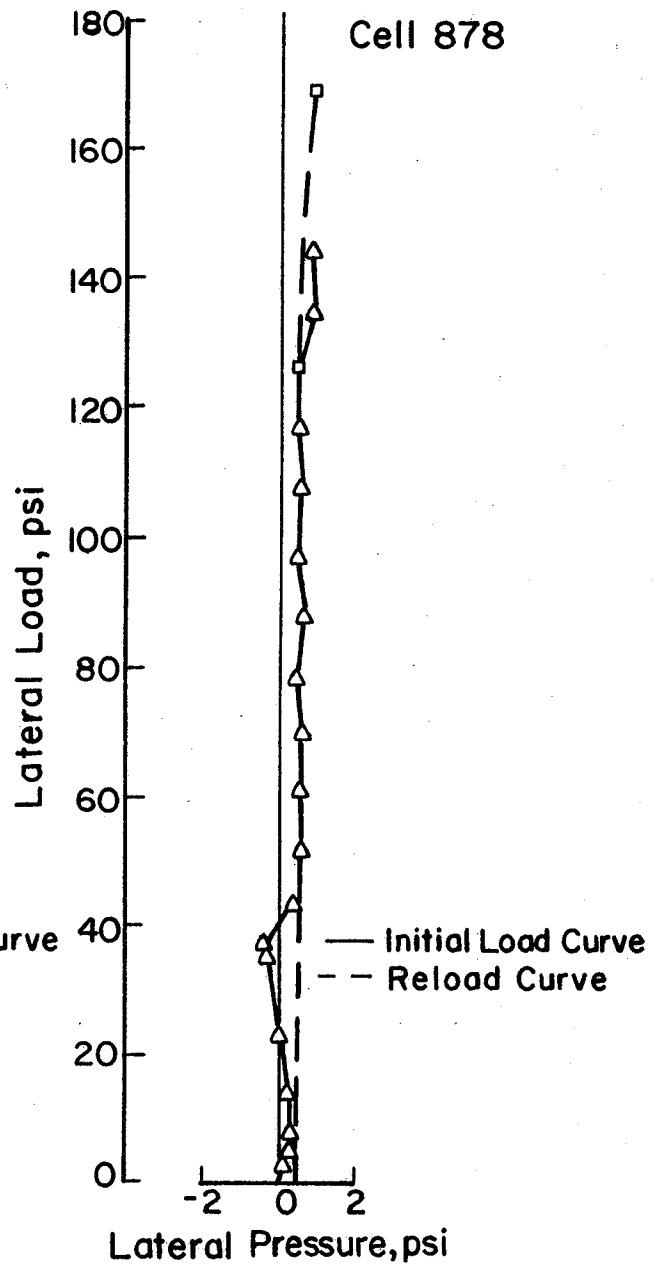
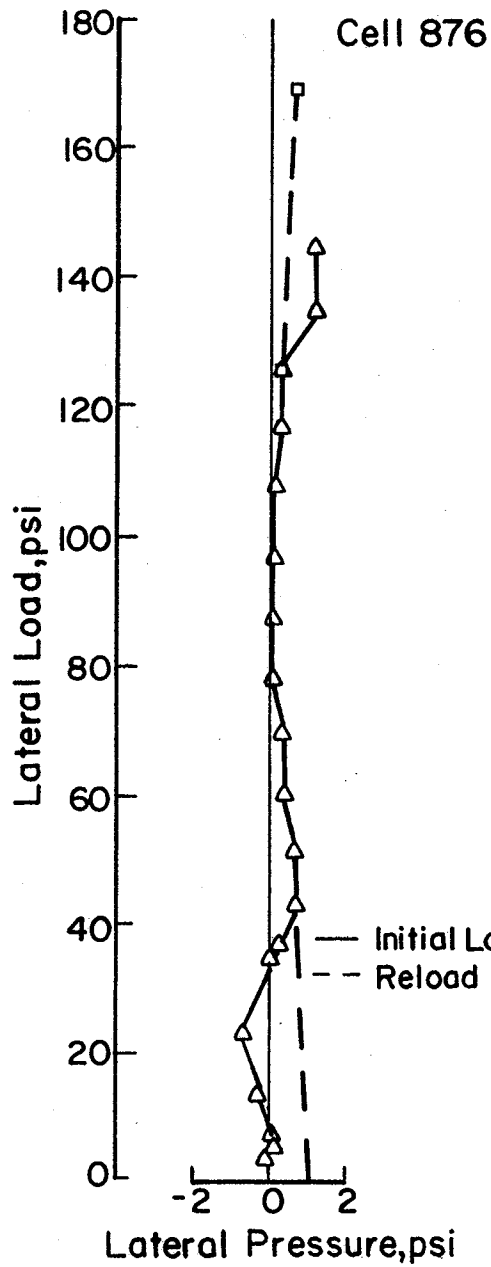


FIG. 26— Lateral Load vs. Lateral Pressure, Cells 876 & 878  
 1 kip = 4.45 kN; 1 psi = 6.9 kN/m<sup>2</sup>

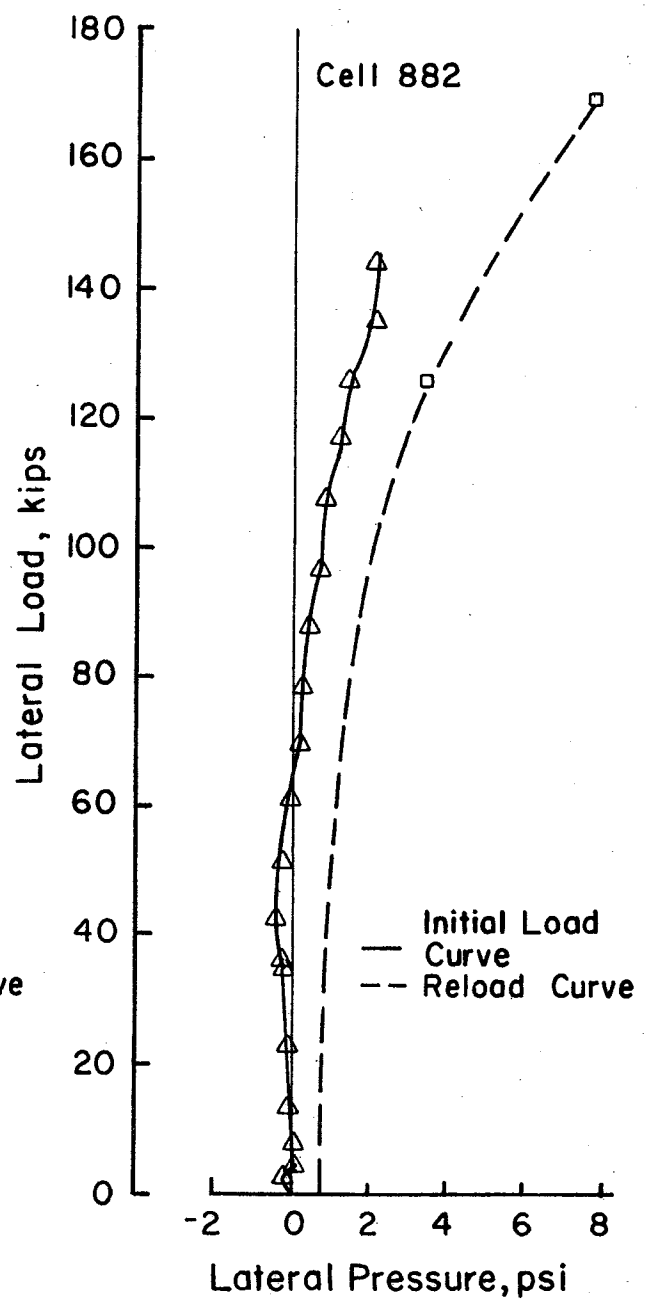
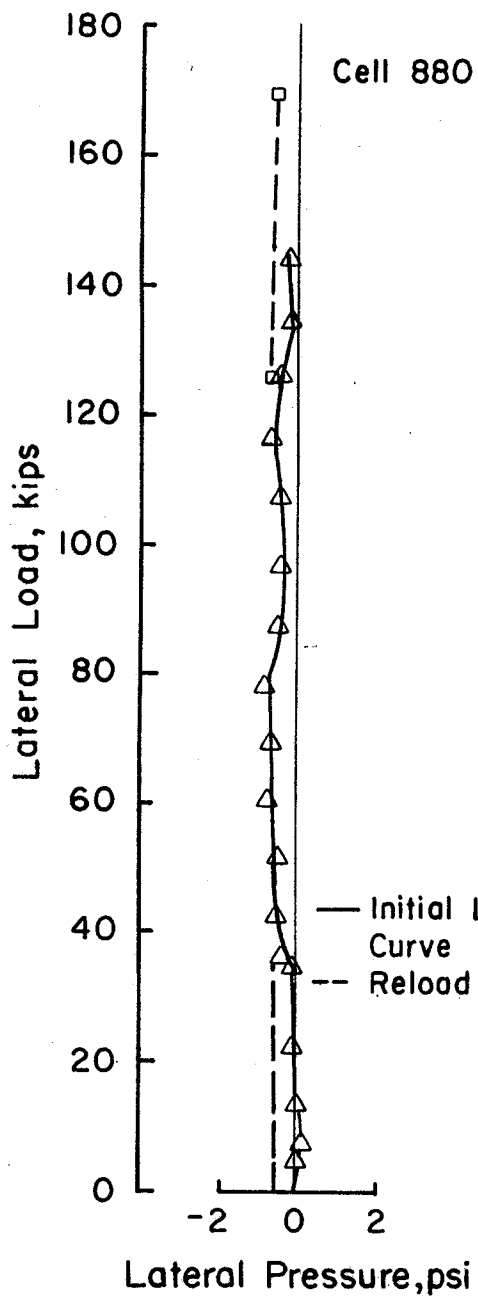


FIG. 27 - Lateral Load vs Lateral Pressure, Cells 880 & 882  
 1 kip = 4.45 kN; 1 psi = 6.9 kN/m<sup>2</sup>

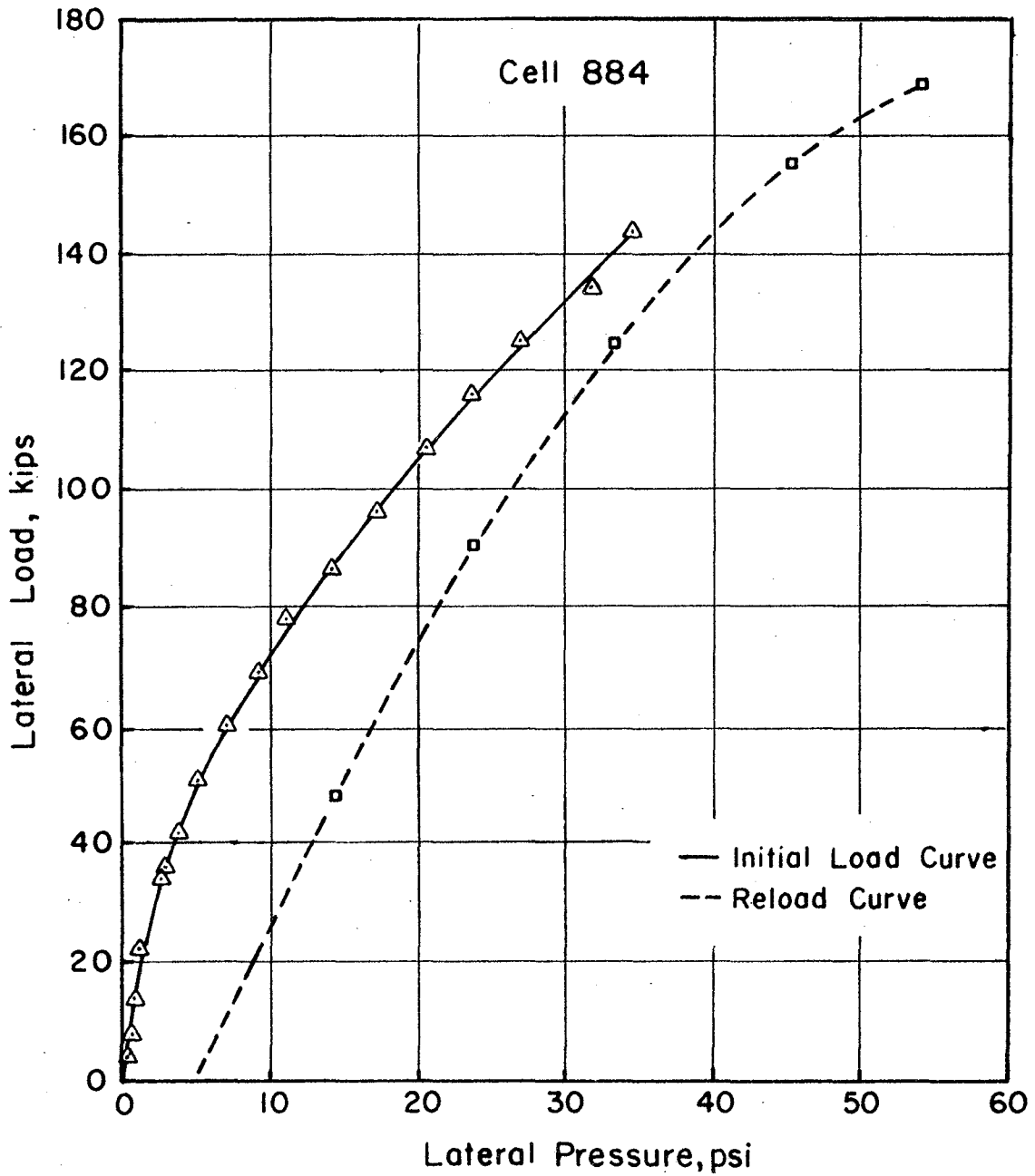


FIG. 28- Lateral Load vs Lateral Pressure,  
 Cell 884; 1 kip = 4.45 kN; 1 psi = 6.9 kN/m<sup>2</sup>

of the reloading curve does not match the original loading curve. However, in most instances the reloading curve appears to fall in line with the loading curve to a fairly good degree once the load of 144 kips (640.5 kN) has been exceeded. Since the pressures on the initial portion of the reloading curve exceeded the original pressures, it is probable that some degree of consolidation occurred in the soil during the original loading of the shaft.

When the lateral pressures were calculated, pressures that were consistently negative were recorded for cells 880 and 883. It is probable that these two cells experienced a loss of contact with the soil as a result of the shaft rotation. This loss of contact could have resulted in a pressure decrease. However, it should be noted that cells 876 and 878, which should also have experienced a loss of soil contact, did not record a significant number of negative pressures. This probably indicates that the initial pressures being used for cells 880 and 883 were too high by 1 to 2 psi (6.9 to 13.8 kN/m<sup>2</sup>).

When the pressure cells were installed it was assumed that the lateral loading would cause the shaft to rotate about a point 10 to 15 ft (3.05 to 4.57 m) deep. Consequently, the top three cells (see Fig. 21) located on the front side of the shaft (cells 875, 877, and 879) and the bottom two cells on the back side (cells 882 and 884) would be recording passive pressures and would have the highest pressure readings. These assumptions were essentially verified by the load test.

The pressure cell data indicate that of the five cells on the front side of the shaft, the top three (cells 875, 877, and 879) showed considerable pressure increases along with a slight increase being recorded by the fourth cell (cell 881). The bottom cell pressure (cell

883) was essentially constant. Of the five cells on the back side of the shaft, only the bottom cell (cell 884) showed a significant increase in pressure. The pressures in the top three cells (cell 876, 878, and 880) remained essentially constant, while the fourth cell (cell 882) showed a slight increase in pressure.

The lateral pressures indicated by cells 875, 877, 879, 881, and 884 are plotted with respect to depth for various lateral loads in Fig. 29. It should be noted that the second cell from the top on the front side of the shaft (cell 877) consistently recorded the highest pressures. The next highest pressures were recorded by the lowest cell on the back side (cell 884). Cell 881 remained essentially constant recording little or no lateral pressure until the latter stages of the load test. This would seem to indicate that the rotation point of the shaft was in the general area of this pressure cell. The pressures obtained from cell 882 did not correlate well with those obtained from cell 884. Cell 882 was located less than 2 ft (0.61 m) above cell 884 and yet did not record a lateral pressure in excess of 1 psi ( $6.9 \text{ kN/m}^2$ ) until the load was over 100 kips (445 kN). Since this cell was located in the slickensided clay, it is possible that some clay fell out from behind the cell during installation, thus creating an insufficient bearing area. It was felt the pressures recorded on cell 882 were erroneous and consequently they were not included in Fig. 29.

#### Analysis of Pressure Cell Data

Pressure Distribution. - Considering the results shown in Fig. 29, it is possible to draw some general conclusions about the shape of the lateral soil pressure distribution curve for cylindrical foundations in

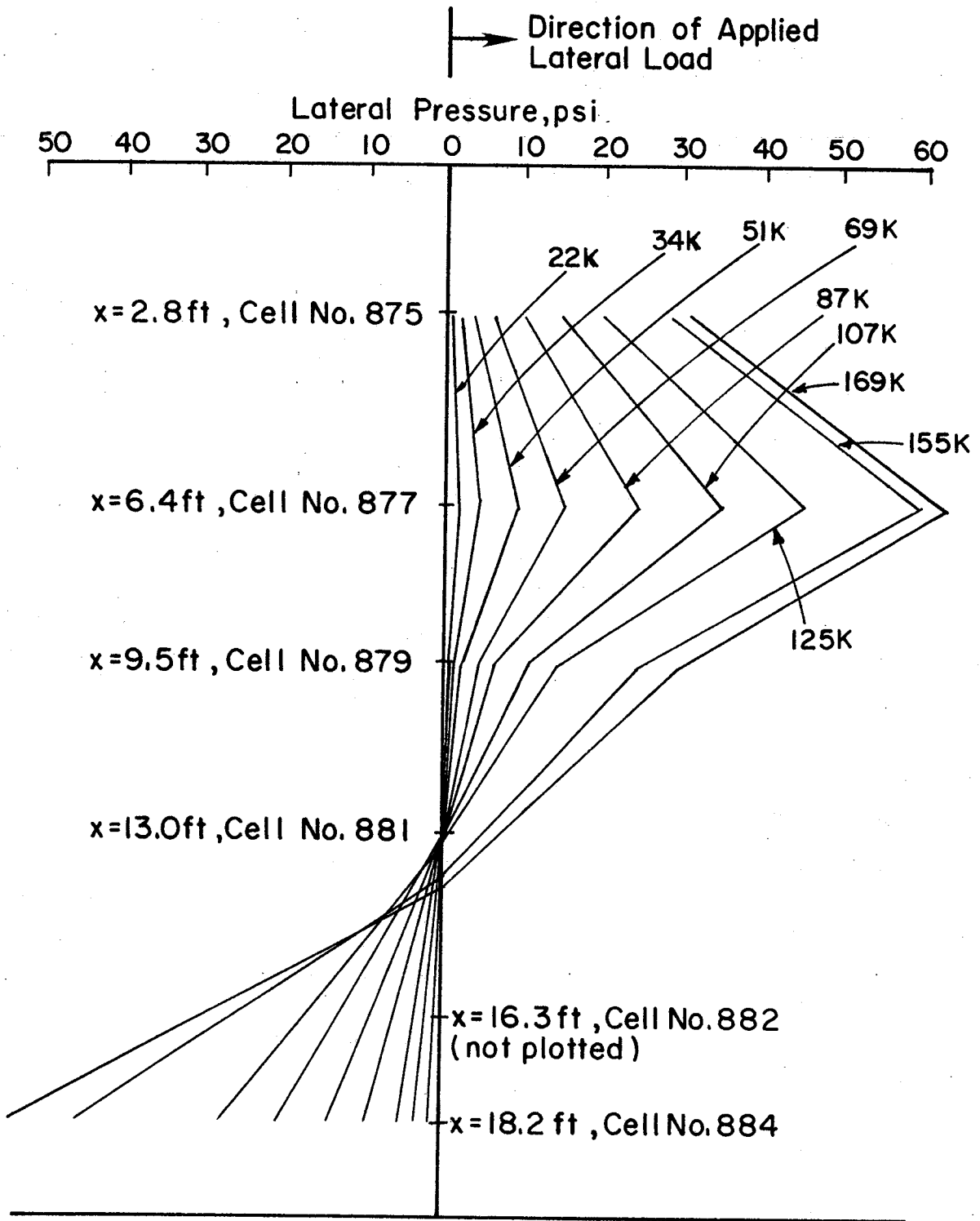


FIG. 29 — Lateral Pressure vs. Depth  
 x = Depth Below Groundline; 1 ft = 0.3048 m ; 1 kip = 4.45 kN ;  
 1 psi = 6.9 kN/m<sup>2</sup>

relatively homogeneous cohesive soil. (The lateral soil pressure distribution will herein be referred to as soil resistance.) For loads that do not exceed the ultimate lateral resistance of the soil, the soil resistance appears to increase from some value in excess of zero at the ground surface to a maximum value that occurs at some depth between the ground surface and half of the foundation embedment. The soil resistance then decreases to zero at the rotation point which occurs roughly between half and three quarters of the foundation embedment depth. Below the rotation point the resistance again increases to a maximum value at the bottom of the foundation. It has been stated by Davisson and Prakash (9) that the upper point of maximum soil resistance shifts downward along the foundation although the shape of the soil resistance curve remains the same. The fixed location of the pressure cells on this test shaft prevented the observation of this phenomenon in this study.

Ultimate Soil Resistance. - Since a structural failure occurred in the test shaft before soil failure was attained, it was not possible to record the ultimate lateral soil resistance. However, a comparison can be made between the soil resistance recorded by the pressure cells for the highest applied lateral load and the calculated ultimate soil reactions predicted by other researchers. As defined in Eq. 4 (p. 14), the soil reaction,  $p$ , is the force per unit length of shaft. It can be calculated by multiplying the soil resistance by the shaft diameter,  $B$ . Fig. 30 presents a comparison of the soil reaction, to a depth of 10 ft (3.05 m), recorded on the test shaft at the maximum load of 169 kips (752 kN) with ultimate soil reactions,  $p_u$ , calculated by methods proposed by Rankine (37), Hansen (12), Matlock (22), and Reese (28). The soil reaction for the test shaft was calculated from the pressures

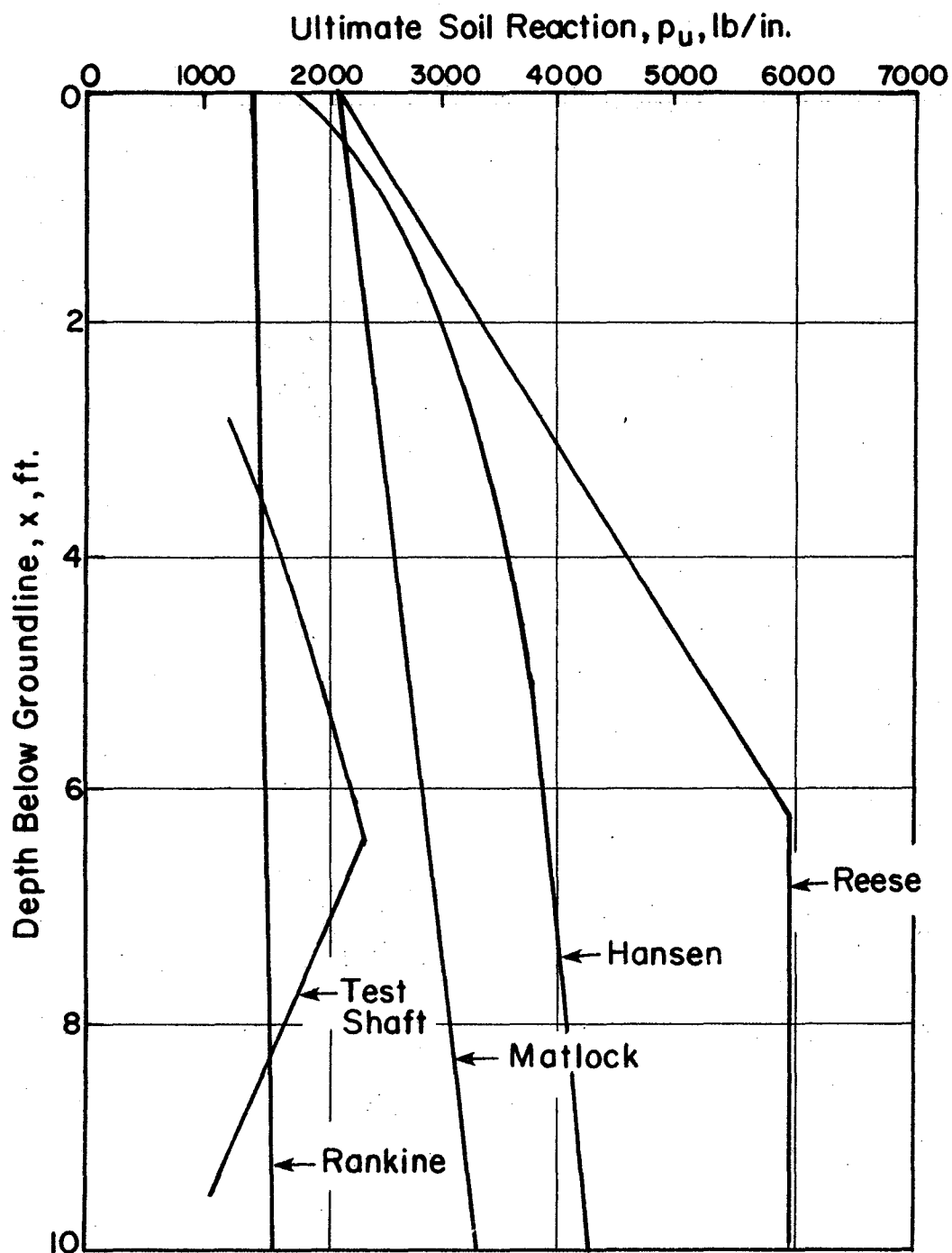


FIG. 30— Ultimate Soil Reaction vs. Depth Below Groundline  
 Note: Test Shaft Data are not Ultimate Values Because  
 Shaft Failed Before Ultimate Load was Reached.  
 1 ft. = 0.3048 m; 1 lb/in. = 1.75 N/cm

recorded on cells 875, 877, and 879. The equations used to predict the ultimate soil reactions according to Rankine, Hansen, Matlock, and Reese are:

$$\text{Rankine: } p_u = (\gamma x + 2C_u) B \dots \dots \dots (13)$$

$$\text{Hansen: } p_u = K_c C_u B \dots \dots \dots (14)$$

$$\text{Matlock: } p_u = \left[ 3 + \frac{\gamma x}{C_u} + \frac{0.5x}{B} \right] C_u B \dots \dots \dots (15)$$

$$\text{Reese: } p_u = \left[ 3 + \frac{\gamma x}{C_u} + \frac{2.83x}{B} \right] C_u B \dots \dots \dots (16)$$

The term  $\gamma$  is the unit weight of the overburden material. The terms  $C_u$ ,  $B$ , and  $K_c$  have been defined in Eqs. 11 and 12 (p. 36), while  $x$  has been defined in Eq. 10 (p. 22).

Fig. 30 indicates that even though the load test did not produce ultimate soil reactions, the Rankine predictions were exceeded, thus verifying the conservative nature of this method. The general form of Eqs. 15 and 16 was developed by Reese (28). The equation used by Matlock has been empirically adjusted using the results of lateral load tests on piles in soft clays. However, in lateral load tests in stiff clays, Matlock's equation has in some instances predicted satisfactory results, while Reese's equation has yielded values in excess of those determined experimentally (39, 31). Additional testing will be needed before it can be determined which of the above equations can best predict ultimate soil reactions. This is especially true since an ultimate value was not attained on this test.

#### Load-Deflection Characteristics

As discussed previously, the initial loads applied to the drilled

shaft were a simulation of the loads produced during the backfilling of the retaining wall studied by Wright et al. (42). The daily loads applied to the retaining wall, calculated from the data presented by Wright et al., are shown in Table 4 along with the loads applied to the test shaft. The resulting deflections are also shown in Table 4. The deflection that occurred during the 13 days when no load was added to the shaft is also shown. The shaft movement during the 13 day period was only 0.042 in. (1.07 mm). This movement was probably due to a combination of creep and a slight amount of structural breakdown of the soil due to the cyclic loading effect of the expanding and contracting cables, caused by temperature variation.

Table 4. - Results of Retaining Wall Loading Simulation of Test Shaft

Day	Calculated Load, kips	Actual Load, kips	Deflection, in.
1	0.068	-	-
2	0.543	-	-
3	1.83	2.45	0.002
4	4.37	4.60	0.007
5	8.47	7.59	0.012
6	14.6	13.3	0.022
7	23.3	22.8	0.054
8	34.9	34.5	0.120
21	34.9	34.5	0.162

The load-deflection curve for the load test is presented in Fig. 31. The shaft had deflected 3.220 in. (8.18 cm) when the structural failure in the shaft occurred at 169 kips (752 kN). The unloading and reloading curves that resulted from the two week delay for repairs of the loading system are also presented in Fig. 31. It appears that the delay had little effect on the shape of the entire curve.

#### Load-Rotation Characteristics

The load-rotation curve for the load test is shown in Fig. 32. The structural failure of the shaft occurred at a rotation of about  $1^{\circ}53'$ . This rotation is considerably less than the  $5^{\circ}$  rotation needed to develop the ultimate soil resistance as indicated by Ivey and Dunlap (16). Fig. 32 also indicates a possible change in slope between the final portion of initial loading curve and the initial portion of the reloading curve of the shaft.

#### Rotation Point of the Test Shaft

Conflicting results on the location of the rotation point of the test shaft were indicated by the results of the inclinometer and the pressure cells. As the lateral load exceeded 100 kips (445 kN) the inclinometer results indicated that the shaft was rotating about a point roughly 8 ft (2.44 m) deep. The rotation point was obtained by dividing the measured deflection of the shaft at the ground surface by the tangent of the rotation angle. The pressure cell readings seemed to indicate that the rotation point was in the area of cell 881, about 13 ft (3.96 m) deep. After the structural failure of the shaft, it became apparent that flexural bending had been occurring below the bottom of the anchor bolts at 8 ft (2.44 m) depth. Consequently, the

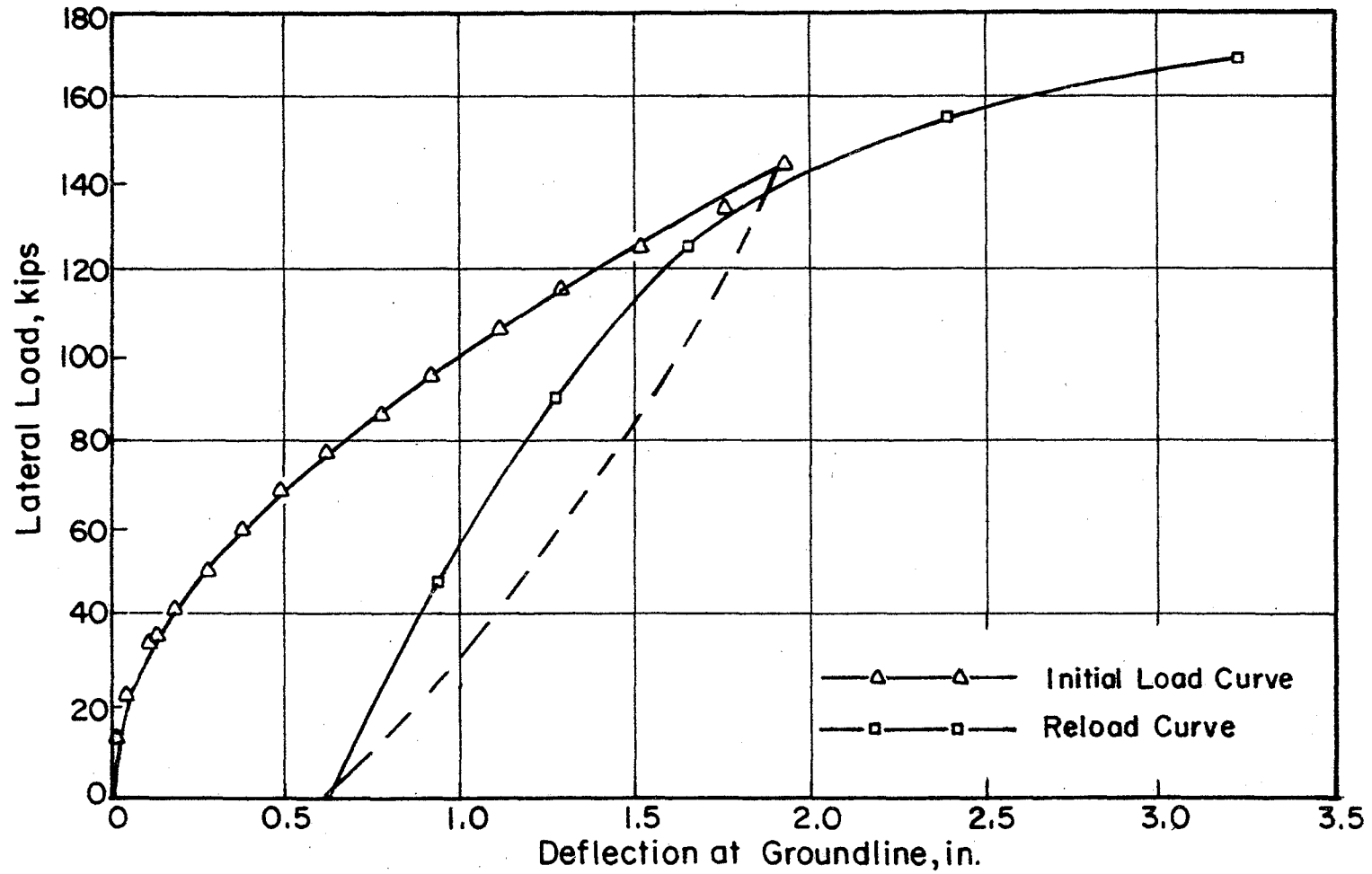


FIG. 31 - Lateral Load vs. Deflection at Groundline  
1 kip = 4.45 kN; 1 in. = 2.54 cm

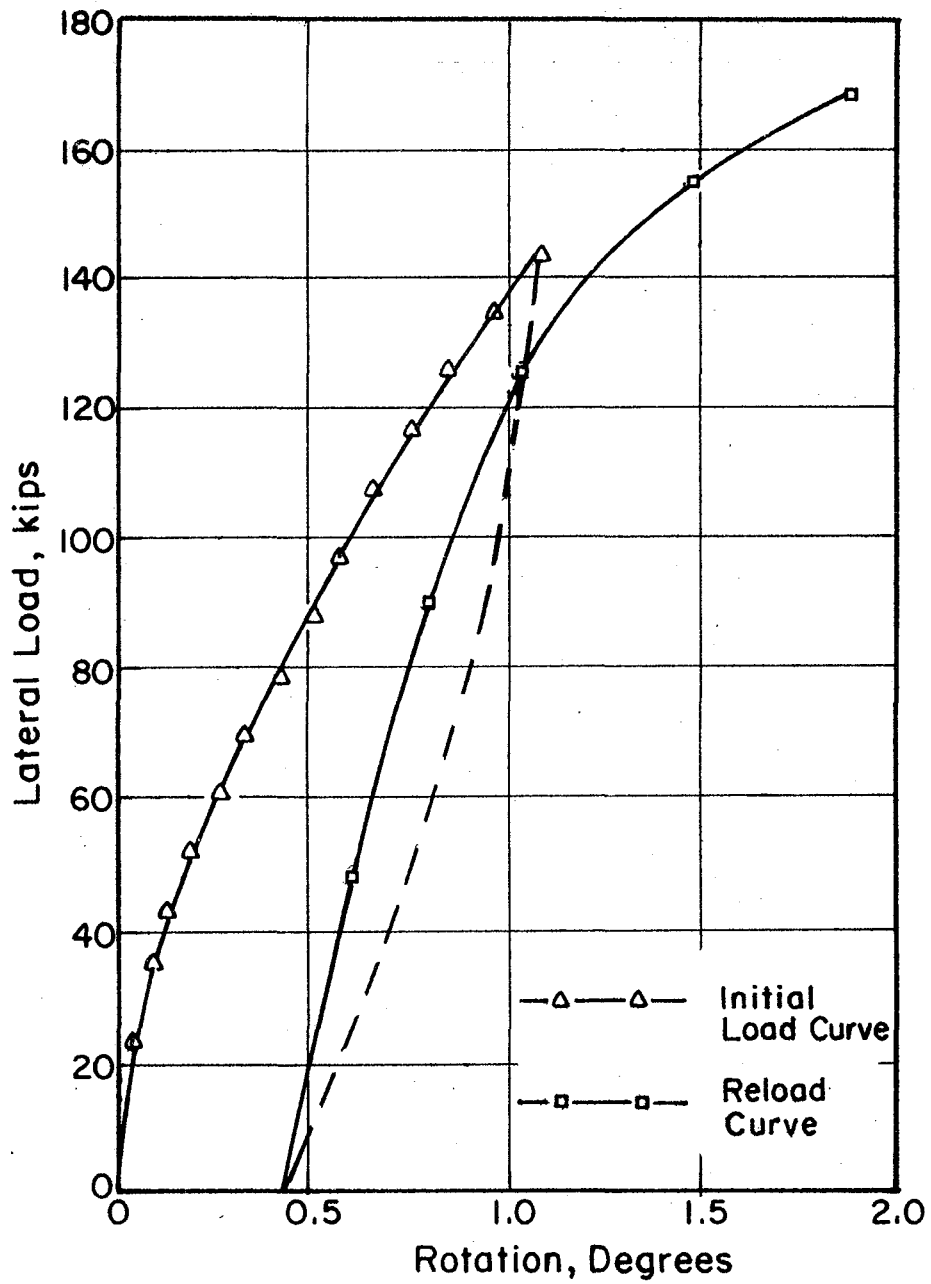


FIG. 32— Lateral Load vs. Rotation  
 1 kip = 4.45 kN

shaft was probably rotating as a unit about a point approximately 13 ft (3.96 m) deep, while at the same time it was experiencing a flexural rotation at a depth of 8 ft (2.44 m).

Analytical studies by Hays et al. (13) indicated that the rotation point was not constant but shifted downward from some point below the middle of the foundation for light loads to a point beyond three quarters of the embedment depth for failure loads. Since the test shaft in this study experienced flexural bending and an ultimate load was not attained, it was not possible to verify Hays' results.

#### Ultimate Loads on Rigid Shafts

It has been shown that a cylindrical foundation will behave as a rigid member if its relative stiffness ratio,  $D/R$  or  $D/T$ , is two or less. It was also shown that this relative stiffness requirement will be satisfied if the depth over diameter ratio,  $D/B$ , is limited to approximately six. The relative stiffness ratio,  $D/R$ , for the test shaft in this study was calculated to be 1.96 while the depth over diameter ratio,  $D/B$ , was 6.6. Therefore, the test shaft generally conformed to the requirements of a rigid shaft.

The methods discussed in the section on rigid foundations were used to calculate the ultimate loads that could be carried by the test shaft and two other rigid shafts for which all needed information was available. The ultimate load is the maximum lateral load that the soil in contact with the foundation can withstand. Continued foundation deflection and rotation may occur with no increase in load when the ultimate load is reached. Calculated ultimate loads are presented in Table 5. It should be noted that for the current study no real

comparison can be made for ultimate loads since the shaft failed structurally. However, a relative comparison can be made between the various calculated ultimate loads and the highest load applied to the shaft. Of the three load tests presented in Table 5, the Bryan test probably offers the best comparison. The Galveston test was conducted without any problems but as shown in the table, the measured load greatly exceeded any of the predicted ultimate loads. This was probably due to a stiff surface layer of clay that had a cohesive shear strength six times greater than the shear strength of the soil on the lower half of the shaft. It should also be noted that two variations of the method presented by Ivey and Dunlap were used to calculate ultimate loads. As stated earlier, this method is a semi-empirical method in which a

Table 5. - Comparison of Lateral Load Test Results with Calculated Ultimate Loads

Method	Load Test		
	TTI Project 211 Current Study	TTI Project 105 Galveston Test	TTI Project 105 Bryan Test
Measured Load, kips	169+	5.50	12.40
Ivey and Dunlap, kips	286	2.88	15.14
Ivey and Dunlap, with $\phi = 0$ , kips	130	1.35	8.72
Ivey and Hawkins, kips	89	0.96	5.94
Broms, kips	260	1.55	9.54
Hays et al., kips	221	1.75	8.94
Hansen, kips	271	2.02	12.40

modifying factor was applied to the Rankine coefficients of passive and active earth pressure. Laboratory tests on cohesive samples to determine the modifying factor for these type of soils were conducted in such a way that the angle of shearing resistance,  $\phi$ , as well as the undrained cohesive shear strength,  $C_u$ , was determined. Consequently, the determined modifying factor assumes the use of both the cohesive shear strength and the angle of shearing resistance when determining the ultimate load of a foundation.

As expected, Table 5 indicates that the Ivey and Hawkins method, which is based on Rankine passive earth pressures, consistently gives the most conservative results. The Ivey and Dunlap method used with the angle of shearing resistance,  $\phi$ , set equal to zero, also gives consistently conservative results, though not nearly as conservative as the Ivey and Hawkins method. The Ivey and Hawkins method underpredicted the measured load for the Galveston test by 473%, while the Ivey and Dunlap method was conservative by 307%. For the Bryan test, the Ivey and Hawkins method was 108% on the conservative side, while the Ivey and Dunlap method was conservative by 42%. The Ivey and Dunlap method, using both the cohesive shear strength and the angle of shearing resistance, consistently predicted the highest ultimate load. The method was conservative by 91% for the Galveston test, but 18% unconservative for the Bryan test. The other three methods, Broms, Hays et al., and Hansen, all predicted ultimate loads between those predicted by the two variations of the Ivey and Dunlap method.

## TENTATIVE DESIGN PROCEDURE

When designing drilled shafts to support precast panel retaining walls, it is probably appropriate to use rigid foundation design procedures. Two reasons for the use of rigid design procedures can be given. First, the lateral loads on most retaining walls should not be of such large magnitude as to necessitate a deeply embedded shaft that would require elastic analysis. Secondly, in most instances rigid design procedures are less complicated than elastic solutions. Many elastic analysis procedures require computer solutions. It should be noted though, that in order to be reasonably assured of rigid foundation behavior, the depth over diameter ratio,  $D/B$ , of the drilled shaft should be limited to about six or less.

Before the depth and diameter of a shaft supporting a retaining wall can be determined, several design parameters have to be obtained. These parameters include the resultant force acting on the retaining wall, the point of application of the resultant force, the undrained cohesive shear strength of the soil, the allowable shaft rotation, and the creep potential of the soil.

### Force Acting on Retaining Wall

The force acting on a retaining wall is the resultant of the lateral pressure in the backfill. As a result of a study conducted on an instrumented precast panel retaining wall, Wright et al. (42) developed an equation to predict the resultant force of a level, cohesionless backfill with no surcharge, acting on a retaining wall. The equation in terms of force is:

$$F_r = 0.25 \gamma h^2 L (K_a + 0.8) \dots \dots \dots (17)$$

where h is the height of the wall and L is the length of the panel, pilaster to pilaster. The term  $\gamma$  has been defined in Eq. 13 (p. 71). The expression  $K_a$  is the Rankine coefficient of active earth pressure. This expression is defined as:

$$K_a = \cos \zeta \left[ \frac{\cos \zeta - \sqrt{\cos^2 \zeta - \cos^2 \phi'}}{\cos \zeta + \sqrt{\cos^2 \zeta - \cos^2 \phi'}} \right] \dots \dots \dots (18)$$

where  $\zeta$  is the angle of the slope of the backfill to the horizontal and  $\phi'$  is the effective angle of shearing resistance of the backfill material.

#### Application Point of Resultant Force

Wright et al. also developed an equation to calculate the point of application of the resultant force,  $F_r$ , of a level backfill with no surcharge. The equation is:

$$\bar{h} = \frac{h}{2} \left[ \frac{K_a + 0.267}{K_a + 0.8} \right] \dots \dots \dots (19)$$

where  $\bar{h}$  is the height of the application point above the base of the retaining wall. The expressions h and  $K_a$  were defined in Eqs. 17 and 18.

#### Soil Shear Strength

The SDHPT often uses the TCP Test as the primary means of determining soil shear strength in routine subsurface investigations.

Laboratory testing to determine soil shear strength is often omitted because of the additional expense involved. The TCP Test consists of driving a 3 in. (7.62 cm) diameter cone attached to a drill rod, with a

170 lb (77 kg) hammer. The hammer is dropped 2 ft (0.61 m) for each blow. The cone is seated with 12 blows and the number of blows, N, required to produce the next foot of penetration is recorded (10).

An improved correlation between the TCP blow count, N, and the undrained cohesive shear strength has recently been reported by Duderstadt et al. (10). The correlation has been reported for highly plastic homogeneous clays (CH) and for homogeneous clays of low to medium plasticity (CL). The results were reported as:

$$\text{Homogeneous CH : } C_u = 0.067N \dots \dots \dots (20)$$

$$\text{Homogeneous CL : } C_u = 0.053N \dots \dots \dots (21)$$

If it is desired by the designer a factor of safety may be applied to the shear strength,  $C_u$ .

Allowable Shaft Rotation

If excessive rotation of the drilled shaft were allowed to occur, objectionable deflection of the panel, retaining wall in terms of aesthetics and possibly serviceability would result. It is therefore desirable to incorporate a factor of safety to guard against this potential problem.

Based on the finding that the ultimate load of a rigid shaft generally occurs at a rotation of  $5^\circ$ , Ivey and Dunlap (16) proposed the following equation to be used as a factor of safety against undesirable rotation:

$$P_\alpha = \frac{Fr}{1 - \frac{(5-\alpha)^2}{25}} \dots \dots \dots (22)$$

where Fr is the resultant force transmitted from the wall to the shaft (from Eq. 17) and  $\alpha$  is the desired limiting angle of rotation.  $P_\alpha$

is the force acting at height  $\bar{h}$  necessary to rotate the shaft through the limiting angle of rotation,  $\alpha$ .

The degree of rotation producing objectionable lateral deflection of a retaining wall is arbitrary. However, in view of the deflections and rotations recorded on the test shaft, it is likely that a total rotation of  $2^\circ$  would be aesthetically objectionable. The total rotation will probably consist of two separate movements. The first is the initial rotation that occurs after the application of the lateral load. The second is a long term rotation that occurs as a result of soil creep. In view of these considerations it is recommended that  $\alpha$  be limited to  $1^\circ$  or less.

#### Soil Creep

The time-dependent deformation behavior of a soil mass under a given set of sustained stresses is referred to as creep. It is a function of several variables, including soil type, soil structure, and stress history (11). Since the load resisted by a retaining wall is a sustained load, the soil in contact with the drilled shafts supporting the wall will be subjected to the creep phenomenon.

Dunlap et al. (11), in a study of sustained loads on drilled shafts, recommended that a factor of safety based on the soil type be applied to the ultimate load causing  $5^\circ$  rotation. A factor of safety of 3 is recommended for soft and stiff fissured clays. For stiff non-fissured clays, a factor of safety of 2 is recommended. It is stated that although these safety factors should result in a rotation that terminates, it is likely that the rotation will be significant and in the order of  $1^\circ$ . Therefore, if an appropriate safety factor for creep is used in

conjunction with a limiting angle of rotation,  $\alpha$  equals  $1^\circ$  or less, it is likely that the total shaft rotation will be limited to  $2^\circ$  or less.

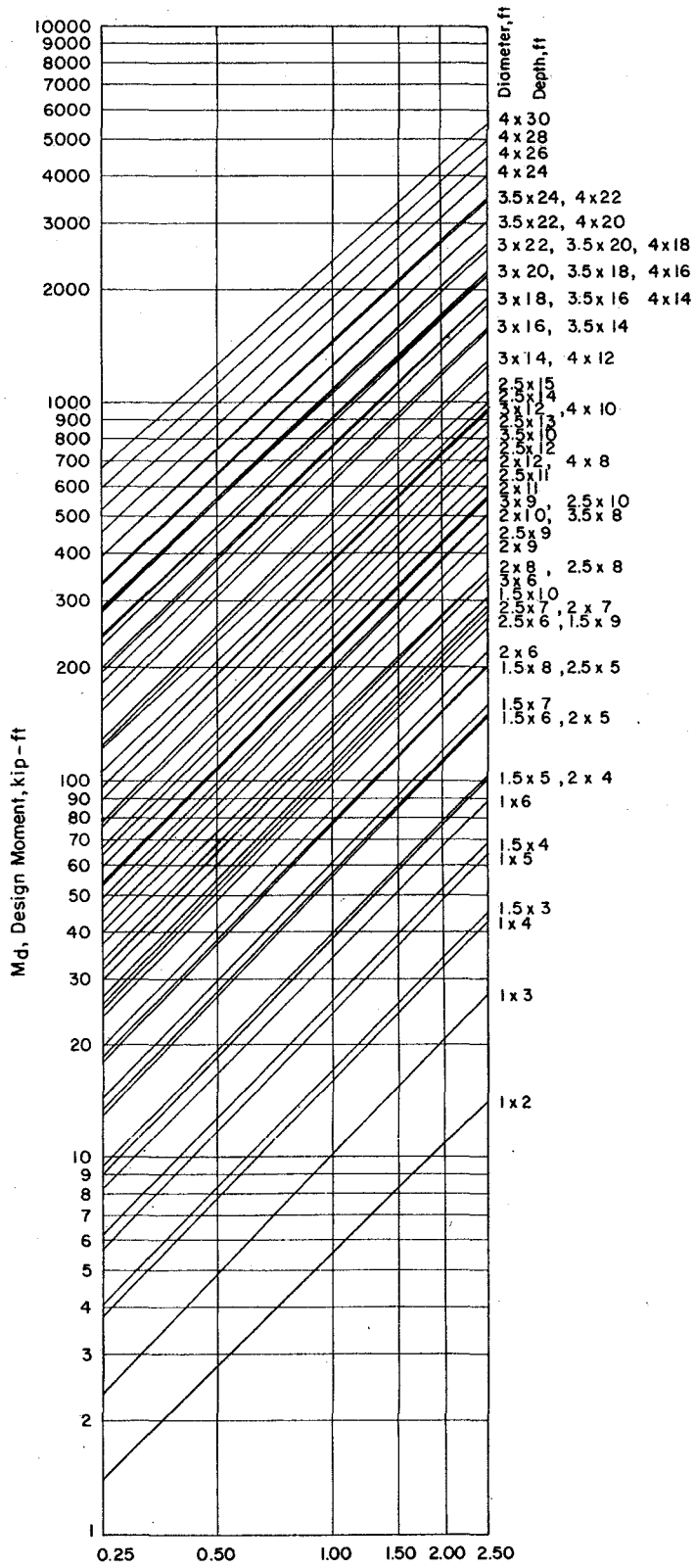
#### Drilled Shaft Design Method

In view of the fact that this study was conducted during the first year of a multi-year research project, insufficient data have been collected for the development of new or improved design criteria. Therefore, at this point in the project it was decided to propose a tentative design procedure based on existing design methods. Based on the results presented in Table 5, the method proposed by Ivey and Dunlap with  $\phi$  equal to zero has been selected. Although this method appears to produce conservative results in comparison to some of the other methods shown in Table 5, it was felt that until more load test data become available this method would provide a safe means of design. In order to expedite design procedures, a design chart using the Ivey and Dunlap method with  $\phi$  equal to zero has been developed by Lytton (19). The chart is presented in Fig. 33.

#### Proposed Design Procedure

The following procedure is recommended as the tentative design method for the design of drilled shafts supporting precast panel retaining walls:

1. Use Eq. 17 to calculate the force,  $F_r$ , that will be applied to the shaft by the retaining wall.
2. Use Eq. 19 to calculate the application point of the force,  $\bar{h}$ .
3. Setting  $\alpha$  equal to  $1^\circ$  or less, calculate the resulting force,  $P_\alpha$ , by means of Eq. 22.
4. Choose the appropriate factor of safety for soil creep and



$C_u$ , Undrained Cohesive Shear Strength, tsf ( $\phi = 0$ )

FIG. 33 - Design Chart I (After Lytton)

1 tsf = 95.8 kN/m<sup>2</sup>; 1 kip-ft = 1.36 kN-m; 1 ft = 0.3048 m

calculate the design force,  $P_d$ , as:  $P_d = (P_\alpha)(F.S.)$ .

5. Calculate the resulting design moment as:  $M_d = (P_d)(\bar{h})$ .
6. Calculate the undrained cohesive shear strength,  $C_u$ , of the soil by use of Eq. 20 or 21. A factor of safety may be applied if desired.
7. Enter Design Chart I with moment,  $M_d$ , on vertical scale and undrained cohesive shear strength,  $C_u$ , on horizontal scale. Find the intersection of  $M_d$  and  $C_u$ . Travel in a vertical direction from intersection of  $M_d$  and  $C_u$  until first diagonal line is encountered. Follow diagonal line to the right side of the chart and read shaft diameter and depth.

#### Example of Design Procedure

The following example is provided as an aid in the design of precast panel retaining wall foundations. A drilled shaft foundation is to be designed for the following situation.

A retaining wall is to consist of panels having a height of 10 ft (3.05 m) and length of 12 ft (3.66 m). The backfill material will be clean sand having an effective angle of shearing resistance,  $\phi'$ , equal to  $36^\circ$  and unit weight,  $\gamma$ , equal to 0.115 kcf ( $18.60 \text{ kN/m}^3$ ). The backfill will have no additional surcharge and will have a horizontal slope. The soil at the construction site is a stiff non-fissured homogeneous clay that has been classified CH. The average N value obtained from the TCP Test conducted at the site was 15. The limiting angle of rotation,  $\alpha$ , is  $1^\circ$ . Apply a factor of safety of 1.3 to  $C_u$ .

Step 1a: Using Eq. 18:

$$K_a = \cos 0^\circ \left[ \frac{\cos 0^\circ - \sqrt{\cos^2(0^\circ) - \cos^2(36^\circ)}}{\cos 0^\circ + \sqrt{\cos^2(0^\circ) - \cos^2(36^\circ)}} \right] = 0.260$$

Step 1b: Using Eq. 17:

$$F_r = (0.25)(.115)(10)^2(12)(0.260 + 0.8) = 36.6 \text{ kips}$$

Step 2: Using Eq. 19:

$$\bar{h} = \frac{10}{2} \left[ \frac{0.260 + 0.267}{0.260 + 0.8} \right] = 2.49 \text{ ft}$$

Step 3: Using Eq. 22:

$$P_\alpha = \frac{36.6}{1 - \frac{(5 - 1)^2}{25}} = 101.7 \text{ kips}$$

Step 4: Calculate  $P_d$ ; soil conditions indicate that F.S. = 2 is appropriate.

$$P_d = (101.7)(2) = 203 \text{ kips}$$

Step 5: Calculate  $M_d$ :

$$M_d = (203)(2.49) = 505 \text{ kip-ft}$$

Step 6: Using Eq. 20:

$$C_u = (0.067)(15) = 1.00 \text{ tsf}$$

Applying F.S. = 1.3:

$$C_u = \frac{1.00}{1.3} = 0.77 \text{ tsf}$$

Step 7: Using Design Chart I:

Shaft diameter = 3 ft

Shaft depth = 16 ft

## CONCLUSIONS AND RECOMMENDATIONS

Even though the test shaft failed structurally during lateral loading and an ultimate load was not attained as hoped, several beneficial observations were made during the test. The conclusions obtained from the first year of the research study, along with recommendations for future studies, are presented below.

### Conclusions

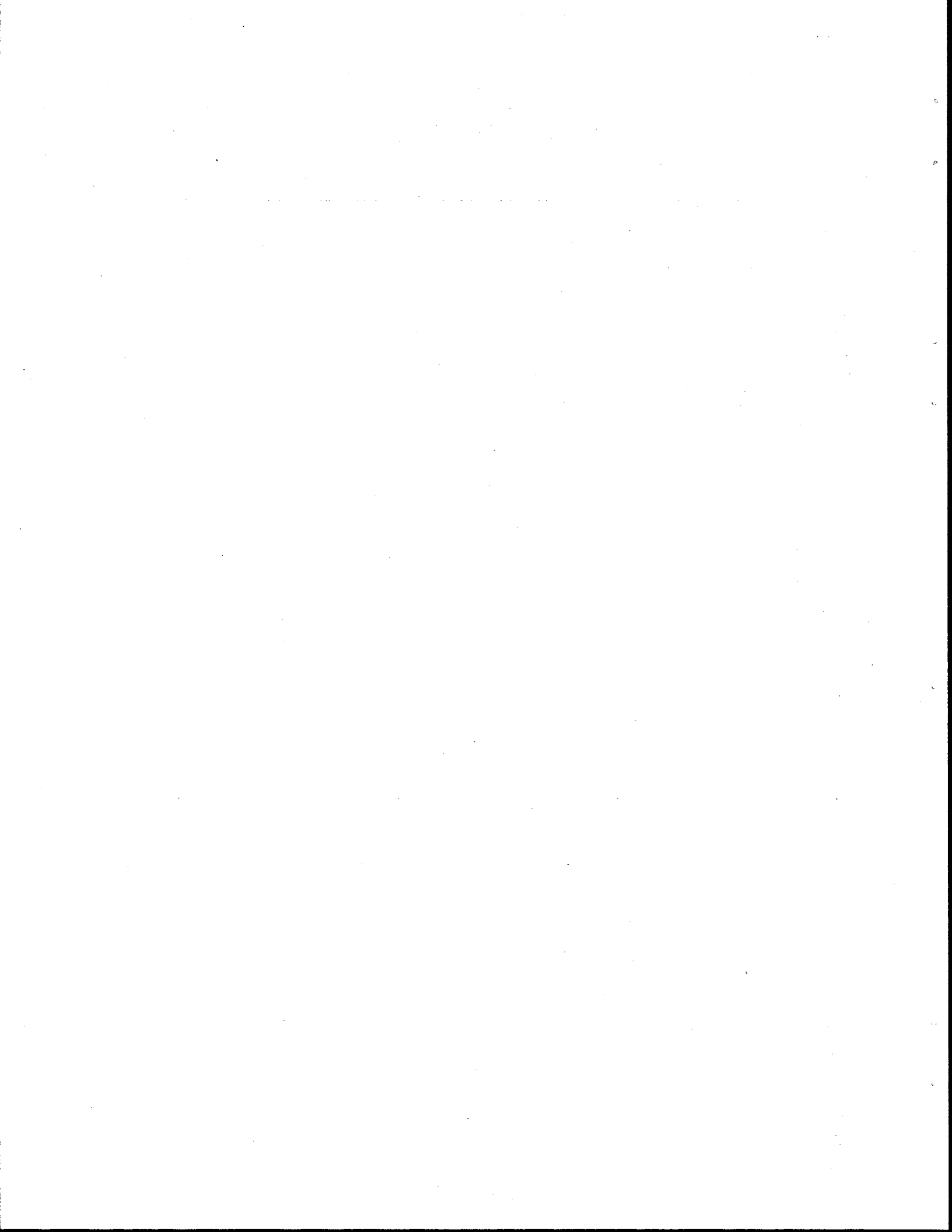
1. It is recognized that the serviceability and aesthetic appeal of a retaining wall depends on the amount of lateral deflection experienced by the wall. However, the magnitude of deflection that may occur before becoming objectionable is arbitrary. When the resultant force corresponding to that measured on the wall reported by Wright et al. (42) was applied to the test shaft, the magnitude of the resulting deflection, rotation, and soil reaction was small. Based on these observations it is concluded that the drilled shafts supporting the precast retaining wall reported by Wright et al. were oversized. It is felt that the dimensions of those shafts could have been reduced by some amount without resulting in an objectionable deflection.
2. Before the structural failure of the test shaft occurred, its lateral deflection was of such magnitude as to probably be aesthetically objectionable. It is concluded that allowable deflection rather than ultimate lateral load may be the controlling criterion for the design of drilled shafts supporting precast panel retaining walls.

3. The Ivey and Hawkins design method, which is based on Rankine's passive earth pressure formula, is not recommended for the design of laterally loaded drilled shafts because of its conservative nature. Fig. 30 indicates that even though the lateral load test did not produce ultimate soil reactions, the Rankine predictions were still exceeded.
4. Based on the comparison of the load tests shown in Table 5, it is concluded that the Ivey and Dunlap method with  $\phi$  equal to zero will produce conservative drilled shaft designs. However, its use is recommended until additional lateral load tests can be conducted.
5. Any desired degree of conservatism may be incorporated in the tentative design procedure by using conservative values of: the limiting angle of rotation,  $\alpha$ ; the factor of safety applied to the undrained cohesive shear strength,  $C_u$ ; and the factor of safety applied for soil creep.

#### Recommendations

1. Future lateral load tests on rigid drilled shafts should be conducted to failure in order to obtain ultimate loads and ultimate soil reactions that are needed to develop improved or new design procedures.
2. Future ultimate load tests should be conducted on shafts of varying depths and diameters.
3. Sustained lateral load tests should be conducted on shafts of varying depths and diameters in order to study the creep phenomenon.

4. Future lateral load tests should be conducted in varying types of soil.
5. A maximum value for the total rotation of a drilled shaft supporting a precast panel retaining wall should be determined.



## APPENDIX I - REFERENCES

1. Adams, J.I., and Radhakrishna, H.S., "The Lateral Capacity of Deep Augered Footings," Proceedings, Eighth International Conference on Soil Mechanics and Foundation Engineering, Vol. 2.1, Moscow, USSR, 1973, pp. 1-8.
2. Bowles, Joseph E., Foundation Analysis and Design, 1st. ed., McGraw-Hill Book Co., New York, 1968, pp. 503-512.
3. Bowles, Joseph E., Analytical and Computer Methods in Foundation Engineering, McGraw-Hill Book Co., New York, 1974, pp. 147-186, 291-314.
4. Bowles, Joseph E., Foundation Analysis and Design, 2nd ed., McGraw-Hill Book Co., New York, 1977, pp. 630-632.
5. Broms, Bengt B., "Lateral Resistance of Piles in Cohesive Soils," Journal of the Soil Mechanics and Foundation Division, ASCE, Vol. 90, No. SM2, Proc. Paper 3825, March, 1964, pp. 27-63.
6. Corbett, David A., Coyle, Harry M., Bartoskewitz, Richard E., Milberger, Lionel J., "Evaluation of Pressure Cells Used for Field Measurements of Lateral Earth Pressures on Retaining Walls," Research Report No. 169-1, Texas Transportation Institute, Texas A&M University, Sept., 1971.
7. D'Appolonia, Elio, D'Appolonia, David J., and Ellison, Richard D., "Drilled Piers", in Foundation Engineering Handbook, Winterkorn, Hans F., and Fang, Hsai-Yang (ed.), Van Nostrand Reinhold Co., New York, 1975, pp. 601-615.
8. Davisson, M.T., and Gill, H.L., "Laterally Loaded Piles in a Layered Soil System," Journal of the Soil Mechanics and Foundation Division, ASCE, Vol. 89, No. SM3, Proc. Paper 3509, May, 1963, pp. 63-94.
9. Davisson, M.T., and Prakash, Shamsheer, "A Review of Soil-Pole Behavior," Highway Research Record No. 39, 1963, pp. 25-48.
10. Duderstadt, Franklin J., Coyle, Harry M., and Bartoskewitz, Richard E., "Correlation of the Texas Cone Penetrometer Test N-Value with Soil Shear Strength," Research Report 10-3F, Texas Transportation Institute, Texas A&M University, Aug., 1977.
11. Dunlap, Wayne A., Ivey, Don L., and Smith, Harry L., "Long-Term Overturning Loads on Drilled Shaft Footings," Research Report 105-5F, Texas Transportation Institute, Texas A&M University, Sept., 1970.
12. Hansen, J. Brinch, "The Ultimate Resistance of Rigid Piles Against Transversal Forces," Danish Geotechnical Institute, Bulletin 12, 1961.

13. Hays, C.O., Davidson, J.L., Hagan, E.M., and Risitano, R.R., "Drilled Shaft Foundation for Highway Sign Structures," Research Report D647F, Engineering and Industrial Experiment Station, University of Florida, Dec., 1974.
14. Heijnen, W.J., and Lubking, P., "Lateral Soil Pressure and Negative Friction on Piles," Proceedings, Eighth International Conference on Soil Mechanics and Foundation Engineering, Vol. 2.1, Moscow, USSR, 1973, pp. 143-147.
15. Ivey, Don L., "Theory, Resistance of a Drilled Shaft Footing to Overturning Loads," Research Report 105-1, Texas Transportation Institute, Texas A&M University, Feb., 1968.
16. Ivey, Don L., and Dunlap, Wayne A., "Design Procedure Compared to Full-Scale Tests of Drilled Shaft Footings," Research Report 105-3, Texas Transportation Institute, Texas A&M University, Feb., 1970.
17. Ivey, Don L., and Hawkins, Leon, "Signboard Footings to Resist Wind Loads," Civil Engineering, Vol. 36, No. 12, Dec., 1966, pp. 34-35.
18. Ivey, Don L., Koch, Kenneth J., and Raba, Carl F., Jr., "Resistance of a Drilled Shaft Footing to Overturning Loads, Model Tests and Correlation with Theory," Research Report 105-2, Texas Transportation Institute, Texas A&M University, July, 1968.
19. Lytton, Robert L., "Design Charts for Minor Service Structure Foundations," Research Report 506-1F, Texas Transportation Institute, Texas A&M University, Sept., 1971.
20. McClelland, Bramlette, and Focht, John A., Jr., "Soil Modulus for Laterally Loaded Piles," Journal of the Soil Mechanics and Foundations Division, ASCE, Vol. 82, No. SM4, Proc. Paper 1081, Oct., 1956, pp. 1081-1 - 1081-22.
21. Mason, H.G., and Bishop, J.A., "Measurement of Earth Pressure and Deflection Along the Embedded Portion of a 40-ft Steel Pile," ASTM Special Technical Publication, No. 154-A, 1954, pp. 1-21.
22. Matlock, Hudson, "Correlations for Design of Laterally Loaded Piles in Soft Clay," Preprints, Second Annual Offshore Technology Conference, Paper No. OTC 1204, 1970, pp. 577-594.
23. Matlock, Hudson, and Reese, Lymon C., "Generalized Solutions for Laterally Loaded Piles," Journal of the Soil Mechanics and Foundation Division, ASCE, Vol. 86, No. SM5, Part I, Proc. Paper 2626, Oct., 1960, pp. 63-91.
24. O'Neill, Michael W., and Reese, Lymon C., "Behavior of Axially Loaded Drilled Shafts in Beaumont Clay," Research Report 89-8, Center for Highway Research, The University of Texas at Austin, Dec., 1970.

25. Osterberg, J.O., "Lateral Stability of Poles Embedded in a Clay Soil," Northwestern University Project 208, Bell Telephone Laboratories, Evanston, Illinois, Dec., 1958.
26. Outdoor Advertising Association of America, Engineering Manual, Outdoor Advertising Association of America, Chicago, Illinois, 1955.
27. Poulos, Harry G., "Behavior of Laterally Loaded Piles: I-Single Piles," Journal of the Soil Mechanics and Foundation Division, ASCE, Vol. 97, No. SM5, Proc. Paper 8092, May, 1971, pp. 711-731.
28. Reese, Lymon C., Discussion of "Soil Modulus for Laterally Loaded Piles," by Bramlette McClelland and John A. Focht, Jr., Transactions, ASCE, Vol. 123, 1958, pp. 1071-1074.
29. Reese, Lymon C., "Laterally Loaded Piles: Program Documentation," Journal of the Geotechnical Engineering Division, ASCE, Vol. 103, No. GT4, Proc. Paper 12862, April, 1977, pp. 287-305.
30. Reese, Lymon C., Cox, William R., and Koop, Francis D., "Analysis of Laterally Loaded Piles in Sand," Preprints, Sixth Annual Offshore Technology Conference, Paper No. OTC 2080, 1974, pp. 473-483.
31. Reese, Lymon C., Cox, William R., and Koop, Francis D., "Field Testing and Analysis of Laterally Loaded Piles in Stiff Clay," Preprints, Seventh Annual Offshore Technology Conference, Paper No. OTC 2312, 1975, pp. 671-690.
32. Seiler, J.F., "Effect of Depth of Embedment on Pole Stability," Wood Preserving News, Vol. 10, No. 11, Nov., 1932, pp. 152-168.
33. Shilts, W.L., Graves, L.D., and Driscoll, G.G., "A Report of Field and Laboratory Tests on the Stability of Posts Against Lateral Loads," Proceedings, Second International Conference on Soil Mechanics and Foundation Engineering, Vol. 5, Rotterdam, Holland, 1948, pp. 107-122.
34. Spillers, William R., and Stoll, Robert D., "Lateral Response of Piles," Journal of the Soil Mechanics and Foundation Division, ASCE, Vol. 90, No. SM6, Proc. Paper 4121, Nov., 1964, pp. 1-9.
35. Stobie, James C., "Pole Footings," Journal of the Institute of Engineers, Australia, Vol. 2, 1930, pp. 58-63.
36. Terzaghi, Karl, "Evaluation of Coefficients of Subgrade Reaction," Geotechnique, London, Vol. 5, No. 4, Dec., 1955, pp. 297-326.
37. Terzaghi, Karl, and Peck, Ralph B., Soil Mechanics in Engineering Practice, 2nd ed., John Wiley & Sons, Inc., New York, 1967, pp. 198-200.
38. Vesic, Aleksandar B., "Bending of Beams Resting on Isotropic

Elastic Solid," Journal of the Engineering Mechanics Division, ASCE, Vol. 87, No. EM2, Proc. Paper 2800, April, 1961, pp. 35-53.

39. Welch, Robert C., and Reese, Lymon C., "Lateral Load Behavior of Drilled Shafts," Research Report 89-10, Center for Highway Research, The University of Texas at Austin, May, 1972.
40. Winkler, E., Die Lehre von Elastizitat und Festigkeit (On Elasticity and Fixity), 1867, Prague, 1967.
41. Woodward, Richard J., Gardner, William S., and Greer, David M., Drilled Pier Foundations, McGraw-Hill Book Co., New York, 1972, 287 pp.
42. Wright, William V., Coyle, Harry M., Bartoskewitz, Richard E., and Milberger, Lionel J., "New Retaining Wall Design Criteria Based on Lateral Earth Pressure Measurements," Research Report No. 169-4F, Texas Transportation Institute, Texas A&M University, Aug., 1975.

## APPENDIX II - NOTATION

The following symbols are used in this report:

- B = foundation diameter;
- $C_u$  = undrained cohesive shear strength;
- D = embedded depth;
- d = width of rectangular vertical strip;
- E = modulus of elasticity of foundation;
- $E_s$  = soil modulus;
- $E_{s0}$  = initial value of soil modulus;
- EI = flexural stiffness of foundation;
- F = applied lateral load;
- $F_r$  = resultant force transmitted from retaining wall to drilled shaft;
- $F_s$  = weight of structure and footing;
- $F_{zd}$  = vertical force beneath foundation;
- H = height of lateral load application;
- h = height of retaining wall;
- $\bar{h}$  = height of application point above base of retaining wall;
- I = moment of inertia of foundation;
- $K_a$  = Rankine coefficient of active earth pressure;
- $K_c$  = earth pressure coefficient;
- k = constant of soil modulus variation;
- $k_h$  = coefficient of horizontal subgrade reaction;
- $k_s$  = coefficient of vertical subgrade reaction;
- $k_0, k_1, k_2$  = constants of soil modulus variation;
- L = length of precast panel;

$L$  = length of rectangular vertical strip;  
 $M$  = applied moment;  
 $M_d$  = design moment;  
 $N$  = blow count from TCP Test;  
 $N_c$  = bearing capacity factor;  
 $n$  = exponent of depth term;  
 $P_d$  = design force;  
 $P_s$  = ultimate soil resistance at groundline;  
 $P_x$  = axial load on foundation;  
 $P_\alpha$  = force acting at height,  $\bar{h}$ , to rotate shaft through angle,  $\alpha$ ;  
 $p$  = soil reaction;  
 $p_u$  = ultimate lateral soil reaction;  
 $q$  = pressure per unit area of contact surface;  
 $q_u$  = unconfined compressive strength;  
 $R$  = relative stiffness factor;  
 $R_1$  = resultant force above rotation point of foundation;  
 $R_2$  = resultant force below rotation point of foundation;  
 $s$  = slope;  
 $T$  = relative stiffness factor;  
 $V$  = shear;  
 $V_{xd}$  = horizontal shear force beneath foundation;  
 $V_{za}$  = vertical shear force above rotation point;  
 $V_{zb}$  = vertical shear force below rotation point;  
 $WF$  = wide flange;  
 $W$  = settlement;  
 $x$  = depth below groundline;

$x_1$  = depth to  $R_1$ ;  
 $x_2$  = depth to  $R_2$ ;  
 $y$  = lateral deflection;  
 $Z$  = depth to rotation point;  
 $\alpha$  = limiting angle of rotation;  
 $\beta$  = damping factor;  
 $\phi$  = angle of shearing resistance;  
 $\phi'$  = effective angle of shearing resistance;  
 $\lambda$  = slope of soil resistance diagram;  
 $\nu_s$  = Poisson's ratio;  
 $\gamma$  = unit weight of overburden material; and  
 $\zeta$  = angle of slope of backfill to horizontal.

NOTES